

Functional characterization of the *R. irregularis* effector RiSP749 and its interactors in tomato and *M. truncatula*

Sofía Hernández Luelmo

Student number: 02002157

Supervisor(s): Prof. Sofie Goormachtig

Scientific tutor: (Dr.) Judith Van Dingenen

Master's dissertation submitted to Ghent University to obtain the degree of Master of Science in Biochemistry and Biotechnology. Major Plant Biotechnology

Academic year: 2021 - 2022

Confidentiality statement

Master thesis 'Functional characterization of the *R. irregularis* effector RiSP749 and its interactors in tomato and *M. truncatula*'

By Sofía Hernández Luelmo

Under the supervision of Prof. Sofie Goormachtig

This document and the information in it are provided in confidence, for the sole purpose of evaluation of the MASTER thesis of Sofía Hernández Luelmo, and may not be disclosed to any third party or used for any other purpose without the explicit written permission of Prof. Dr. Sofie Goormachtig, VIB-UGent Center for Plant Systems Biology.

Acknowledgements

First of all, I would like to thank Prof. Sofie Goormachtig for opening me the doors of her lab and giving me the opportunity to perform this Master thesis. I would also like to thank Dra. Judith Van Dingenen for all her support, corrections and enthusiasm, I really learnt a lot from all your comments and your positivity keeps me motivated even in the most stressing moments.

The Rhizosphere Group also worth my attention and greetings, as they have completely included me in the team since the first day and make me feel at home. I hope I can stay and keep growing with all of you.

Finally, I would like to thank my flatmate, Lia, for all the patient and for taking out a smile from me even in the worst days, my mother, for pushing me to grow and start this amazing path in science and life, and the rest of my family and friends for being always close even in the distance.

Table of contents

Acknowledgements.....	i
List of Abbreviations	v
English summary	x
Part 1: Introduction.....	1
1. Sustainable agriculture	1
1.1. The need for sustainable agricultural alternatives	1
1.2. The bio-fertilizer Arbuscular mycorrhizal fungi (AMF) as sustainable alternative for tomato cultivation	1
2. Arbuscular mycorrhizal fungi (AMF).....	2
2.1. <i>Medicago truncatula</i> , AM symbiosis model species.....	3
2.2. <i>Rhizophagus irregularis</i> DAOM197198 as a AMF model strain in research.....	4
2.3. AMF development.....	4
2.4. The AMF common symbiosis signalling pathway (CSSP)	6
2.4.1. Implication of DELLA in CSSP regulation and mycorrhization.....	8
2.5. AMF nutrient exchange.....	9
2.5.1. Transporters involved in nutrient exchange.....	10
3. Plant defenses activation during mycorrhization	12
3.1. Different layers of defense responses	12
3.2. Defense mechanisms induced during AM symbiosis.....	14
3.3. AMF effectors.....	14
3.4. <i>R. irregularis</i> effectors.....	15
Part 2: Aims of the Research Project	17
Part 3: Results.....	19
1. In silico analysis of RiSP749 and its interactors in tomato and <i>M. truncatula</i>.....	19
1.1. <i>R. irregularis</i> effector RiSP749	19
1.2. Candidate RiSP749 interactors in tomato: SIRSZ22 and SIGNAT	19
1.3. Candidate homologous interactors of RiSP749 in <i>M. truncatula</i>	22
2. Validating the interaction between RiSP749 and two candidate interactors SIRSZ22 and SIGNAT in tomato, and their homologs in <i>M. truncatula</i>	23
2.1. Nuclear colocalization of RiSP749 and the candidate tomato interactor proteins SIRSZ22 and SIGNAT	24
2.2. Binary Y2H validated the interaction between RiSP749 and the tomato proteins SIRSZ22 and SIGNAT	25

2.3.	Ratiometric Bimolecular Fluorescence Complementation (rBiFC)	26
2.4.	Binary Y2H assays validate the interaction between RiSP749 and the <i>M. truncatula</i> homologs of SIRSZ22 and SIGNAT	28
3.	Functional characterization of RiSP749 during AM symbiosis	30
3.1.	Time series evaluation of mycorrhization in WT <i>M. truncatula</i> plants.....	30
3.2.	Effect of RiSP749 overexpression on AM colonization of <i>M. truncatula</i> plants	33
3.3.	Effect of RiSP749 OE on the expression of its protein interactors	36
4.	Functional characterization of candidate interactors in tomato.....	38
4.1.	Pattern of promoter activity of SIGNAT in tomato mycorrhizal roots	38
4.2.	Effects of tomato <i>SIRSZ22</i> silencing on mycorrhization.....	39
Part 4: Discussion		41
1.	RiSP749 interacts with the tomato protein SIRSZ22.....	42
2.	RiSP749 is expressed at early stages of mycorrhization in <i>M. truncatula</i>	43
3.	RiSP749 overexpression reduces the expression of multiple AM symbiosis inducible genes	44
4.	RiSP749 induces SIRSZ22 <i>M. truncatula</i> homologs during mycorrhization	47
5.	<i>SIRSZ22</i> silencing increased AM colonization in tomato.....	49
6.	Conclusions	49
Part 5: Materials and Methods		52
1.	Plant and fungal material.....	52
2.	Cloning	52
3.	<i>In silico</i> analysis	53
4.	Yeast-two-hybrid (Y2H) assay	53
5.	Transient expression of proteins in leaves of <i>Nicotiana benthamiana</i>	53
5.1.	Ratiometric bimolecular fluorescent complementation (BiFC)	53
5.2.	Colocalization	54
6.	Generation of <i>M. truncatula</i> and tomato hairy root composite plants	54
7.	GUS staining and analysis	54
8.	Colonization analysis, ink staining and Trouvelot method.....	55
9.	RNA extraction, cDNA synthesis and qRT-PCR analysis	55
References		56
Addendum		71
1.	Figures.....	71
2.	Tables.....	74

3. Detailed Protocols	77
3.1. Tomato and <i>M. truncatula</i> -AMF bioassay	77
3.2. Cloning	78
3.3. Yeast transformation	80
3.4. Tobacco transformation.....	81
3.5. RT-qPCR.....	81
3.6. GUS staining	82

List of Abbreviations

3-AT	3-Amino-1,2,4-Triazol
AD	Activation domain
AMF	Arbuscular Mycorrhiza Fungi
AM	Arbuscular mycorrhiza
AMT	Ammonium Transporter
BAP	6-benzylaminopurine
BD	Binding Domain
CACNA1S	calcium channel alpha-1 subunit
CCaMK	CALCIUM-, CALMODULIN-DEPENDENT SERINE/THREONINE PROTEIN KINASE
CEBIP	CHITIN ELICITOR BINDING PROTEIN
CO	Chito oligosaccharides
CoIP	co-immunoprecipitation
CRN	CRINKLER
CSSP	Common Symbiosis Signalling Pathway
DAMP	Damage-Associated Molecular Patterns
DMI	Does Not Make Infection
ENOD11	<i>EARLY NODULATION 11</i>
ER	Endoplasmic Reticulum
ERF	ETHYLENE RESPONSE FACTOR
ETI	Effector triggered immunity
EV	Empty Vector
FAS	fatty acid synthase
FLIP	Fluorescence Loss In Photobleaching

FRAP	Fluorescence Recovery After Photobleaching
GA	Gibberellic Acid
GFP	Green Fluorescent Protein
GNAT	Gcn5 N-Acetyl Transferase
GPAT	glycerol-3-phosphate acyl transferase
GR	Green Revolution
H	Histidine
H2B	Histone 2B
HA1	H ⁺ -ATPases1
HAK10	High-Affinity Potassium Transporter
HIGS	Host-induced gene silencing
HMGR1	3-HYDROXY-3-METHYLGLUTARYL COENZYME A REDUCTASE 1
HRGP	Hydroxyproline-rich Glycoproteins
IPD3	INTERACTING PROTEIN DMI3
IRM	intraradical mycelium
JA	Jasmonic acid
L	Leucine
LCO	Lipo-chito oligosaccharides
LYK	Lysine Motif-Receptor Like Kinase
LYR	Lysine Motif-Receptor
LysM	Lysine Motif
Ma	Million years ago
MAMP	Microbe-associated molecular patterns
MAX2	More Axillary Growth 2

MIG1	MYCORRHIZA INDUCED GRAS
MS	Mass spectrometry
MS	Murashige & Skoog
N	Nitrogen
NB-LRR	NUCLEOTIDE-BINDING LEUCINE RICH REPEAT
NFP	Nod Factor Perception
NF-Y	Nuclear Factors-Y
NIN	Nodule Inception
NLE1	NUCLEAR LOCALISED EFFECTOR 1
NLS	Nuclear Localization Signal
NOPE1	NO PERCEPTION 1
NPF	Nitrate Transporter 1/Peptide transporter family
NSP	NODULATION SIGNALLING PATHWAY
OE	Overexpression
P	Phosphorous
PAM	Periarbuscular membrane
PaPDR1	Petunia PLEIOTROPIC DRUG RESISTANCE 1
PPA	Pre-Penetration Apparatus
PRR	PATTERN RECOGNITION RECEPTOR
PT	Phosphate Transporter
PTI	Pattern-Triggered Immunity
qRT-PCR	Quantitative- Reverse Transcriptase Polymerase Chain Reaction
RAM	REQUIRED FOR ARBUSCULAR MYCORRHIZATION
RIP	mRNA co-immunoprecipitation

RNAi	RNA interference
rBiFC	Ratiometric Bimolecular Fluorescence Complementation
RFP	Red Fluorescence Protein
RRM	RNA-recognition motif
RSZ	Arginine/Serine, Zinc-Knuckle splicing factor
SA	Salicylic Acid
SIS1	SL-INDUCED PUTATIVE SECRETED PROTEIN
SKP1	S-phase kinase-associated protein
SL	Strigolactones
SLM	SECRETED LYSIN MOTIF
SLP1	Secreted LysM Protein 1
snRNP	Small nuclear Ribonucleoprotein
SP7	Secreted Protein 7
STR	STUNTED ARBUSCULE
SUT	SUCROSE Transporter
SWEET	Sugar Will Eventually be Exported Transporters
SYM	Symbiosis
SYMRK	SYMBIOSIS RECEPTOR-LIKE KINASE
T	Threonine
T3SS	Type 3 Secretion System
TF	Transcription Factor
UAS	Upstream Activation Sequence
WPI	Weeks post inoculation
WT	Wild-type

X-Gluc 5-bromo-4-chloro-3-indolyl- β -glucuronide

Y2H Yeast two Hybrid

English summary

Arbuscular mycorrhizal fungi (AMF) establish symbiotic interactions with the majority of the land plants and important crops such as tomato. During AM symbiosis, the fungus provides nutrients to the plant in exchange for plant photoassimilates. AMF tune host plant physiology in order to overcome the transiently activated host plant defense response induced upon fungal detection and to establish a successful colonization and a complete symbiosis. In plant-pathogen interactions and nodulation, effectors are essential for that purpose. Also, AMF secrete effectors during host plant colonization, thus, their role in symbiosis has been presumed. In this thesis, we focused on RiSP749, an effector from the model AMF species *Rhizophagus irregularis*, and its role during symbiosis with *Medicago truncatula* and tomato. RiSP749 interacted *in planta* with the tomato splicing factor SIRSZ22 and *in vitro* with its *M. truncatula* homologs (MtRSZ21, MtRSZ22a and MtRSZ22b). In addition, RiSP749 induces *MtRSZ21*, *MtRSZ22a* and *MtRSZ22b* expression during mycorrhization in *M. truncatula* roots. RiSP749 also interacted *in vitro* with SIGNAT, although this interaction could not be confirmed *in planta*. In *M. truncatula*, *RiSP749* was mostly expressed at early stages of colonization and repressed the expression of both early mycorrhiza inducible genes (*MtNIN*, *MtDELLA1*, *MtNSP2* and *MtCYCLOPS*) and functional arbuscule marker genes (*MtPT4* and *MtRAM1*). However, *RiSP749* OE lines did not or only slightly reduced colonization frequency, whereas more arbuscules were formed in the outer cortical cell layers, indicating that a constitutive expression of *RiSP749* at late stages of mycorrhization impairs the normal arbuscule development in the plant cortical cells. Moreover, the silencing of *SIRSZ22* in roots of mycorrhized tomato plant showed increased level of colonization, whereas SIPT4, SIPT5 and SIRAM1 were not affected. Overall, these experiments suggest that the *R. irregularis* effector RiSP749 has a role in mycorrhization, probably during hyphal elongation prior to arbuscule formation and some of its functions might be exerted by the interaction with SIRSZ22 and MtRSZ21, MtRSZ22a and MtRSZ22b, homologs in tomato and *M. truncatula*, respectively.

Part 1: Introduction

1. Sustainable agriculture

1.1. The need for sustainable agricultural alternatives

The imbalance between the world population and food production grows every year threatening food security. While the world population grows 1,1 % annually, and expects to reach 12 billion people by the end of this century, annual crop yield is decreasing due to land degradation, water scarcity and climate change, among others (FAO, 2020).

The Green Revolution (GR) was one of the key drivers in the exponential population growth that began in the 1960s. The industrialization and automatization of agriculture, as well as the use of fertilizers and pesticides profoundly remodeled the agricultural sector and drastically increased the production. Cereal production tripled since the start of GR with only 30% expansion in used land (Pingali, 2012). However, in the last decade, the crop production has stabilized, and agriculture mostly relies on the application of fertilizers and pesticides to keep the production rates. The use of chemical fertilizers increased more than 40% from 2000 to 2018, reaching 188 million tons in 2018 (Pahalvi *et al*, 2021), with a significant crop yield increment but also negative consequences for the environment (Yousaf *et al*, 2017). Up to 50% of the nitrogen (N) and 90% of the phosphorous (P) of the current fertilizers applied on the fields are not absorbed by the plants and leach into the soil and groundwater (Ye *et al*, 2020; Pahalvi *et al*, 2021). This overuse of fertilizers contributes to land degradation, reduces soil microbial diversity and productivity, decreases soil organic matter, and pollutes the air, water and soil causing also human health problems (Fan *et al*, 2014). At biological level, the application of high amounts of fertilizer, altering the microbiome composition and promoting the growth of pathogenic strains leading to an increased frequency of diseases and pests (Li *et al*, 2017). Therefore, in order to meet the foreseeable food-demand without polluting the environment and overexploiting natural resources, i.e. 38% of the land and 70% of the water coming from freshwater bodies are used for agriculture worldwide (FAO, 2020), a novel agricultural sector which makes use of sustainable agricultural systems is required.

Novel ecological and sustainable alternatives that are being considered to reduce or replace the use of chemical fertilizers and pesticides are e.g. the use of manure, bio-fertilizers, better land management practices involving new monitoring technologies and genetically modified plants, among others (Geng *et al*, 2019; Fukuda *et al*, 2012).

1.2. The bio-fertilizer Arbuscular mycorrhizal fungi (AMF) as sustainable alternative for tomato cultivation

Bio-fertilizers are biological products containing living organisms that promote plant growth. For example, plant growth promoting bacteria and fungi such as *Burkholderia* or *Trichoderma* (Ye *et al*, 2020), nitrogen fixing bacteria such as *Rhizobium* (Bhattacharjee *et al*, 2008) or Arbuscular Mycorrhizal Fungi (AMF) such as *Funneliformis mosseae* (Amani Machiani *et al*, 2021). Applying these organisms on agricultural fields can reduce the required fertilizer input, promote a more efficient use of nutrients by the plant, assimilate inorganic forms of certain nutrients into more

accessible forms for the plants, or provide nutrients directly to the plant (Ye *et al*, 2020). The mechanisms of plant growth promotion vary between bio-fertilizers.

Symbiosis with AMF is a widespread association observed in many economically important crops such as soybean, wheat, corn and tomato. During mycorrhization, AMF provides water and multiple nutrients, especially P, to the plant. P is an essential plant nutrient deficient in 67% of the total farmed land and presents low solubility (Schachtman *et al*, 1998). The growth of AMF hyphae outside the plant roots allows plants to access to P distant from the root surface and provide plants with the required amount of this mineral, which reduces their dependence on chemical fertilizers (Smith *et al*, 2011). Hence, AMF is an interesting sustainable alternative to fertilizers in agriculture (Chen *et al*, 2018; Siciliano *et al*, 2007; Nacocon *et al*, 2021).

One of the crops that could strongly benefit from the use of AMF as bio-fertilizers is the important vegetable crop tomato (*Solanum lycopersicum*). The most important trait in tomato cultivation is fruit flavor and nutritional quality. Multiple studies evidenced that tomato plants colonized with AMF have increased levels of carotenoids, citric acid, minerals, certain amino acids, sugars and antioxidant components in their fruits (Chialva *et al*, 2016; Bona *et al*, 2017; Schubert *et al*, 2020; Rodriguez & Sanders, 2015; Hart *et al*, 2015). Mycorrhized tomato plants also showed a higher nutraceutical value with increased concentrations of the antioxidant lycopene in their fruits and a higher anti-oestrogenic power evidenced by the enhanced ability of mycorrhized tomato fruit extracts to inhibit the 17- β -oestradiol-human oestrogen receptor binding (Giovannetti *et al*, 2012). Additionally, AM symbiosis reduces the vegetative growth of tomato plants, leading to early flowering and fruit maturation (Bona *et al*, 2017), as well as bigger fruit size, thus, increasing yield (Nzanza *et al*, 2012; Salvioli *et al*, 2012). These tomato yield improvements are achieved without or with a strongly reduction in P fertilization (Ziane *et al*, 2021; Schubert *et al*, 2020). Beside the AMF positive effects on fruit development, AMF application can improve tomato performance under abiotic stresses such as salt-stress (Balliu *et al*, 2015), waterlogged (Calvo-Polanco *et al*, 2014), water scarcity (Chitarra *et al*, 2016) or heat conditions (Duc *et al*, 2018), by increasing the expression of tomato aquaporins (SIPIP1;7), improving plant homeostasis and moderating oxidative stress (Duc *et al*, 2018; Calvo-Polanco *et al*, 2014).

2. Arbuscular mycorrhizal fungi (AMF)

AMF belong to the phylum Glomeromycota and establish symbiotic associations with more than 70% of the land plants, indicating a low host specificity. Their hyphal network is widely spread across the soil and highly abundant, i.e. more than 100 meters of hyphae per cubic centimeter of soil (Parniske, 2008). Interestingly, arbuscular mycorrhiza (AM) symbiosis was essential for the terrestrialization of land plants 450 million years ago (Ma) (Humphreys *et al*, 2010). During evolution, AM symbiosis created a monophyletic group of plants able to colonize land by generating an enhanced root system enabling attachment to the soil and absorption of nutrients and water (Chen *et al*, 2018).

AMF have aseptate multinucleate hyphae and mainly propagate asexually by forming spores. Moreover, they can undergo hyphal fusion between related species and exchange genetic material increasing their genetic diversity (De Novais *et al*, 2017), although the level of relatedness required for nuclei exchange has not yet been determined. Only 240 AMF species

have been described within the phylum Glomeromycota based on morphological differences (Krüger *et al*, 2012; Lee *et al*, 2013). However, the presence of different functionalities, growth patterns and genetic compositions in diverse AMF communities, suggest a much wider diversity. Indeed, by means of molecular studies a considerable genetic variability between strains and even within a single spore has been found (Lee *et al*, 2013). Additionally, taxonomic classification of AMF based on their genomes presents an additional challenge because AMF are multinucleate organisms, and occasionally, contain nuclei with different genetic information (Serghi *et al*, 2021).

One of the traits used for the classification of AMF is the colonization patterns. Two main colonization patterns have been distinguished in AMF, the Paris-type and the Arum-type (Dickson *et al*, 2007). Arum-type colonization is more common in crop plants and is characterized by mostly intercellular hyphae and intracellular branched arbuscules. On the other hand, Paris-type structures mainly appear in trees and forest herb plants. In this morphotype, coiled intracellular hyphae and arbuscules predominate (Stoian *et al*, 2019; Dickson, 2004). These morphotypes are primarily determined by the host plant, which, depending on the species, form only one type of structure, intermediate structures or both type of structures. Both structures can appear simultaneously in the same plant, for example in *Ranunculus*. In some species, such as *Zea mays*, the fungal morphotype depends on the particular plant cultivar (Dickson, 2004). In contrast, in tomato the structure formed depends on the colonizing fungi. *Rhizophagus irregularis*, *Glomus mosseae*, and *Glomus versiforme* form Arum-type structures during tomato colonization, while *Glomus coronatum*, *Gigaspora margarita* and *Scutellospora calospora* form Paris-type (Dickson, 2004).

AM symbiosis is widely spread across different environments and host plants, which suggests a high degree of adaptation and coordination between the fungus and the host plant. In fact, the outcome of AM symbiosis strongly depends on the genotypes of both the plant and the fungus (Burleigh *et al*, 2002; Croll *et al*, 2008; Avio *et al*, 2006; Munkvold *et al*, 2004). Variations in the activated genetic program influences the colonization rates, the growth of the extra- and intraradical mycelium, the mycelium viability or nutrient uptake capacity (Hohnjec *et al*, 2005). However, fungal strains show little host specificity, they can establish interactions with many different plants, and one plant can be colonized by many different AMF species and even strains of the same species. Although, interestingly, some level of host preference has been proven by the positive correlation between the biodiversity of AMF strains and plant species, demonstrating different levels of functional compatibility (Serghi *et al*, 2021; Angelard *et al*, 2010), but the exact mechanisms involved in the selection of the host plant-AMF preferred combination remain unknown (Lee *et al*, 2013).

2.1. *Medicago truncatula*, AM symbiosis model species

Within the plant species that interact with AMF, *Medicago truncatula* has been widely used as a legume model species for plant-microbe interactions and most of the molecular mechanisms involved in AM symbiosis establishment have been studied this plant species (Gavrin & Schornack, 2019). Working with tomato and other interesting crops such as wheat (*Triticum sp.*) or rice (*Oryza sativa*) is challenging due to their complex genomes, the absence of standardized

protocols and their reduced mycorrhization potential. In contrast, *M. truncatula* genome sequence is available (Young *et al*, 2011), it counts with a germplasm and mutant collection (Tadege *et al*, 2008) and databases about spatio-temporal gene expression studies (Benedito *et al*, 2008). Moreover, *M. truncatula* has a high mycorrhization potential, and occupies little space. All these characteristics make *M. truncatula* an ideal model species in this field.

2.2. *Rhizophagus irregularis* DAOM197198 as a AMF model strain in research

AMF depends on the plant to obtain their nutritional requirements. Thus, they are obligate mutualistic symbionts and can only be propagated in plant root cultures (Song *et al*, 2011). This characteristic, together with their complex genome, have hindered their transformation, massive production and commercial utilization of AMF. Nowadays, only transient transformation with fluorescent reporter genes (DsRed and GFP) driven by the promoters of two genes from the AMF *G. mossae* that are expressed in early symbiosis, have been achieved by particle bombardment (Helber & Requena, 2008).

Among the efforts to facilitate the study of AMF, transcriptomic and genomic data has been generated from *R. irregularis* (Tisserant *et al*, 2013, 2012; Lin *et al*, 2014), *Gigaspora rosea* (Tang *et al*, 2016), *G. margarita* (Salvioli *et al*, 2016) and *Rhizophagus clarus* (Sędziewska Toro & Brachmann, 2016). However, only the genome of *R. irregularis* DAOM197198 have been fully sequenced (Tisserant *et al*, 2013) and specific primers for its identification by qRT-PCR based on its mitochondrial genome have been designed (Badri *et al*, 2016). Furthermore, the production of AMF in higher amounts and without plant contamination has been achieved through a two-compartment system for *in vitro* propagation of AMF established two decades ago. This system was designed and optimized using *R. irregularis* DAOM197198, although it allows the production of other AMF species as well (St-Arnaud *et al*, 1996; Rosikiewicz *et al*, 2017).

Within the diversity of AMF species, *R. irregularis* is used as an AMF model species because of its broad host range, its worldwide distribution and its positive effects on plant performance during symbiosis, compared with the other mentioned species.

2.3. AMF development

Establishment of AM symbiosis can be divided in three phases: the pre-symbiotic phase, the penetration phase and the intraradical growth or arbuscular phase (Gutjahr & Parniske, 2013; Figure 1). The **pre-symbiotic phase** is initiated when, under P limiting conditions, the plant roots exude strigolactones (SLs) as a signal for the initiation of AM symbiosis establishment. SL are secreted through the G-subfamily ABC transporter PLEIOTROPIC DRUG RESISTANCE 1 (PaPDR1 in *Petunia*)/MtABCG59 (Kretzschmar *et al*, 2012; Banasiak *et al*, 2020). In the *Solanaceae* family, SLs are secreted *via* the hypodermal passage cells, the only non-suberized cells from the exodermis (Sasse *et al*, 2015). Interestingly, these cells are also the only entry points of the fungus during mycorrhization (Sharda & Koide, 2008). Therefore, the secretion of SLs through hypodermal passage cells may guide AMF to the preferred colonization locations. SLs recognition by the fungus enhances spore germination and hyphal branching towards the plant roots (Akiyama *et al*, 2005). SL concentration gradient is established in the soil from the plant root surface due to their instability, guiding the growth of the fungal hypha (Besserer *et al*, 2006; Gomes & Selman,

2005). Interestingly, beside SLs, other plant secreted molecules may be involved in priming the AM symbiosis. This hypothesis is supported by the necessity of the N-acetylglucosamine transporter NO PERCEPTION 1 (NOPE 1) in maize and rice to induce AMF germination and establish AM symbiosis (Nadal *et al*, 2017). NOPE1 secreted compounds are required for the transcriptional reprogramming of the fungus during the pre-symbiotic phase of mycorrhization. In response, AMF secrete a mix of sulfated and non-sulfated lipo-chito-oligosaccharides (LCOs) (Maillet *et al*, 2011) and short chain chito-oligosaccharides (CO4/CO5) (Genre *et al*, 2013), also known as Myc factors. Myc factors are recognized by the plant *via* lysine motif (LysM) receptor-like kinases, the initial point of the common symbiosis signaling pathway (CSSP). This signaling pathway is common with nodulation, another type of symbiosis established between legumes and rhizobia and which is closely intertwined with mycorrhization during plant evolution (Oldroyd, 2013).

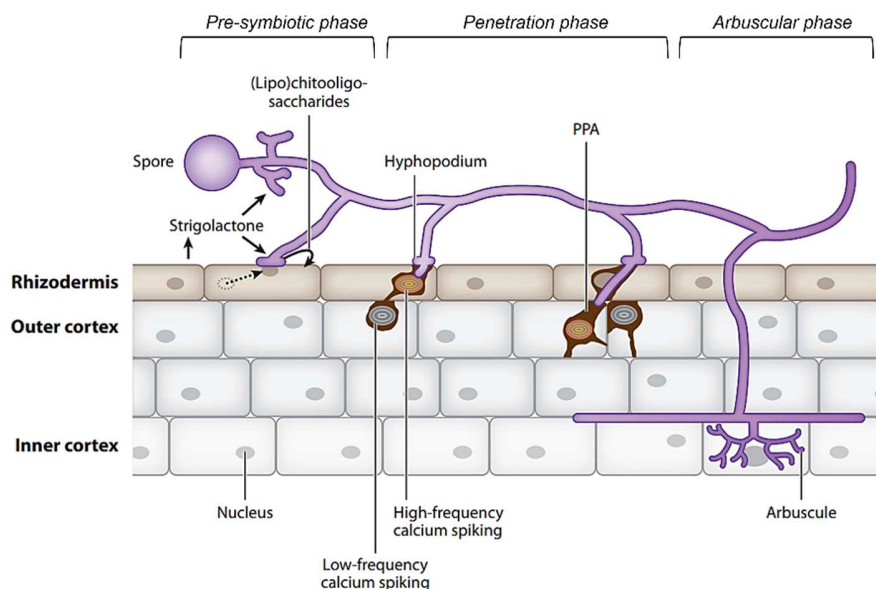


Figure 1: AM symbiosis establishment. During the pre-symbiotic phase, plant releases SLs to promote AMF spore germination and hyphal branching towards the plant root. At the same time, the fungus secretes LCOs that are detected by LysM receptors from the plant which activates the common symbiosis signaling pathway (CSSP). Once the fungus reaches the host plant root surface it forms a hyphopodium and penetrates into the plant epidermal cell, initiating the penetration phase. The intracellular growth of the fungus is accommodated by the pre-penetration apparatus (PPA) formed by the plant. Once in the cortex, during the arbuscular phase, the fungal hyphae elongate intercellularly and eventually penetrates into a cell from the inner cortex forming branched structures known as arbuscules (from the Latin 'arbusculum', which means little tree). (Gutjahr & Parniske, 2013)

Once the fungus reaches the host plant surface, it forms a hyphopodium. The hyphopodium is an infective structure of the fungus formed at the contact point of the host plant root. It serves as a fungal entry point into the host plant epidermis. Hyphopodium formation is triggered by plant produced cutin monomers (Wang *et al*, 2012; Murray *et al*, 2013). Once hyphopodium is formed, the host plant assembles the **pre-penetration apparatus (PPA)** to start the penetration phase. The PPA is a cytoplasmic bridge consisting of membrane invaginations held by the cytoskeleton and surrounded by a very dense endoplasmic reticulum (ER) cisternae, responsible for providing the elements required for perifungal membrane formation (Siciliano *et al*, 2007). The PPA

formation and growth is guided by the nucleus of the infected plant cell which initially moves towards the hyphopodium and then to the inner phase of the cell (Genre *et al*, 2005; Parniske, 2008). Similarly, the symplastic growth of the fungal hyphae is guided by the PPA (Pimprikar & Gutjahr, 2018). The fungus only penetrates the root when the PPA is formed, indicating a strict control of the fungal infection by the host plant and a specific identification of the fungus (Siciliano *et al*, 2007).

In the outer cortex, the fungal hyphae elongate intercellularly, and eventually penetrate in the inner cortical cells forming branched structures known as **arbuscules**, where nutrient exchange takes place (Chen *et al.*, 2018; Gutjahr & Parniske, 2013; Figure 1). The branched fungal hyphae are surrounded by a periarbuscular membrane (PAM), consisting of the plant plasma membrane and enriched in organic and inorganic nutrient transporters (An *et al*, 2019; Harrison *et al*, 2002; Manck-Götzenberger & Requena, 2016; Banasiak *et al*, 2021). The fungal membrane and the PAM are separated by an acidified space called the periarbuscular space. The periarbuscular space is acidified by plant H⁺-ATPases (MtHA1/SIHA1) located at the PAM membrane, which creates an electrochemical gradient necessary for an efficient nutrient exchange (Krajinski *et al*, 2014).

The lifespan of arbuscules is short, i.e. one week, and they are only functional for two to three days when they are fully mature (Kobae & Hata, 2010; Kobae & Fujiwara, 2014; Kobae, 2019; Toth & Miller, 1984). This short life ensures maintenance of an efficient nutrient exchange (Luginbuehl & Oldroyd, 2017). The arbuscule grows and branches until it reaches its maximum size, after which it degenerates. Degeneration is characterized by the separation of the cytoplasm of the arbuscular hyphae from the rest of the hyphae through septation by which the arbuscule collapses and disappears (Toth & Miller, 1984; Kobae & Fujiwara, 2014).

2.4. The AMF common symbiosis signalling pathway (CSSP)

The CSSP is a conserved set of plant proteins that tunes AM establishment transducing the symbiosis signals (Genre & Russo, 2016; Figure 2). The CSSP pathway involves plant LysM-receptor like kinases that recognize Myc factors, calcium signaling proteins that act downstream of the generated calcium spiking, and symbiosis specific transcription factors (TF). Multiple LysM receptors involved in mycorrhization have been identified in different plant species. *M. truncatula* expresses NOD FACTOR PERCEPTION (MtNFP), LYSIN MOTIF-RECEPTOR LIKE KINASE (MtLYR3) and LYSIN MOTIF-RECEPTOR LIKE KINASE 9 (MtLYK9), which are involved, although not essentially, in mycorrhization (Gibelin-Viala *et al*, 2019; Maillet *et al*, 2011; Gough *et al*, 2018). In tomato, LYSIN MOTIF-RECEPTOR LIKE KINASE 10 and 12 (SILYK10, and SILYK12) have been identified as the main Myc factor receptors involved in AM (Buendia *et al*, 2016; Girardin *et al*, 2019; Liao *et al*, 2018). In legumes, such as *Lotus japonicus* and *M. truncatula*, the SYMBIOSIS RECEPTOR-LIKE KINASE (LjSYMRK) and DOES NOT MAKE INFECTION (MtDMI2) proteins act as co-receptors of the LysM receptor kinases (Antolín-Llovera *et al*, 2014; Stracke *et al*, 2002) and interact with 3-HYDROXY-3-METHYLGLUTARYL COENZYME A REDUCTASE 1 (HMGR1; Kevei *et al.*, 2008), involved in the mevalonate biosynthesis pathway.

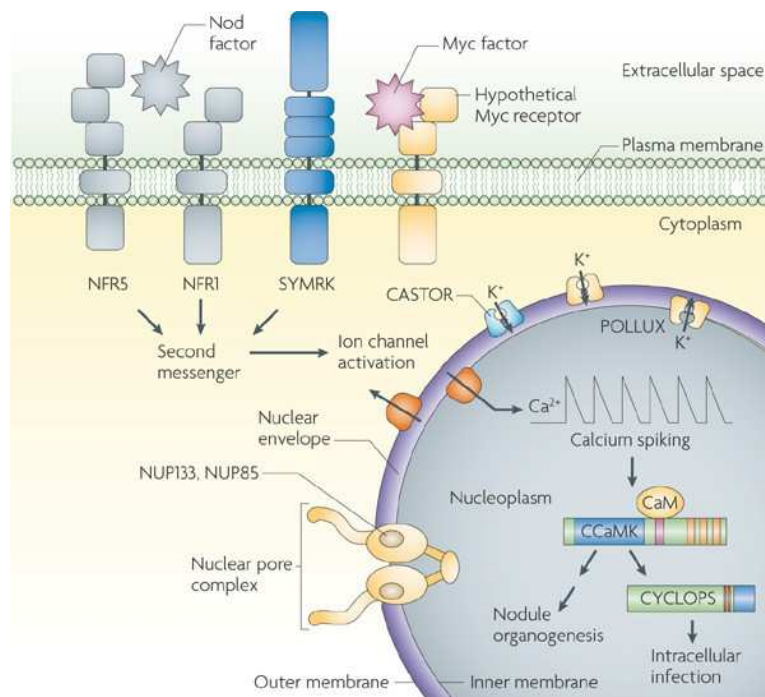


Figure 2: Common symbiosis signaling pathway (CSSP) components. The CSSP pathway is a set of proteins conserved among most of the plants and activated both during nodulation and arbuscular mycorrhiza symbiosis. Is initiated by the recognition of Myc or Nod factors by LysM plant membrane receptors, the signal is transduced until the nucleus where a calcium spiking takes place, activating Calcium dependent calmodulin kinase, which, together with CYCLOPS induces the expression of specific transcription factors (TF) involved in the accommodation of the bacteria or the fungus, respectively, and the establishment of a complete symbiosis. (Parniske, 2008)

Mevalonate has been proposed as a second messenger for the activation of channels involved in nuclear **calcium spiking** (Oldroyd, 2013), such as the LjCASTOR and LjPOLLUX/MtDMI1, cation channels from the nuclear envelope (Capoen *et al*, 2011), MCA8, an ATP-powered Ca²⁺ pump localized in the nuclear envelope (Capoen *et al*, 2011), and NUP85, NENA and NUP133, nucleoporins (Kanamori *et al*, 2006; Saito *et al*, 2007; Groth *et al*, 2010; Riely *et al*, 2007; Genre & Russo, 2016). Calcium spiking induces CALCIUM-, CALMODULIN-DEPENDENT SERINE/THREONINE PROTEIN KINASE (LjCCaMK)/MtDMI3 which associates with the transcriptional activator LjCYCLOPS/INTERACTING PROTEIN DMI3 (MtIPD3) (Yano *et al*, 2008; Horváth *et al*, 2011). Together, these proteins modify host plant gene expression directly, by binding to the NODULE INCEPTION (MtNIN) promoter (Singh *et al*, 2014), or by phosphorylation and activation of multiple TFs from the GRAS family involved in AM establishment (Parniske, 2008; Genre *et al*, 2005). MtNIN represses *EARLY NODULATION 11* (*MtENOD11*) expression, which induces the expression of the Nuclear Factors-Y (NF-Y) subunit genes *MtNF-YA1*, *MtNF-YA2* and *MtNF-YB1*, involved in the stimulation of cortical cell division during colonization (Guillot *et al*, 2016; Soyano *et al*, 2013). Two main GRAS TFs activated during AM symbiosis establishment are NODULATION SIGNALLING PATHWAY 1 and 2 (MtNSP1, MtNSP2; Delaux *et al*, 2013), which are involved in strigolactones biosynthesis (Maillet *et al*, 2011; Liu *et al*, 2011b), and REQUIRED FOR ARBUSCULAR MYCORRHIZATION 1 (MtRAM1), specifically induced during mycorrhization and required for hyphopodium, arbuscule formation and branching (Park *et al*,

2015). RAM1 and NSP2 interacts in the host plant nucleus, probably forming heterodimers for the regulation of AM symbiosis specific gene expression and competing with NSP1-NSP2 heterodimers that regulate transcription mostly related to nodulation (Gobbato *et al*, 2012). MtRAM1 regulates the expression of MtRAM2, a glycerol-3-phosphate acyl transferase (GPAT) involved in cutin biosynthesis, which promotes hyphopodia formation (Wang *et al*, 2012; Gobbato *et al*, 2012; Gobbato, 2015). Additionally, RAM2, together with *FatM*, an acyl-ACP thioesterase, is responsible *de novo* lipid biosynthesis in arbusculated cells (Bravo *et al*, 2017; Jiang *et al*, 2017). Although this pathway has been mainly studied in legumes and during nodulation, orthologues of the CSSP genes have been found in all other mycorrhizal host plants such as rice (Banba *et al*, 2008).

2.4.1. Implication of DELLA in CSSP regulation and mycorrhization

DELLA is a GRAS TF family involved in repression of gibberellic acid (GA) signaling (Silverstone *et al*, 1998), and an important regulator of arbuscule development during mycorrhization (Foo *et al*, 2013; Floss *et al*, 2013) as *della1/della2 M. truncatula* mutant shows a strong reduction of arbuscule numbers in mycorrhized roots (Floss *et al*, 2013). Nevertheless, the arbuscules that appear in this mutant are fully mature, which suggest that DELLA has a role in the initial stages of arbuscule development. DELLA forms a complex with CCaMK-CYCLOPS inducing *RAM1* expression and arbuscule development (Pimprikar *et al.*, 2016; Figure 3). In addition, DELLA interacts with MYCORRHIZA INDUCED GRAS 1 (MIG1) to promote radial cell expansion in order to accommodate arbuscules in the cortical cells (Heck *et al*, 2016) (Figure 3). Overall, these intrinsic pathways indicate a fine-tuning and intertwined signaling during mycorrhization.

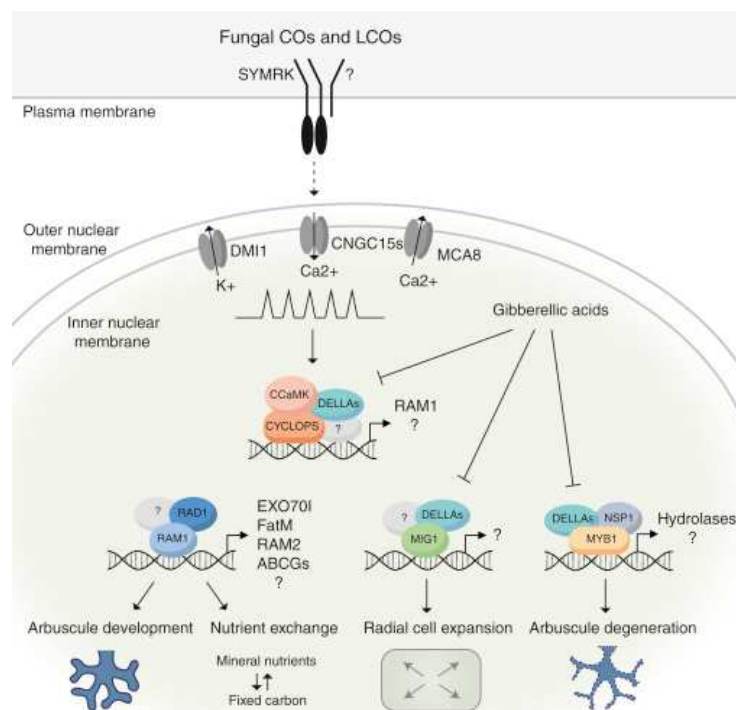


Figure 3: DELLA and CSSP interplay in arbuscule development. The common signaling symbiosis pathway (CSSP) transduces the signals for symbiosis establishment, including arbuscule development, nutrient exchange and

arbuscule degradation. DELLA regulates the CSSP signaling pathway at multiple levels, influencing in arbuscule development. (Luginbuehl & Oldroyd, 2017)

2.5. AMF nutrient exchange

Many nutrients are transferred from the fungus to the plant, from which P is the most important for symbiosis establishment (Ryan *et al*, 2000). P is present in essential biomolecules such as nucleic acids, phospholipids and ATP, and necessary for enzyme activity modulation or energy metabolism. In nature, plants overcome P deficiency by expressing high affinity phosphate transporters in their roots, increasing the number of root hairs and the length of the roots to enlarge the absorption surface or secreting organic acids to reduce soil pH, which facilitates P uptake (Péret *et al*, 2011). However, these mechanisms have a limited action distance, creating areas of depleted P around plant roots. Then, in order to access to further resources of P, the plant establishes symbiotic interactions with AMF (Etesami *et al*, 2021; Péret *et al*, 2011). Low concentrations of P availability in the soil promotes symbiosis establishment, and the host plant switches its phosphate-uptake route from rhizodermal-uptake to symbiotic-uptake (Wang *et al*, 2017). Molecular evidence of the change in the P uptake route during mycorrhization is the downregulation of the genes involved in direct rhizodermal-uptake of P, such as PHOSPHATE TRANSPORTER 2 or 6 (OsPT2, OsPT6) from rice, while the symbiotic-uptake P transporters, such as MtPT4 from *M. truncatula* or OsPT11 from rice, are upregulated (Paszkowski *et al*, 2002; Yang *et al*, 2012; Grunwald *et al*, 2009). The symbiotic pathway can even account for all P uptake necessary for the plant (Smith *et al*, 2004). High P concentrations, in contrast, reduce the level of mycorrhization by e.g. reducing the SL content in root exudates (López-Ráez *et al*, 2008; Yoneyama *et al*, 2007) or activating plant defenses (Lehnert *et al*, 2017). This P-inhibiting response on symbiosis is a plant energy-saving mechanism regulated systemically. This has been demonstrated by root experiments in which half of the root system is located in a high P concentration and the other half is situated in a low P concentration compartment (Balzergue *et al*, 2013, 2011). Beside P uptake, AMFs also provide other mineral nutrients to the plant such as N, sulphur, manganese and potassium (Balliu *et al*, 2015).

AMF colonization is shown to promote the photosynthetic rate of the plant (Bago *et al*, 2000) to ensure the supply of sugar and lipids to the fungus (Kaschuk *et al*, 2009; Keymer *et al*, 2017). During symbiosis, sugars are redistributed in the host plant, increasing the delivery of photoassimilates to the plant roots. Despite the increased demand of carbon due to the association with the fungus, mycorrhized plants show higher biomass and sugar content in leaves indicating that the additional effort demanded by the fungus is compensated, at least under P limiting conditions (Pedone-Bonfim *et al*, 2013; Kaschuk *et al*, 2009). Indeed, the energy metabolism, both the plant's Krebs cycle and plastid metabolism, is more active in mycorrhized plants to increase the level of carbon that is required for the fungus (Wewer *et al*, 2014; Keymer *et al*, 2017). The host plant provides 20% of its photosynthates, mainly in the form of sugars and lipids, to the fungi. Thus, considering all terrestrial plants, approximately 5 billion tons of carbon per year are consumed by AMF, highlighting the importance of this symbiotic relationship and its contribution to carbon cycling (Parniske, 2008).

2.5.1. Transporters involved in nutrient exchange

The exchange of all nutrients mentioned above takes place in arbuscules. Multiple mycorrhiza-specific and mycorrhiza-induced transporters have been described at the PAM. The most studied transporters are P transporters from the proton-coupled Phosphate Transporter 1 (PHT1) family. One of these P transporters is MtPT4 which is specifically expressed in arbusculated cells of *M. truncatula* and from which the expression increases with an increased colonization level (Harrison *et al*, 2002; Pumplin *et al*, 2012). Due to the exclusive expression of *MtPT4* in the PAM, it has become a marker gene of arbusculated cells. This transporter is essential for an efficient symbiosis as *mtpt4* mutants show reduced levels of mycorrhizal colonization and a premature collapse of arbuscules (Javot *et al*, 2007). In the *Solanaceae* family, three arbuscular mycorrhiza-specific phosphate transporters have been identified StPT3, StPT4 and StPT5 in potato and SIPT3, SIPT4 and SIPT5 in tomato, with the last two being orthologues of MtPT4 (Nagy *et al.*, 2005; Figure 4).

The PAM also contains N transporters from the AMMONIUM TRANSPORTER (AMT) family and the Nitrate Transporter 1/Peptide transporter family (NPF). *LjAMT2;2* from *Lotus japonicus*, is an ammonium high-affinity transporter exclusively expressed in arbusculated cells and the highest up-regulated gene upon plant colonization with the AMF *G. margarita* (Guether *et al.*, 2009; Figure 4). The ability of AMF to transfer nitrates to the plant as a N source has only recently been described, and so far, nitrate transporters have been found only in gramineous species such as rice or sorghum (*Sorghum bicolor*). Grasses express low affinity nitrate transporter NPF4.5 in arbusculated cells, and this symbiotic nitrate route is responsible for the delivery of 42% of the N supply to mycorrhized plants (Wang *et al.*, 2020). Also the fungus increases the expression of fungal ammonium transporters in arbusculated cells to deliver N into the periarbuscular space. In *R. irregularis*, three ammonium transporters expressed in arbuscules have been described, RiAMT1, RiAMT2 and RiAMT3 (Calabrese *et al*, 2016). Other mineral nutrients such as potassium, sulfates, or metals such as zinc, iron or manganese are also taken up by the plant via the arbuscules. However, not much is known about the transporters involved. An example for potassium transport is the High-Affinity Potassium Transporter 10 (SIHAK10) which is localized on the PAM in arbusculated cells from tomato (Liu *et al.*, 2019).

The PAM membrane also contains sugar and lipid transporters to provide nutrients to the fungus. Two families of sugar transporters have been studied during mycorrhization, the Sugar Will Eventually be Exported Transporters (SWEET) family and the SUCrose Transporter (SUT) family (Figure 4). MtSWEET1b is a glucose transporter protein expressed in arbuscule containing cells from *M. truncatula*. *mtsweet1b* mutants still show normal colonization rates indicating that it probably acts redundantly with other MtSWEET transporters expressed at the PAM (An *et al*, 2019). In potato (*Solanum tuberosum*), at least three StSWEET transporters StSWEET2c, StSWEET7a and StSWEET12a from the 35 StSWEET genes identified in its genome are induced upon mycorrhization (Manck-Götzenberger & Requena, 2016). The SUT family was suggested to balance the amount of photoassimilates that is provided to the fungus by taking up part of the sugars that SWEET transporters release into the periarbuscular space back to the plant cell (Bitterlich *et al*, 2014). SUT transporters are also expressed in the stem and leaves of the host plant indicating a role in carbohydrate redistribution in mycorrhized plants (Garcia *et al*, 2016).

The downregulation of *SISUT2* in tomato plants increases mycorrhization levels, although the plant shows a reduction in growth, probably due to an excessive amount of nutrients provided to the fungus (Bitterlich *et al*, 2014). In contrast, the overexpression of *StSUT1* in potato also promotes AMF colonization in high P soil conditions (Gabriel-Neumann *et al*, 2011).

The discovery of the absence of genes involved in the cytoplasmic type I fatty acid synthase (FAS-I) complex required for FA synthesis in the *R. irregularis* genome (Wewer *et al*, 2014), and the increased demand of lipids in mycorrhized roots (Gaude *et al*, 2012) lead to the hypothesis that the plant also supplies lipids to the fungus during symbiosis. Currently, it is shown that two Half-ABC transporters from the G-subfamily, STUNTED ARBUSCULE (MtSTR and MtSTR2), identified in *M. truncatula* may be responsible for lipid transport, although their substrate has not yet been identified (Bravo *et al*, 2017). MtSTR and MtSTR2 form heterodimers that localize at the PAM membrane and their activity is necessary for arbuscule development (Gutjahr *et al.*, 2012; Zhang *et al.*, 2010; Figure 4). The role of STR and STR2 in lipid transport is supported by the conservation of this function in other transporters from the ABCG family (Wang *et al*, 2011; Fabre *et al*, 2016).

Overall, the huge amount of mycorrhiza induced transporters, many of them exclusively expressed in arbusculated cells, suggests a high level of specialization in AM symbiosis, probably derived from the long process of co-evolution of host plants and AMF.

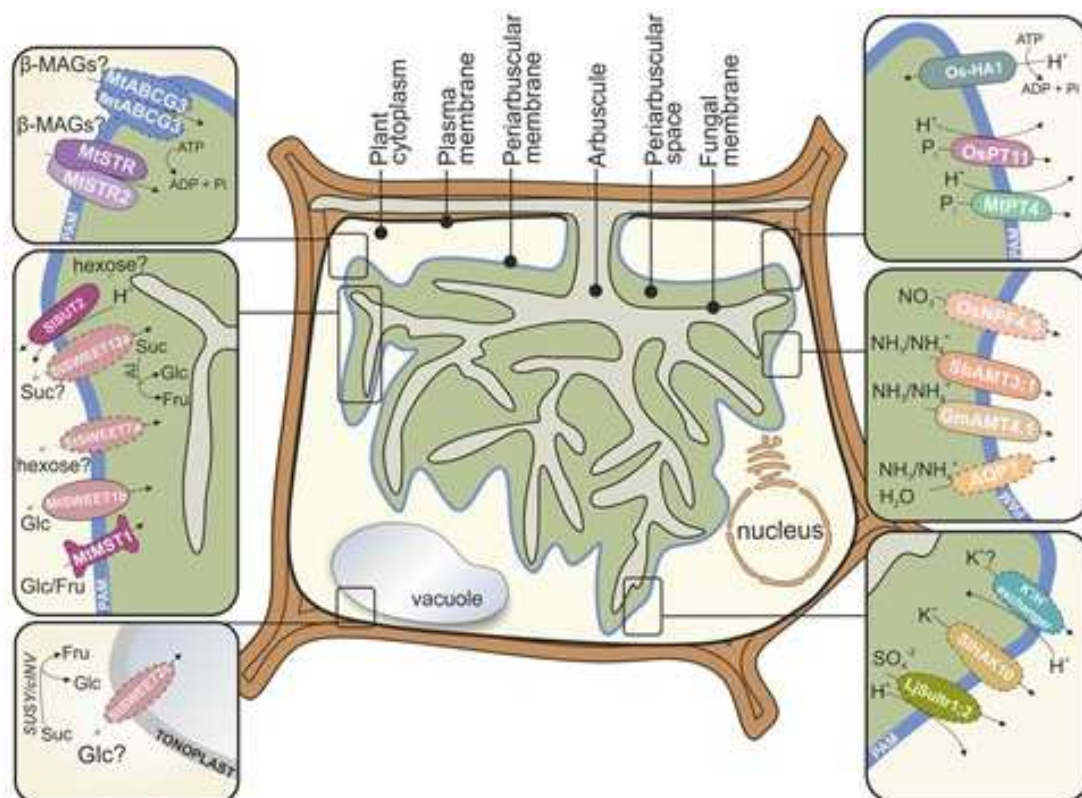


Figure 4: Transporters present at the PAM. The PAM is enriched in nutrient transporters, especially phosphate transporters, sugar transporters, lipid transporters and nitrogen transporters. (Banasiak *et al*, 2021)

3. Plant defenses activation during mycorrhization

3.1. Different layers of defense responses

Plants are sessile organisms that are confronted with many different microbes. As a result, plants have developed a sophisticated and inducible immune system consisting of different layers of defense responses. The first layer depends on **constitutive defense responses**, consisting out of plant elements that are constitutively present such as the cell walls, waxy epidermal cuticles or bark (Van Zandt, 2007). These defenses are unspecific, prevent plant infection and confers strength and rigidity to the plant (Freeman & Beattie, 2008). The second layer of defense is called the **pattern-triggered immunity (PTI)** or innate immunity. During their attack, plant pathogens cause damage to the host plant cell wall releasing oligosaccharides (damage-associated molecular patterns, DAMPs). Additionally, pathogens carry molecules called microbe-associate molecular patterns (MAMPs) such as chitin or flagellin, that are conserved parts of molecules not existing in plants. MAMPs and DAMPs are detected by plant cell membrane receptors, PATTERN RECOGNITION RECEPTORS (PRRs), which activate a signaling cascade resulting in PTI (Boller & Felix, 2009). During PTI, antimicrobial molecules, such as reactive oxygen species, phytoalexins, phospholipases or phenylpropanoids accumulate in the pathogen penetration zone. Besides, the plant defense hormones, salicylic acid (SA) and jasmonic acids (JA), are increased to subsequently stimulate defense signaling (Bari & Jones, 2009; Wu & Zhou, 2013; Boller & Felix, 2009). Pathogens can circumvent this PTI by releasing effector proteins which interact with plant macromolecules shutting down the defense responses. In response to the effectors, the plant express NUCLEOTIDE-BINDING LEUCINE RICH REPEAT (NB-LRR) proteins which recognize these effectors or their action and activate plant **effector triggered immunity (ETI)** also known as gene-for-gene resistance (Boller & Felix, 2009). Next, co-evolution between the pathogen and its host plant results in the development of new strategies of the pathogen to invade the host plant and evade the immune system, while the plant simultaneously finetunes its defense mechanisms to avoid pathogen infection (Naveed *et al*, 2020).

Filamentous fungal and oomycete pathogenic effectors are small, secreted proteins, usually smaller than 300 amino acids with multiple Cys-disulfide bonds that stabilize their tertiary structure (Lo Presti *et al*, 2015). They usually do not contain any domain or have homology with known proteins. In oomycetes, the RXLR and the CRINKLER (CRN) motifs have been related with effector translocation into the host plant cell (Liu *et al*, 2011a), but in fungi none of these motifs have been identified yet (Raffaele *et al*, 2010). These small, secreted proteins deregulate host plant immunity to favor fungal colonization (Rovenich *et al*, 2014; Lo Presti *et al*, 2015). Effectors are mainly targeted to the endoplasmic reticulum (ER)- Golgi apparatus secretion route *via* their N-terminal secretion peptide, and their expression is usually host-dependent, as they are important determinants of plant-pathogen host-specificity (Hung *et al*, 2014).

Effectors can act in the apoplast or inside the plant cells (Figure 5). Fungal apoplastic effectors mainly bind chitin or inhibit plant secreted enzymes and the secretion systems of those enzymes (Hou *et al*, 2019). Upon fungal detection, the plant secretes chitinases, which bind and degrade chitin causing PRR-mediated fungal recognition and hyphal lysis (Rovenich *et al*, 2014). In response, phytopathogenic fungi secrete chitin-binding effector proteins, which compete with

chitinases for binding chitin. An example is the Secreted LysM Protein 1 (Slp1) from *Magnaporthe oryzae*, which competes with CHITIN ELICITOR BINDING PROTEIN (CEBiP) from rice to bind chitin during the rice blast disease (Mentlak *et al*, 2012). An example of an effector directly targeting plant secreted enzymes is the *Cladosporium fulvum* effector Avr2 targeting the tomato cysteine protease Rcr3 (Van Esse *et al*, 2008), whereas an example of an effector that prevents the secretion of these enzymes is the AVRblb2 effector from *Phytophthora infestans*, which inhibits the papain-like cysteine protease C14 secretion system during potato infection (Bozkurt *et al*, 2011). Fungal cytoplasmic effectors interfere with PTI signaling by interacting with host plant proteins (Figure 5). They can exert multiple functions upon binding, e.g. sequestering, marking them for degradation, impairing their interaction with other proteins, modifying their subcellular localization or tuning host plant gene expression (Rovenich *et al.*, 2014; Figure 5). Fungal effectors mimic molecules from the host plant, enabling their movement across different subcellular compartments and subvert host defenses by binding their target (Figueroa *et al*, 2021). Examples of cytoplasmic effectors are the BcCrh1 effector from the necrotrophic fungus *Botrytis cinerea*, which causes plant cell death during strawberry infection (Bi *et al*, 2021), and HaRXL44, a nuclear-localized effector from *Hyaloperonospora arabidopsidis* that targets the Mediator subunit 19a (MED19a) for proteosomal degradation during *Arabidopsis thaliana* infection, hindering the expression of multiple defense related genes (Caillaud *et al*, 2013).

Most of the plant defenses research has been done in phytopathogens due to the important economic consequences for the agricultural sector (Heil & Bostock, 2002; Yang *et al*, 2021). However, plant defenses are also activated upon contact with a huge range of commensal microbes which do not cause any disease to the plant (Teixeira *et al*, 2019).

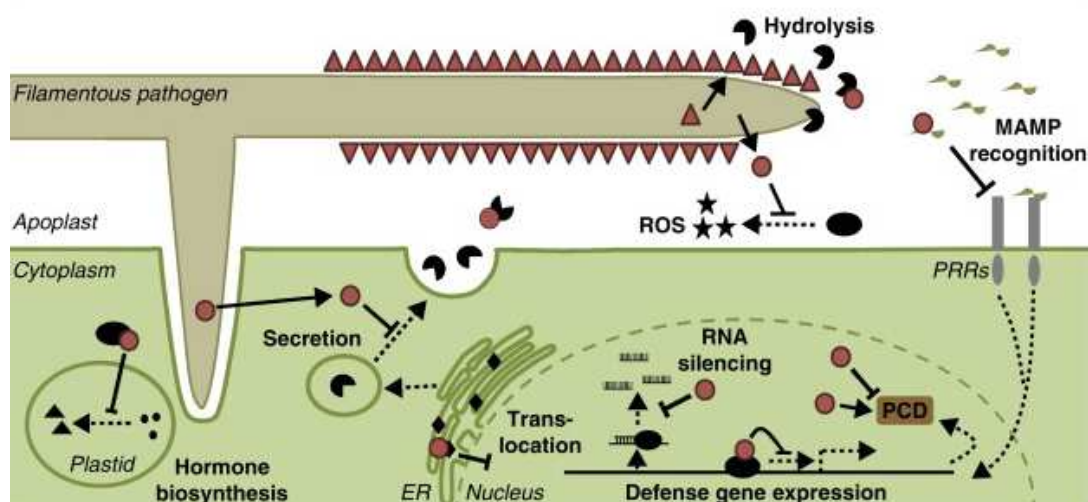


Figure 5: Different action mechanisms of fungal effectors. During filamentous fungus infection, the fungus secretes apoplastic and cytoplasmic effectors. The main functions of apoplastic effectors include sequestering hydrolases produced by the infected plant to promote fungal cell wall degradation or the oligosaccharides resulting from this degradation to avoid the recognition by plant PRR receptors. Cytoplasmic effectors are fungal proteins translocated into the infected plant cell interfering with its physiology. Cytoplasmic effectors bind different proteins from the plant modifying its turnover rate, impairing or modifying the interaction with their targets, altering their subcellular location or interfering with their expression. (Rovenich *et al*, 2014)

3.2. Defense mechanisms induced during AM symbiosis

The initial AMF recognition by the plant leads to a mild, transient and localized activation of plant defense responses (Jung *et al*, 2012). Plant defense plays an important role in the maintenance of the mutualistic status of the association by controlling fungal growth to prevent the symbiosis from becoming a pathogenic relationship (Lambais & Mehdy, 1998; García-Garrido & Ocampo, 2002).

In the initial steps of the symbiosis, chitin and glucan molecules from the AM-fungal surface as well as cellulose, pectin, xyloglucan and hydroxyproline-rich glycoproteins (HRGP) resulting from plant cell wall degradation are recognized by PRRs activating PTI (Gómez-Gómez & Boller, 2000). However, the levels of cell wall degrading enzymes secreted by AMF are low compared to many fungal pathogens, resulting in less PTI activation (Tisserant *et al*, 2013). Secondly, AMF cause an oxidative burst after penetrating the host plant root cortical cells (Salzer *et al*, 1999), which is an important secondary messenger for the activation of the hypersensitive response (Zurbriggen *et al*, 2010). Nonetheless, the accumulation of catalase and ascorbate peroxidases, responsible for H₂O₂ degradation, modulates this oxidative burst and the downstream defense responses such as SA accumulation (Blilou *et al*, 2000; Herrera Medina *et al*, 2003) or phytoalexin production (Lambais, 2000). High SA content prevents hyphopodium formation and delays mycorrhization (Song *et al*, 2011; Maharshi *et al*, 2019). Another level of defense regulation is the nutritional status of the plant. High P levels and low sucrose concentration inhibit mycorrhization by inducing defense related genes such as glucanases or the isoflavonoid medicarpin, an AMF spore germination inhibitor (Guenoune *et al*, 2001). In contrast, low P levels and sufficient photosynthates supply leads to downregulation of plant defenses and the production of coumestrol and daidzein, which stimulates hyphal growth and AMF colonization (Larose *et al*, 2002). Finally, a fine-tuned molecular interplay between symbiotic and plant defense genes regulates the mycorrhization levels. Symbiosis (SYM) genes repress defense responses, which promotes mycorrhization (Song *et al*, 2011). An example of this regulation is the *sym30* pea mutant which shows increased levels of SA in the root cortex cells, hindering the establishment of the symbiosis (Blilou *et al*, 1999).

3.3. AMF effectors

Like plant pathogenic fungi, AMF were also proposed to secrete effectors. In the past decade, a large set of effector proteins encoded in AMF genome of multiple species has been predicted (Liao *et al*, 2014; Martin *et al*, 2008; Tisserant *et al*, 2013; Lin *et al*, 2014). These genes were mainly expressed during the active colonization of the host plant, which indicates that they might have an important role during mycorrhization (Martin *et al*, 2008; Plett & Martin, 2015). Additionally, a small set of the predicted effectors appear to be common between different AMF species and host plants indicating that these proteins are probably essential for symbiosis establishment (Kamel *et al*, 2017). Nevertheless, most of them are specific from a single AMF species and their expression varies depending on the host plant, linking AMF effectors with host plant specificity and indicative for co-evolution process between both organisms (Prasad Singh *et al*, 2019; Zhong *et al*, 2016). Thus, the AMF secretome is influenced by the phylogenetic

evolutionary history, the fungal lifestyle, the environmental conditions, and the host plant (Lanfranco *et al*, 2018).

Currently, the genome of only seven AMF species have been sequenced, four of them from the genus *Rhizophagus*, and the functions of most of the predicted effectors remain unknown. Although, the characterization of those proteins might help to untangle remaining questions about AM symbiosis establishment (Lanfranco *et al*, 2018).

3.4. *R. irregularis* effectors

For the AMF model species, *R. irregularis* strain DAOM197198, 220 effector candidates have been *in silico* predicted from the published genomes and transcriptomes (Tisserant *et al*, 2013) based on multiple criteria: the presence of a signal secretion peptide, the presence of cysteines, internal repeats, PFAM domains and nuclear localization signals (NLS) (Sędziewska Toro & Brachmann, 2016; Kamel *et al*, 2017; Zeng *et al*, 2018). However, to date, only five effectors (SP7, SIS1, RiCRN1, RiSLM and RiNLE1) have been functionally characterized during symbiosis with the legume *M. truncatula* and only for two of them, a plant host interactor protein has been identified (Zeng *et al*, 2020; Wang *et al*, 2021; Tsuzuki *et al*, 2016; Klop Holz *et al*, 2011; Voß *et al*, 2018). Therefore, still a lot of research is necessary to untangle the role of effectors in AM establishment.

SECRETED PROTEIN 7 (SP7) was the first AMF effector described during symbiosis with *M. truncatula* (Klop Holz *et al*, 2011). SP7 is secreted at the early stages of AM symbiosis into the host plant cytoplasm and is translocated to the plant nucleus. In the nucleus, SP7 interacts with ETHYLENE RESPONSE FACTOR (ERF) 19 suppressing its function in ethylene signaling that is involved in plant defenses (Klop Holz *et al*, 2011). SP7 was shown to be expressed both in intra- and extraradical mycelium (Kamel *et al*, 2017), indicating an additional role beside the suppression of plant immunity. A hypothesis is that SP7 is cleaved by the protease KEX2 into small peptides which have a still unknown activity, either in the plant or the fungus (Kamel *et al*, 2017).

A second effector reported for *R. irregularis*, is the SL-INDUCED PUTATIVE SECRETED PROTEIN (SIS1). SIS1 is induced upon SL treatment during hyphal elongation in the pre-symbiotic stages of mycorrhization. Host-induced gene silencing (HIGS) of SIS1 in plants showed reduced levels of colonization and stunted arbuscules indicating that SIS1 contributes to the establishment of symbiosis in arbuscule formation (Tsuzuki *et al*, 2016).

RiCRN1 is a CRN-like effector secreted by *R. irregularis* during arbuscule formation. Although CRN proteins have been mainly characterized in pathogenic oomycetes, where they have roles in plant cell death (Liu *et al*, 2011a), RiCRN1 is not involved in cell death processes during symbiosis. RiCRN1 accumulates in plant cell nuclear bodies during symbiosis in parallel with MtPT4. Silencing of RiCRN1 in HIGS-RiCRN1 hairy root constructs hampered symbiosis in *M. truncatula* and its ectopic expression caused a reduction in arbuscule size and lower expression levels of MtPT4, suggesting a role in arbuscule development (Voß *et al*, 2018).

A recently characterized AMF effector is SECRETED LYSIN MOTIF (RiSLM). RiSLM is one of the highest expressed effector proteins in intraradical mycelium during symbiosis with *M. truncatula*. RiSLM binds *in vitro* chitin-oligosaccharides and protects fungal cell walls from chitinases

degradation. In planta, RiSLM interferes with the chitin-triggered immune responses preventing the oxidative burst and plant defense gene expression. HIGS-RiSLM *M. truncatula* hairy roots showed reduced levels of fungal colonization (Zeng *et al*, 2020).

Finally, the *R. irregularis* effector NUCLEAR LOCALISED EFFECTOR 1 (RiNLE1) is translocated to the host nucleus where it interferes in the mono-ubiquitination of the plant core nucleosome protein HISTONE 2B (H2B). Mono-ubiquitination of H2B has been related with the expression of defense genes. Hence, RiNLE1 might suppress defense-related gene expression by which it enhances AMF colonization levels (Wang *et al*, 2021).

In conclusion, the established studies have demonstrated the relevance of these effectors during AM. However, not much is yet known about the AMF effectors and their action mechanisms during symbiosis. In this project, we focus on the characterization of the *R. irregularis* effector RiSP749 and the role of its interaction with two plant proteins in mycorrhization in two host plants, tomato and *M. truncatula*.

Part 2: Aims of the Research Project

Climate change and overpopulation are threatening food production (FAO, 2020). In order to achieve the required food production rates without negatively impact the environment, sustainable and eco-friendly agricultural improvements are necessary (Geng *et al*, 2019). Biofertilizers appear as promising substitutes for the current pollutant chemical fertilizers (Ye *et al*, 2020). Arbuscular Mycorrhizal Fungi (AMF) are natural biofertilizers that establish symbiotic interactions with 80% of the land plants providing mineral nutrients, mainly P, to the host plant (Chen *et al*, 2018). In symbiotic interactions, effectors have revealed to be essential for overcoming the plant defense response activated in the initial stages of mycorrhization and establishing a complete symbiosis (Okazaki *et al*, 2013). The effector secretome and the genome of the AMF model species *R. irregularis* has been recently published (Tisserant *et al*, 2013; Kamel *et al*, 2017), but to date, only five AMF effectors have been functionally characterized. Hence, a role for many of these effectors during mycorrhization is still missing.

In this thesis, we aim to characterize the mode-of-action of the *R. irregularis* effector RiSP749 during symbiosis with the important commercial vegetable tomato and the legume model species *M. truncatula*. For that purpose, we will first perform an *in silico* analysis of the RiSP749 candidate tomato interactors SIRSZ22 and SIGNAT and their closest homologs in *M. truncatula* (MtSRZ21, MtRSZ22a, MtRSZ22b, MtGNATYoaA, MtGNATa and MtGNATb) in order find information about their possible role in mycorrhization and work in parallel with both plant species. Next, we will validate the interaction between RiSP749 and the tomato interactors, as well as with their *M. truncatula* candidate homologs *in vitro* through binary Yeast Two Hybrid (Y2H) assay, and further confirm it *in planta* by means of ratiometric Bimolecular Fluorescence Complementation (rBiFC). In order to evaluate expression of RiSP749 and its interactors during different stages of mycorrhization, we will grow *M. truncatula* wild-type (WT) plants mycorrhized with *R. irregularis* and harvest them at 2, 4 and 6 weeks post inoculation (wpi). To study the effects of RiSP749 on *M. truncatula* mycorrhization, transgenic *M. truncatula* roots overexpressing *RiSP749* (RiSP749 OE) will be generated. Colonization rates will be evaluated using the Trouvelot method (Vierheilig *et al*, 1998a). In parallel, to checked the response of *MtSRZ21*, *MtRSZ22a*, *MtRSZ22b*, *MtGNATYoaA*, *MtGNATa* and *MtGNATb* candidate interactors and other symbiosis induced genes to RiSP749 their expression levels will be measured through qRT-PCR analysis. Finally, some preliminary experiments will be done in tomato to investigate the role of SIRSZ22 and SIGNAT in AM symbiosis. On one hand, to investigate the promoter activity of *SIGNAT* and its responsiveness to AMF colonization, we will generate pSIGNAT-GUS reporter lines. On the other hand, the role of SIRSZ22 in mycorrhization will be checked by generating composite tomato plants with transgenic roots expressing a *SIRSZ22* RNAi construct that downregulates *SIRSZ22* expression. qRT-PCR analysis will be used to analyze the expression of *RiSP749* and mycorrhiza inducible genes in these lines.

Together, these experiments will provide a further understanding of the role of RiSP749 in symbiosis with tomato and *M. truncatula*, and the importance of the interaction with the tomato proteins SIGNAT and SIRSZ22 to exert that role. By this, we will increase our knowledge in effector functioning and their importance for symbiosis establishment. On the long term, this project will

provide important knowledge to improve mycorrhization of tomato in the field, and, hence, allow the use of AMF as a reliable and sustainable biofertilizer and bioprotectant in agriculture.

Part 3: Results

1. *In silico* analysis of RiSP749 and its interactors in tomato and *M. truncatula*

1.1. *R. irregularis* effector RiSP749

The predicted *R. irregularis* secretome has only been recently described (Sędzielewska Toro & Brachmann, 2016; Kamel *et al*, 2017; Zeng *et al*, 2018). Making use of these databases, a screening was done previously in the host lab to select a number of candidate effectors that fulfil the following characteristics: the presence of a predicted secretory signal peptide, a nuclear localization signal (NLS), conserved protein domains, and a non-apoplastic localization. From the resulted list of candidate putative effectors, this project focuses on the characterization of the effector RiSP749.

RiSP749 is a predicted effector from the AM fungus *R. irregularis* strain DAOM197198 (Kamel *et al*, 2017). This effector has a predicted and validated signal peptide and a NLS (Toon Leroy Master thesis, 2021, Table 1). It has a RNA recognition motif 1 (RRM_1, PFAM00076) and is 361 amino acids (aa) long. Based on a protein blast with NCBI, RiSP749 is homologous to U11/U12 small nuclear ribonucleoprotein 35 kDa protein from *R. irregularis* and *R. clarus* and does not have effector homologs with a percentage of identity higher than 50% in the genome of *R. clarus* or *G. rosea*.

Table 1: *R. irregularis* effector RiSP749 in silico analysis. Scheme of RiSP749 structure and information about the signal peptide sequence, the non-apoplastic localization, the nuclear localization signal, the length, conserved domains and homologous proteins in the genome of *R. irregularis*.



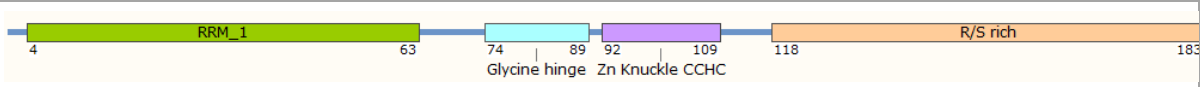
Signal peptide	MWYAKNFLQLILIIQEMWYA
Non-Apoplastic	0,83 probability
Nuclear localization signal (NLS)	RKESGQLRFGARDRPFKR
Length	361 aa
Conserved domain	RNA recognition motif 1 (RRM1) [PF00076]
Homology	U11/U12 small nuclear ribonucleoprotein 35 kDa protein

1.2. Candidate RiSP749 interactors in tomato: SIRSZ22 and SIGNAT

In a previous master thesis (Toon Leroy), a yeast two hybrid (Y2H) screening (Erfelink *et al*, 2018) was performed in order to find candidate tomato interactor proteins of RiSP749. From the possible interactors, two have been selected for further study, encoded by the genes LOC101266050 and LOC101247959, and which will be called SIRSZ22 and SIGNAT, respectively, throughout the thesis from now on. SIRSZ22 is an alternative splicing factor of 183 aa from the arginine/serine (RS)-rich domain family. This family is characterised by the presence of a RS-rich

domain, a Zn-finger motif of the CCHC-type, and a N-terminal RRM (Table 2). A protein blast using NCBI was performed to check the number homologs of SIRSZ22 described in tomato, *M. truncatula* and *A. thaliana* (Figure 6). In tomato, only LOC101248804, with an identity percentage of 94,39% (e-value 1×10^{-38}), encodes for another alternative splicing factor from RSZ22 family. In *M. truncatula*, three candidate homologs were found, LOC112417497 (MtRSZ21) from the RSZ21 family, which has a 59% aa identity to SIRSZ22 (e-value 4×10^{-37}), and LOC112418704 (MtRSZ22a) and LOC112419871 (MtRSZ22b) from the RSZ22 family, which have a 59% (e-value 2×10^{-33}) and a 58% (e-value 3×10^{-31}) aa identity with SIRSZ22, respectively. In *A. thaliana*, this family has three members and one unclassified protein, and another three homologs from the closely related family RSZ21 (Figure 6). *A. thaliana* alternative splicing factors AtRSZ22 and AtRSZ21 bind to the U1 small nuclear riboprotein particle (snRNP) 70K protein recruiting the U1 snRNP, necessary for the normal and alternative splicing of the messenger RNA (mRNA) (Golovkin & Reddy, 1998). AtRSZ22 and AtRSZ21 mostly differ in their expression pattern, AtRSZ22 is more highly expressed in cell suspensions while AtRSZ21 is more expressed in roots (Golovkin & Reddy, 1998).

Table 2: Tomato protein SIRSZ22 in silico analysis. The structure of the protein, the name of the gene, homologous proteins, protein length, conserved domain and interesting bibliographic information are included.

	
Gene	LOC101266050 (SIRSZ22)
Homology	Alternative splicing factor RSZ22
Length	183 aa
Conserved domains	<ul style="list-style-type: none"> • Arginine/serine (RS)-rich domain • Zn-finger motif of the CCHC-type • N-terminal RRM • Glycine Hinge
Background knowledge	<i>A. thaliana</i> RSZ22 interacts with U1 snRNA 70K

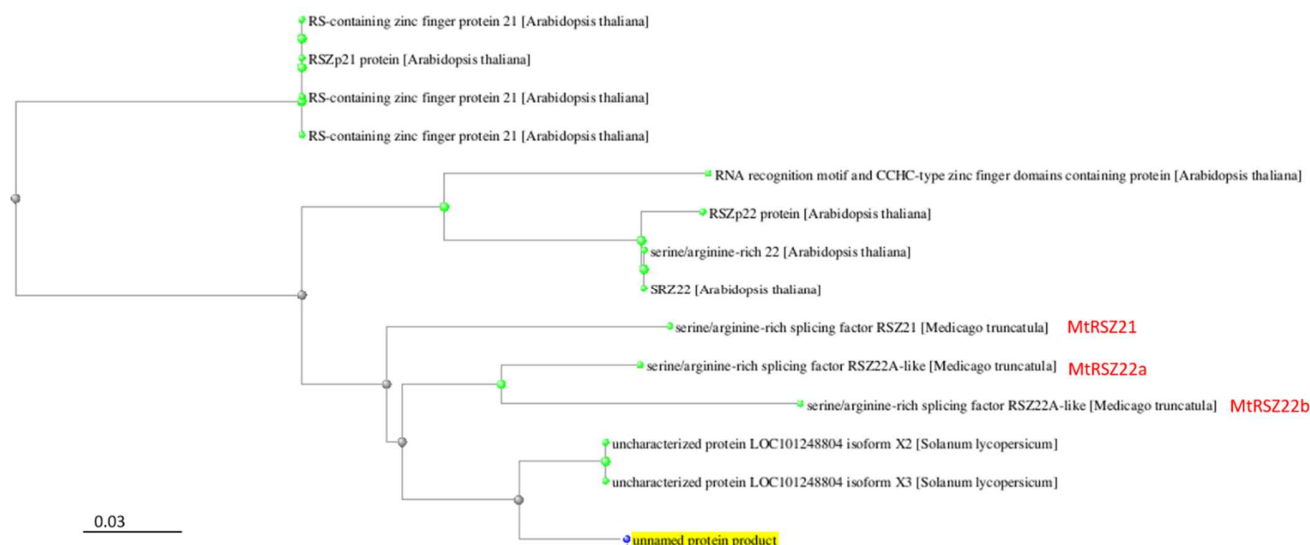


Figure 6: Phylogenetic tree of the alternative splicing factor RSZ proteins from *S. lycopersicum* (tomato), *M. truncatula* and *A. thaliana*. Tomato genome encodes for another uncharacterized alternative splicing factor RSZ22 with two transcriptional variants. In *M. truncatula* we found three possible homologs, while in *A. thaliana* eight homologs were found, three RSZ22, four RSZ21 and one that is not classified. The phylogenetic distance appears to be smaller between *M. truncatula* and tomato compared with *A. thaliana*. In red, the names used for the *M. truncatula* homologs that were studied as candidate interactors of RiSP749.

SIGNAT is an N-acetyltransferase (NAT) p20-like protein of 205 aa (Table 3). NAT proteins is a superfamily of proteins present in all living organisms, which uses acetyl-Coenzyme A (CoA) to transfer acyl groups to multiple substrates (Ud-Din et al., 2016; Table 3). They are involved in a wide range of functions including stress responses (Armbruster et al, 2020) and transcriptional regulation (Song et al, 2003). Interestingly, two NAT complexes (NataA and NatB) antagonistically regulate the turnover of Nod-like receptors in *A. thaliana* (Xu et al, 2015). We performed a protein blast using NCBI to find the SIGNAT homologs in tomato, *M. truncatula* and *A. thaliana* and a phylogenetic tree was built with the proteins found (Figure 7). NAT is a large family of proteins, hence many more homologs were found compared with SIRSZ22, although the phylogenetic distance between plant species was also higher. Tomato counts seven uncharacterized homologous proteins to SIGNAT. In *M. truncatula*, we found 17 candidate homologs with LOC25490856 (80% identity and 7×10^{-54} e-value; MtGNATYoA), LOC11420857 (80% identity and 1×10^{-54} e-value; MtGNATa), and LOC11443152 (94% identity and 3×10^{-53} e-value; MtGNATb) being the three closest homologs (Table 4). *A. thaliana* genome only encoded for four homologs.

Table 3: Tomato protein SIGNAT in silico analysis. The structure of the protein, the name of the gene, homologous proteins, protein length and conserved domain are included.

Gene	LOC101247959 (SIGNAT)

Homology	N-acetyltransferase (NAT) p20-like
Length	205 aa
Conserved domain	Domain: Acetyltransferase 3

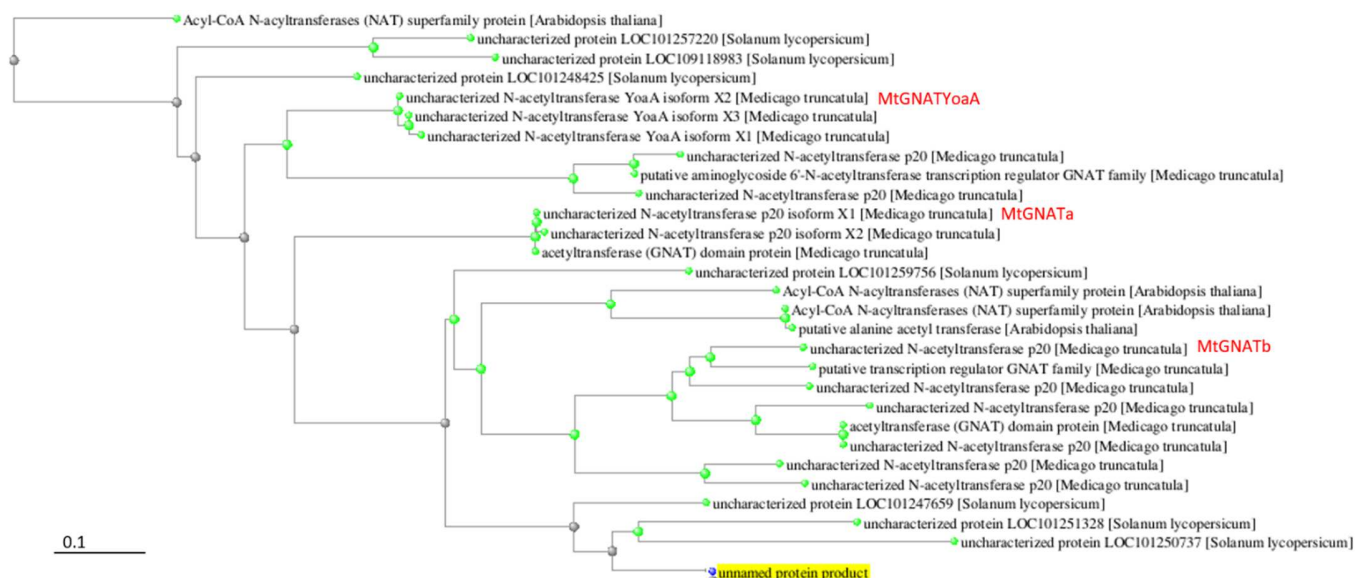


Figure 7: Phylogenetic tree of the N-acetyl transferase (NAT) proteins from *S. lycopersicum* (tomato), *M. truncatula* and *A. thaliana*. Eight uncharacterized NAT proteins were found in tomato, in *M. truncatula* we found 17 possible homologs, while in *Arabidopsis* only four homologs were found. A clustering by species was not seen in this phylogenetic tree. In red, the names used for the *M. truncatula* homologs that were studied as candidate interactors of RiSP749.

1.3. Candidate homologous interactors of RiSP749 in *M. truncatula*

Due to the low mycorrhization rate and the strong silencing capacity of tomato of ectopically expressed fungal effectors, we also used the legume model species *M. truncatula* for phenotyping and mycorrhization experiments. Furthermore, as *M. truncatula* is a widely used model species for AMF research, large databases on expression studies exist and can be used to exploit (Benedito et al., 2008; Table 4 and S1). Therefore, we selected MtSIRSZ21, MtRSZ22a and MtRSZ22b (Figure 6), the closest homologs of SIRSZ22, and MtGNATYoaA, MtGNATa and MtGNATb (Figure 7), the closest homologs of SIGNAT, from protein blast of the genome of *M. truncatula*. Then, by using the *M. truncatula* genomic atlas and Legume Graph-Oriented Organizer (LEGOO) (Carrère et al, 2020), we explored their expression profiles during symbiotic interactions. MtNIN, a symbiotic induced TF (Guillotín et al, 2016), induces *MtRSZ21* expression during nodulation (Liu et al, 2019b). *MtRSZ22a* expression is induced under high P soil concentrations (Grunwald et al, 2009), and is responsive to the nodulation bacteria *Sinorhizobium meliloti* (De Bang et al, 2017). *MtGNATa* is induced by MtNIN during nodulation (Liu et al, 2019b) but repressed by the LysM receptor MtNFP after inoculation with the oomycete *Aphanomyces euteiches* (Rey et al, 2016). *M. truncatula* hypermycorrhizal B9 mutant, impaired

in the detection of P, showed reduced expression of *MtGNATa* at high P concentrations compared with WT *M. truncatula* plants, while the opposite is shown at low P conditions (Truong *et al*, 2015). Mycorrhiza induced genes are more expressed in the B9 mutant, which might indicate that mycorrhiza induced genes repress *MtGNATa* (Truong *et al*, 2015). Finally, *MtGNATb* expression is induced by MYC-factors and NF-YA1 (Rey *et al*, 2016; Camps *et al*, 2015) but repressed in mycorrhizal fungi colonized roots (Luginbuehl & Oldroyd, 2017), indicating a role in the early stages of mycorrhization. No link with AMF or symbiotic interactions was found for the *M. truncatula* homologs non-mentioned.

Table 4: *M. truncatula* homologs of SIRSZ22 and SIGNAT. NCBI gene name, abbreviation, identity and homology with the tomato candidate homologs and the results of the LEGOO exploration of possible AMF-related expression patterns are indicated in the table.

SIRSZ22 <i>M. truncatula</i> homologs				
Gene	Abbreviation	Identity	E-value	Expression profile
LOC112417497	MtRSZ21	59%	4×10^{-37}	Induced by MtNIN
LOC112418704	MtRSZ22a	59%	2×10^{-33}	<ul style="list-style-type: none"> • Upregulated in high Pi soil concentrations • Nodulation responsive
LOC112419871	MtRSZ22b	58%	3×10^{-31}	NA
SIGNAT <i>M. truncatula</i> homologs				
Gene	Abbreviation	Identity	E-value	Expression profile
LOC25490856	MtGNATa	80%	9×10^{-54}	<ul style="list-style-type: none"> • Repressed by MtNFP and in <i>M. truncatula</i> B9 hypermycorrhized mutants • Induced by MtNIN
LOC11420857	MtGNATYoaA	80%	1×10^{-54}	NA
LOC11443152	MtGNATb	94%	3×10^{-53}	<ul style="list-style-type: none"> • Repressed by AMF • Induced by MtNF-YA1 and MYC factors

2. Validating the interaction between RiSP749 and two candidate interactors SIRSZ22 and SIGNAT in tomato, and their homologs in *M. truncatula*

Microbial effectors exert their function during host plant colonization by binding host plant proteins, nucleic acids or other macromolecules (Ahmed *et al*, 2018). Therefore, it is important to find the host plant interactor macromolecule to further characterize the effector function. RiSP749 has been found to interact with two tomato proteins SIRSZ22 and SIGNAT in a previous performed Y2H-seq screening (Toon Leroy master thesis). Here, we first determined the subcellular localization of all proteins, and performed two complementary protein-protein interaction experiments to validate the interaction of RiSP749 with both proteins.

2.1. Nuclear colocalization of RiSP749 and the candidate tomato interactor proteins SIRSZ22 and SIGNAT

To be able to interact, both proteins should colocalize in the same subcellular region. In Toon Leroy master thesis, a preliminary experiment was performed proving the nuclear localization of RiSP749, SIRSZ22 and SIGNAT. Here, we performed additional experiments to determine the colocalization of both tomato proteins with the effector RiSP749 in plant nucleus by transient expression in *Nicotiana benthamiana* (tobacco) leaves.

Constructs encoding N-terminal GFP tagged RiSP749, and eCFP-fused SIRSZ22 and SIGNAT proteins were created and transiently expressed in tobacco leaves separately (Supplementary Figure S1), and in combinations, i.e. RiSP749 with SIRSZ22 or RiSP749 with SIGNAT (Figure 8). Then, the location of the fluorescent signal was checked with confocal imaging. RiSP749 and SIRSZ22 localized in the nucleus, while SIGNAT was located both in the cytoplasm and the nucleus (Figure 8). RiSP749 colocalize with both proteins in the nucleus, but not in the nucleolus (Figure 8).

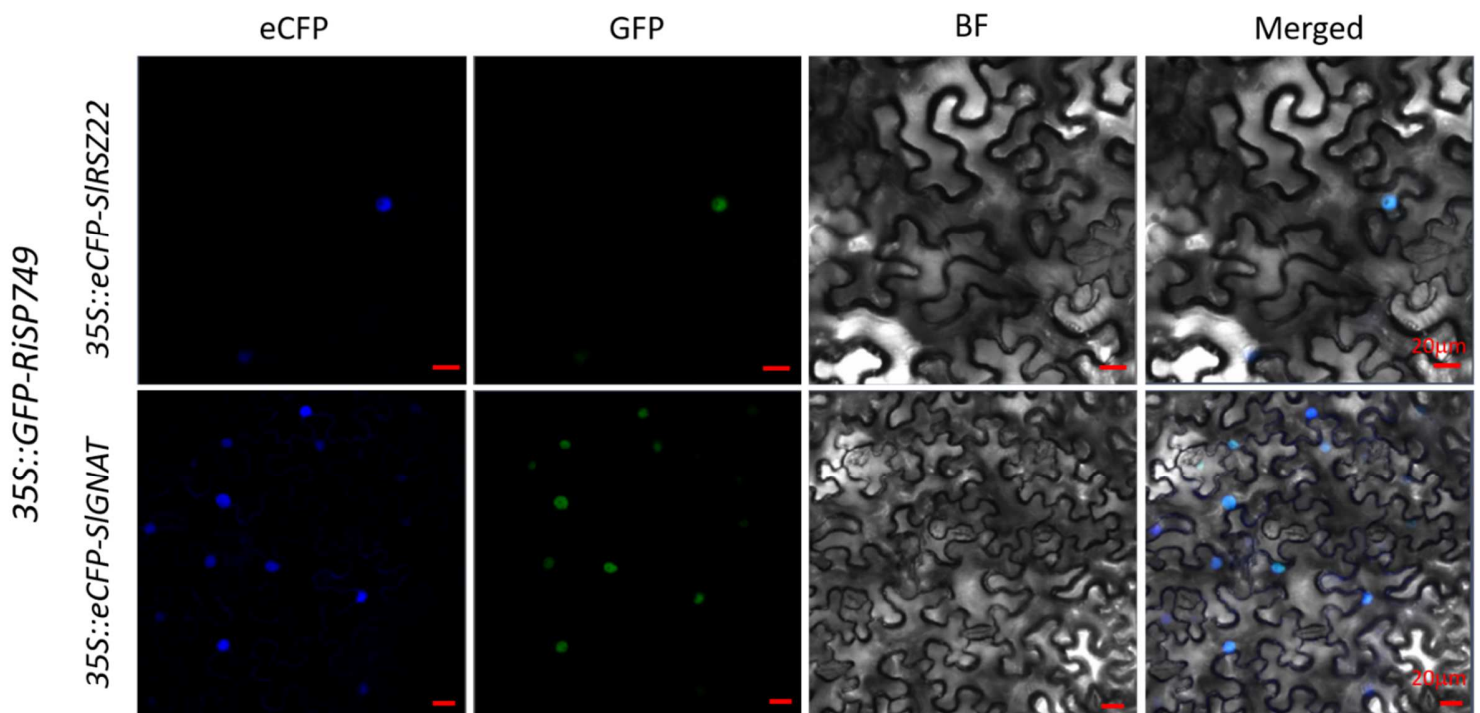


Figure 8: Co-localization of RiSP749 and tomato interactors SIRSZ22 and SIGNAT in the nucleus. RiSP749 was fused to GFP at the N-terminus, while the tomato interactors SIRSZ22 and SIGNAT were N-terminally fused to eCFP. SIRSZ22 and RiSP749 were exclusively located in the nucleus, while SIGNAT was located both in the nucleus and in cytoplasm (see also Supplementary Figure S1). The light blue signal in the Merged column indicates colocalization.

2.2. Binary Y2H validated the interaction between RiSP749 and the tomato proteins SIRSZ22 and SIGNAT

Once colocalization was confirmed, we first performed a binary Y2H to validate the interaction between RiSP749 and the tomato proteins SIRSZ22 and SIGNAT that were found in the Y2H-seq screening.

The RiSP749 coding sequence was N-terminal fused with the transcription factor (TF) GAL4 binding domain (BD) in the bait vector *pGBKT7*, while the candidate interactors SIRSZ22 and SIGNAT were fused to the GAL4 activation domain (AD) in the prey vector *pGADT7*. Both constructs were introduced in the *Saccharomyces cerevisiae* strain PJ69-4 which is auxotroph for leucine (L), threonine (T) and histidine (H). The HIS3 gene, involved in the biosynthesis of H, in this strain is driven by the upstream activation sequence (UAS) that is recognized by the GAL4 TF. Thus, if the bait and the prey proteins interact, the BD and the AD of GAL4 come together inducing the expression of HIS3 and allowing the transformed yeast colonies to grow in a media without H. As negative controls, *S. cerevisiae* strains were transformed with the effector and the empty prey vector and with the candidate tomato interactors and the empty bait vector. For all controls, growth was present in SD-T, SD-L and SD-LT media but not in SD-LTH media in any of the dilutions (1, 10⁻¹, 10⁻², 10⁻³) (Supplementary Figure S2), indicating that the transformation was successful, but that in absence of an interaction, GAL4 is not reconstructed and *HIS3* is not expressed. Figure 9 shows that both BD-RiSP749 with AD-SIRSZ22, and BD-RiSP749 with AD-SIGNAT co-transformed colonies are able to grow in SD-LTH media with increasing concentrations of 3-Amino-1,2,4-Triazol (3-AT), an inhibitor of the *HIS3* gene, indicating that RiSP749 interacts with both candidate tomato interactors. Interestingly, the interaction of RiSP749 with SIRSZ22 appears to be stronger than with SIGNAT as evidenced by the growth at higher concentrations of 3-AT, i.e. 10mM compared with 2,5mM, in every dilution.

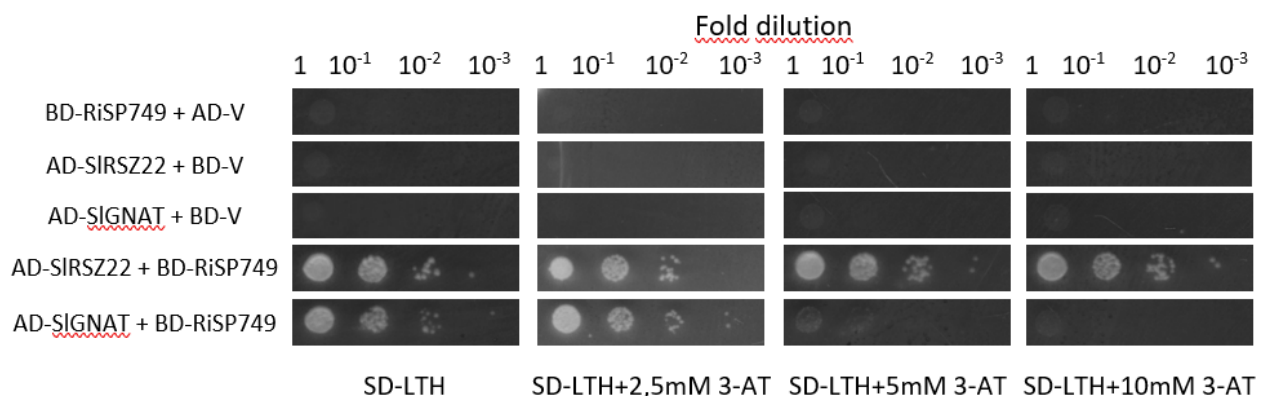


Figure 9: Binary Y2H-assay of RiSP749 and the candidate tomato interactors SIRSZ22 and SIGNAT. Transformation of *S. cerevisiae* strain PJ69-4 with the *R. irregularis* effector RiSP749 fused to the binding domain (BD) of the TF GAL4, and the tomato proteins SIRSZ22 and SIGNAT fused to the activation domain (AD) of the TF GAL4 resulted in growth in the screening media SD-LTH. Four serial dilutions of the culture were done and increasing concentrations of 3-Amino-1,2,4-Triazol (3-AT) (0, 2.5, 5 and 10mM) were added to the medium to test the strength of the interaction. As controls, *S. cerevisiae* strain PJ69-4 was co-transformed with BD- RiSP749 and the empty *pGADT7* vector (AD-V) or with the interactors SIRSZ22 and SIGNAT and the empty *pGBKT7* vector (BD-V). Controls do not grow in SD-LTH media, evidencing that there is no autoactivation of GAL4 and no leaking expression of *HIS3*, but they grew in SD-L, SD-T and SD-LT probing that transformation was successful (see Supplementary Figure S2).

2.3. Ratiometric Bimolecular Fluorescence Complementation (rBiFC)

The interaction between RiSP749 and the two tomato proteins SIRSZ22 and SIGNAT was confirmed *in vitro* using Y2H assay. Next, the interaction was validated *in planta* by rBiFC. In this technique both interacting proteins are introduced into the same vector pBiFCt-2in1-NN (RiSP749/SIRSZ22, and RiSP749/SIGNAT), ensuring their expression in an equal gene dosage, and each protein was N-terminally fused to a part of the yellow fluorescent protein (cYFP and nYFP; Grefen & Blatt, 2012). Additionally, the vector encodes the red fluorescent protein (RFP) under the same promoter as a marker for transformation and expression, allowing to perform a ratiometric quantification of the interaction by comparing the yellow fluorescent signal of a reassembled YFP with the free RFP level (Figure 11). The interaction between the *A. thaliana* proteins MORE AXILLARY GROWTH 2 (AtMAX2) and S-PHASE KINASE-ASSOCIATED PROTEIN 1 (AtSKP1) was used as a positive control (Figure 10, 11). AtMAX2 is a F-box protein involved in SL signalling and AtSKP1 is part of the E3 ubiquitin ligase complex (Stirnberg *et al*, 2007). Their interaction is strong, hence, a ratio above 1 between yellow and red fluorescence signal is expected (Figure 11). The interaction between the *R. irregularis* effector RiSP190 and an unknown tomato protein (Solyc07g045450) found in a Y2H-screening performed with RiSP190 but which interaction could not be later confirmed by binary Y2H, was used as negative control for the experiment (Figure 10, 11). In this case, no yellow signal is expected, the ratio yellow/red fluorescence signal should be close to 0 (Figure 11).

pBiFCt-2in1-NN (SIRSZ22/RiSP749) and *pBiFCt-2in1-NN (SIGNAT/RiSP749)* vectors were transiently expressed in tobacco leaves and their expression was evaluated by means of confocal microscopy. *pBiFCt-2in1-NN (SIRSZ22/RiSP749)* showed a strong YFP signal in the nucleus of the infiltrated tobacco leaves, from which the YFP/RFP signal was significantly higher than the negative control (p-value $9,37 \cdot 10^{-7}$; Figure 10 and 11). RiSP749 and SIRSZ22 interact in the nucleus of the plant cells, but the signal was not present in the nucleolus (Figure 11). Interestingly, in some nuclei, we saw a heterogeneous distribution of the fluorescent signal (Figure 11). *pBiFCt-2in1-NN (SIGNAT/RiSP749)* did not show yellow signal (Figure 10), and no-significative difference was found in the YFP/RFP fluorescence ratio compared with the negative control (Figure 11), indicating that RiSP749 and SIGNAT do not interact *in planta*.

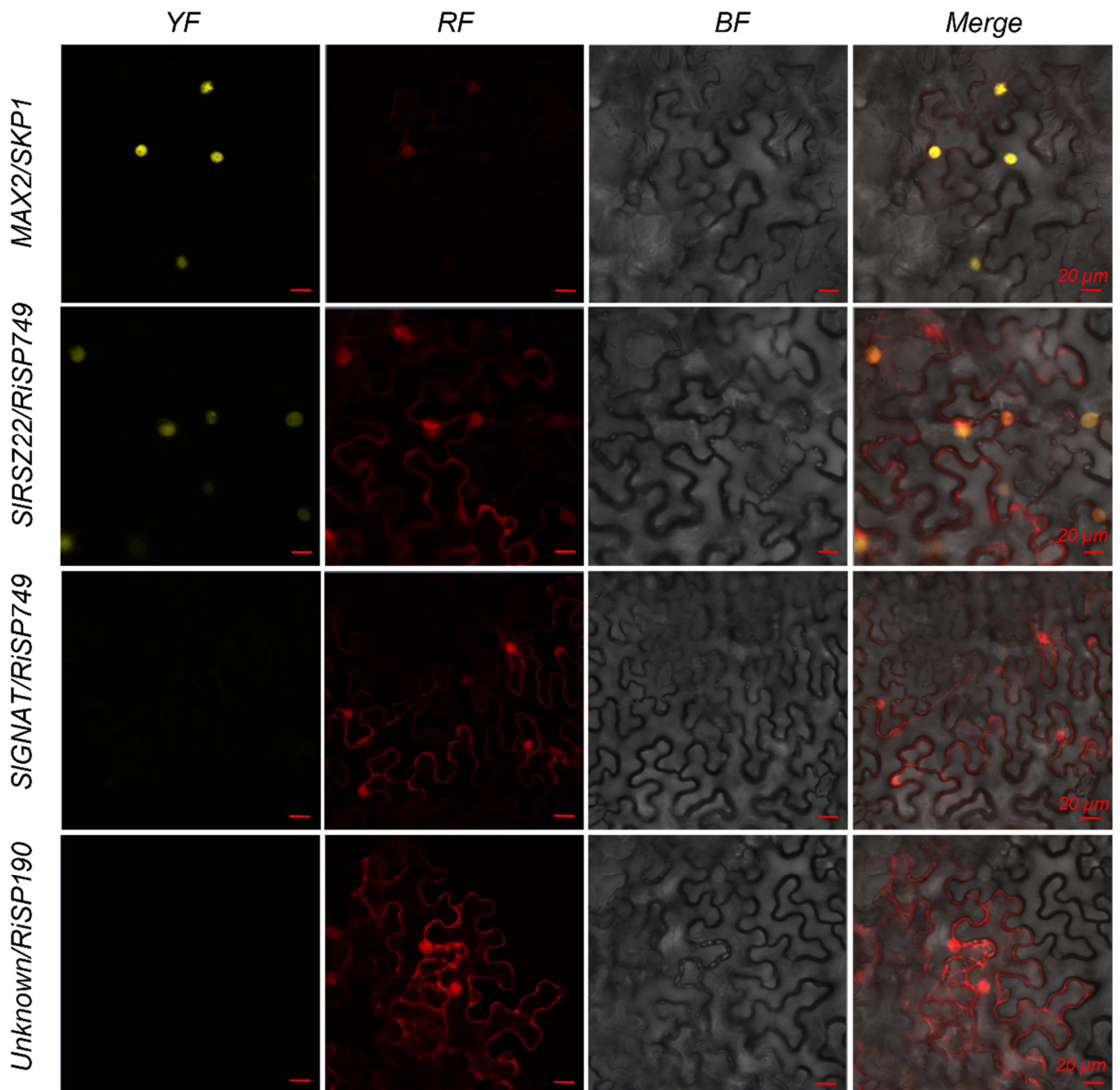


Figure 10: In planta analysis of the interaction between RiSP749 and SIRSZ22, and between RiSP749 and SIGNAT. On one hand, RiSP749 and SIRSZ22 and, on the other hand, RiSP749 and SIGNAT were introduced into a different pBiFct-2in1-NN vector. They were fused at the N-terminus to a part of YFP (n-YFP and c-YFP) for ratiometric bimolecular fluorescence complementation (rBiFC) analysis. AtMAX2/AtSKP1 was used as positive control, while Unknown/RiSP190 was used as negative control. The presence of YFP signal indicates that both proteins interact, while the RFP signal is a marker of the successful expression of the vector and allows the quantification of the interaction. The first column is the YFP channel, the second column is the RFP channel, the third column is the bright field (BF) and the last column is the merge of the previous three.

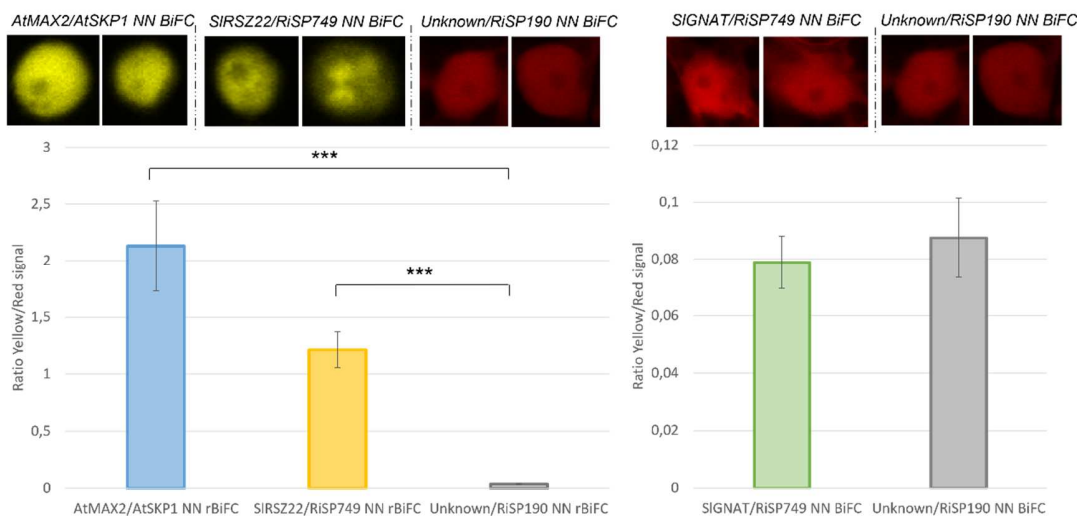


Figure 11: Quantification of the interaction between RiSP749 and SIRSZ22, and RiSP749 and SIGNAT using rBiFC. The ratio of the yellow/red fluorescence signal was quantified for the SIRSZ22/RiSP749, the SIGNAT/RiSP749 and the positive control, AtMAX2/AtSKP1, and compared with the ratio of the negative control, Unknown/RiSP190. A significant difference is seen between the positive control (p -value $3,81 \times 10^{-5}$, Student's t-test) and the RiSP749-SIRSZ22 (p -value $9,37 \times 10^{-7}$, Student's t-test) ratio compared with the negative control. Detailed illustrations of the interaction in the nucleus are displayed above the graph for each construct. *** P -value < 0.001 compared with the negative control, Student's t-test

Altogether, these results confirmed that both RiSP749 and the tomato proteins SIRSZ22 and SIGNAT localize in the nucleus of the host plant. Moreover, we proved that RiSP749 interacts with the tomato protein SIRSZ22. In contrast, although RiSP749 and SIGNAT colocalize in the nucleus of the host plant, their interaction is unlikely as, although they interact *in vitro* by means of a binary Y2H assay, rBiFC results proved that this interaction does not take place *in planta*. However, additional independent experiments should be performed to further confirm this result.

2.4. Binary Y2H assays validate the interaction between RiSP749 and the *M. truncatula* homologs of SIRSZ22 and SIGNAT

Considering that *M. truncatula* was used for the RiSP749 phenotyping and mycorrhization experiments, we checked whether the interaction with RiSP749 is conserved for the *M. truncatula* homologs of SIRSZ22 and SIGNAT. For that purpose, a binary Y2H assay was performed.

As controls, *S. cerevisiae* strain PJ69-4 was co-transformed with RiSP749 fused to the BD of GAL4 TF and the *pGADT7* empty vector, and *M. truncatula* candidate orthologs of SIRSZ22 (MtRSZ21, MtRSZ22a, and MtRSZ22b) and MtGNATb fused to the AD of GAL4 were co-transformed with the *pGBKT7* empty vector (Unfortunately, MtGNATyOaA and MtGNATa could not be cloned during this master thesis). These colonies grew in SD-L, SD-T and SD-LT at every dilution (1 , 10^{-1} , 10^{-2} , 10^{-3}) but they could not grow in the selective media SD-LTH, indicating that there is no autoactivation and leaking expression of *HIS3* (Supplementary Figure S3).

Then, BD-RiSP749 was co-transformed with each of the *M. truncatula* candidate orthologs of SIRSZ22 (MtRSZ21, MtRSZ22a and MtRSZ22b) and MtGNATb fused to AD. RiSP749-MtRSZ21, RiSP749-MtRSZ22a and RiSP749-MtRSZ22b grew in SD-LTH media even when supplemented with 10mM of 3-AT at 10^{-2} dilution, indicating a strong interaction (Figure 12). However, RiSP749-MtGNATb co-transformed yeast colonies did not show growth in SD-LTH media (Figure 12), meaning that MtGNATb does not interact with RiSP749 *in vitro*.

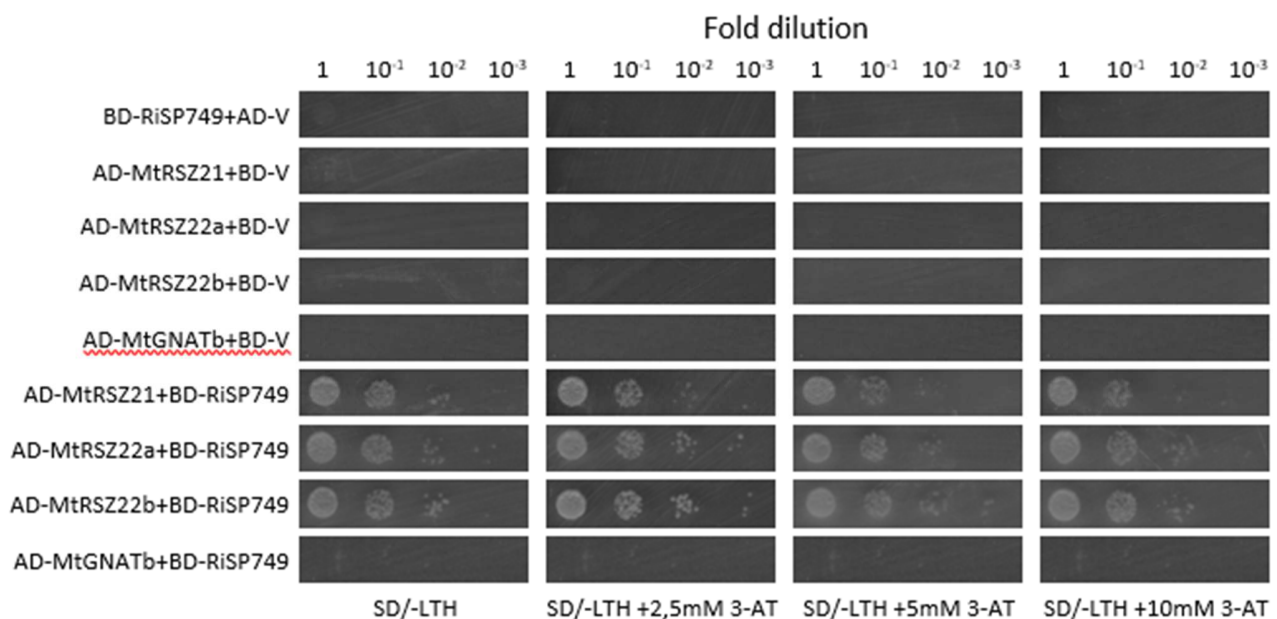


Figure 12: Binary Y2H assay of RiSP749 and the *M. truncatula* candidate orthologs of SIRSZ22 and SIGNAT. Transformation of *S. cerevisiae* strain PJ69-4 with the *R. irregularis* effector RiSP749 fused to the binding domain (BD) of the TF GAL4 and the *M. truncatula* proteins SIRSZ21, SIRSZ22a, SIRSZ22b and SIGNATb fused to the activation domain (AD) of the TF GAL4 resulted in growth in the screening media SD-LTH, except for the RiSP749-SIGNATb combination. Four serial dilutions of the culture were done and increasing concentrations of 3-Amino-1,2,4-Triazol (3-AT; 0 mM, 2.5 mM, 5 mM and 10 mM) were added to the medium to test the strength of the interaction. As controls, *S. cerevisiae* strain PJ69-4 was co-transformed with BD-RiSP749 and the empty pGADT7 vector (AD-V) or with the interactors MtRSZ21, MtRSZ22a, MtRSZ22b and MtGNATb and the empty pGBKT7 vector (BD-V). Controls do not grow in SD-LTH media but they did in SD-L, SD-T and SD-LT (See Supplementary Figure S3), evidencing that there is no leaking expression of HIS3.

Considering that all three *M. truncatula* homologs of SIRSZ22 interact with RiSP749 in the binary Y2H assay, we hypothesized that the binding motif of RiSP749 is conserved among all of them. Hence, we performed a multi sequence alignment using Clustal Omega (EBI; Sievers & Higgins, 2018) in order to identify the most probable regions involved in the interaction (Figure 13). The first 74 aa of all four proteins showed a high percentage of identity, which corresponds with the RRM_1 motif (Barta *et al*, 2010; Lopato *et al*, 1999). Moreover, a highly conserved part corresponding with the Zn Knuckle CCHC motif was observed. Both domains, RRM and CCHC motifs, are involved in the functional mechanism of this group of proteins (Lopato *et al*, 1999) and might be good candidate domains involved in RiSP749 binding. However, the ability to interact with RiSP749 does not mean that all of them are actual targets of this effector during

mycorrhization. Further analysis should be performed to assess which domain interacts with RiSP749 as well as the nature of the interaction during mycorrhization.

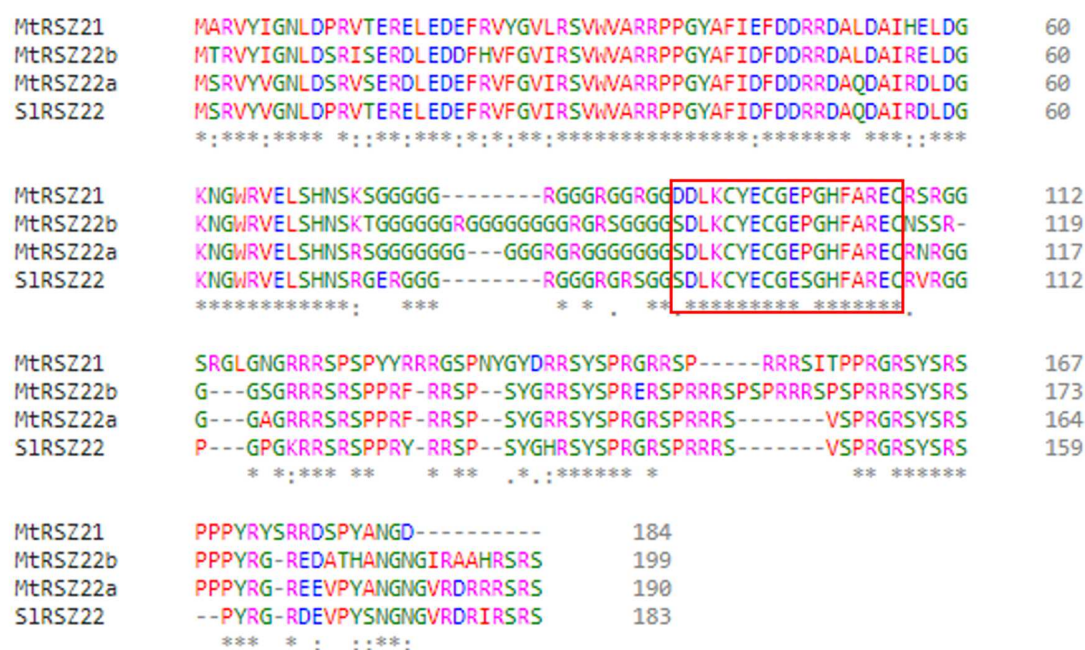


Figure 13: Multi-sequence alignment of SIRS222 and its *M. truncatula* homologs. The protein sequences of SIRS222, MtRSZ21, MtRSZ22a and MtRSZ22b were aligned using Clustal Omega algorithm from EBI in order to find conserved regions among these proteins.

Overall, these experiments demonstrated that RiSP749 interacts with both tomato and *M. truncatula* proteins of the RSZ family, probably through a conserved domain of their sequence which should be tested in the future. Moreover, we concluded that RiSP749 does not interact with MtGNATb. This result should be confirmed with additional independent experiments, and the interaction with the other two SIGNAT candidate *M. truncatula* orthologs (MtGNATYoaA and MtGNATa) should be studied as well.

3. Functional characterization of RiSP749 during AM symbiosis

To study the function of RiSP749 in AM symbiosis, we used the model species *M. truncatula* inoculated with *R. irregularis* spores. Mycorrhization intensity and the AM-related expression of RiSP749 and its *M. truncatula* interactor orthologs were evaluated at three time points, 2, 4 and 6 wpi, in WT *M. truncatula* plants. In addition, the effect of RiSP749 on mycorrhization was investigated by generating composite plants with transgenic roots that overexpressed RiSP749.

3.1. Time series evaluation of mycorrhization in WT *M. truncatula* plants

WT plants of *M. truncatula* cultivar Jemalong A17 were germinated and inoculated with *R. irregularis* spores, and roots were harvested at 2, 4 and 6 wpi. As control, non-inoculated plants were grown and harvested at the same time points. Fresh root weight was measured at 4 and 6 wpi but no significant differences were observed between mock and mycorrhized plants (Supplementary Figure S4). Colonization was evaluated according to the Trouvelot method (Vierheilig *et al*, 1998a), and demonstrated a positive increase in the level of colonization (F%),

the intensity of mycorrhization (m%, M%), and the content of arbuscules (a%) over time, although not significant (Figure 14A). At early time points during symbiosis, a higher proportion of intraradical hyphae is expected as the fungus is still penetrating into the host plant and elongating intercellularly, while at later time points more arbuscules are formed (Figure 14C). This increase allowed us to establish a relation between the time point and the stages in mycorrhization. The increase in colonization was further confirmed by an increased expression of the functional symbiotic marker gene, the phosphate transporter *MtPT4*, and the fungal housekeeping gene *RiEF1 α* along time measured in the full root system (Figure 14B).

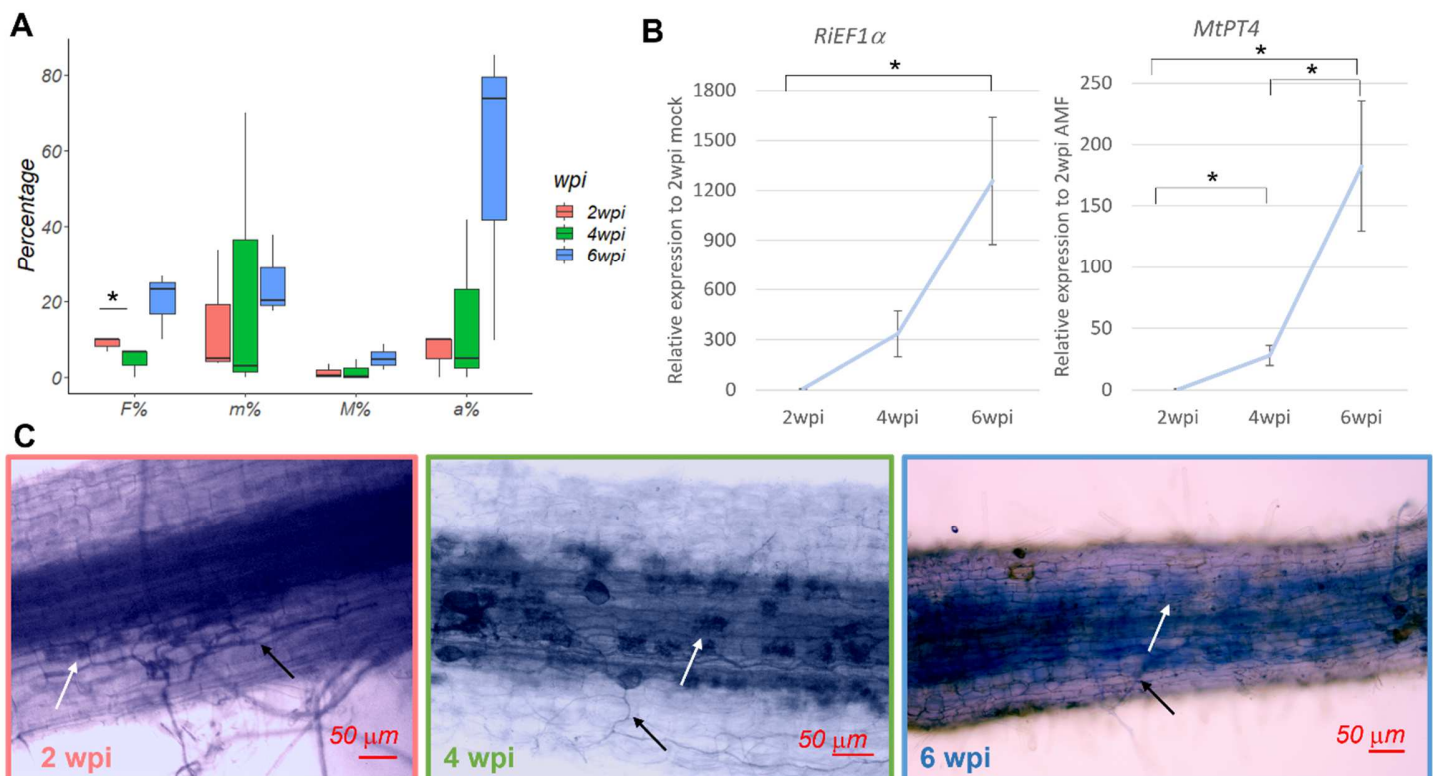


Figure 14: Colonization of wild-type *M. truncatula* plants inoculated with *R. irregularis*. *M. truncatula* WT plants were germinated, inoculated and their roots were harvested at 2, 4 and 6 weeks post inoculation (wpi). Non-inoculated plants were used as control. (A) Colonization quantification with Trouvelot method (Vierheilig et al, 1998b) by analyzing 30 root pieces of 1cm per sample. F% represents the frequency of mycorrhiza in the root system, M% is the intensity of the mycorrhizal colonisation in the root system, m% indicates the intensity of the mycorrhizal colonization in the root fragments and a% shows the arbuscule abundance in mycorrhizal parts of root fragments. Colonization was measured for three to four roots in each repeat. Asterisk indicates significantly different in the frequency of colonization between 2 and 4 wpi (p -value < 0.05, Student's t -test). (B) Expression of the *R. irregularis* housekeeping gene *RiEF1 α* and the symbiotic marker gene *MtPT4* in the mycorrhized roots. Relative expression to 2wpi mock sample 1 and normalized against the *M. truncatula* housekeeping genes *MtTUB1* and *MtGADPH*. Values are means of three independent repeats (three to four plants each) with their standard error. Asterisks indicate significantly different expression between the marked samples (p -value < 0.05, Student's t -test). (C) Representative images of 2, 4, and 6 wpi. Fungus has been ink coloured and appears in darker blue. White arrows indicate arbuscules, black arrows indicate intraradical hyphae.

Next, we used these *M. truncatula* mycorrhized roots to measure *RiSP749* expression during AMF colonization. When *RiSP749* expression was normalized to the tomato housekeeping genes

MtTUB1 and *MtGADPH*, *RiSP749* transcripts decreased over time (Figure 15A). Likewise, when the expression of *RiSP749* was normalized to *RiEF1 α* , to correct for differences in AMF colonization, *RiSP749* appeared also to be the highest expressed at early time points and its expression decreased over time (Figure 15A).

Furthermore, to investigate whether the *M. truncatula* homologs of *SIRSZ22* and *SIGNAT* demonstrate an AM-dependent expression which could suggest a role in AM symbiosis, or an expression profile related to the expression of *RiSP749*, their expression was measured in colonized roots and compared with control roots at all sampling times (Figure 15 B and C, for *SIRSZ22* and *SIGNAT* homologs, respectively). Expression of two of the *SIRSZ22* homologs, *MtRSZ22a* and *MtRSZ22b* tended to be induced in mycorrhized roots (AMF) compared with non-inoculated control roots (mock) and was significantly induced for *MtRSZ22a* at 6wpi, while the expression of the third *SIRSZ22* homolog *MtRSZ21* remained unchanged (Figure 15B). In contrast, the expression of all three *SIGNAT* homologs *MtGNATYoaA*, *MtGNATa* and *MtGNATb* remained mostly unchanged between AMF and mock roots (Figure 15C). Additionally, in general the expression of all *SIRSZ22* and *SIGNAT* homologs tend to decrease over time, with the exemption of the transcripts of *MtGNAYoaA* which increase over time (Figure 15 B and C).

In conclusion, the *M. truncatula* colonization level increases overtime, contrary to the expression level of *RiSP749*. Moreover, less *RiSP749* is accumulated per fungal unit, indicating that *RiSP749* is mostly expressed at early time points. From the *RiSP749* *M. truncatula* interactor homologs, *MtRSZ22a* and *MtRSZ22b* were responsive to mycorrhization as shown by higher expression levels in AMF roots than in control conditions, and they showed a similar pattern than *RiSP749*, as their expression decreases over time, while mycorrhization increases.

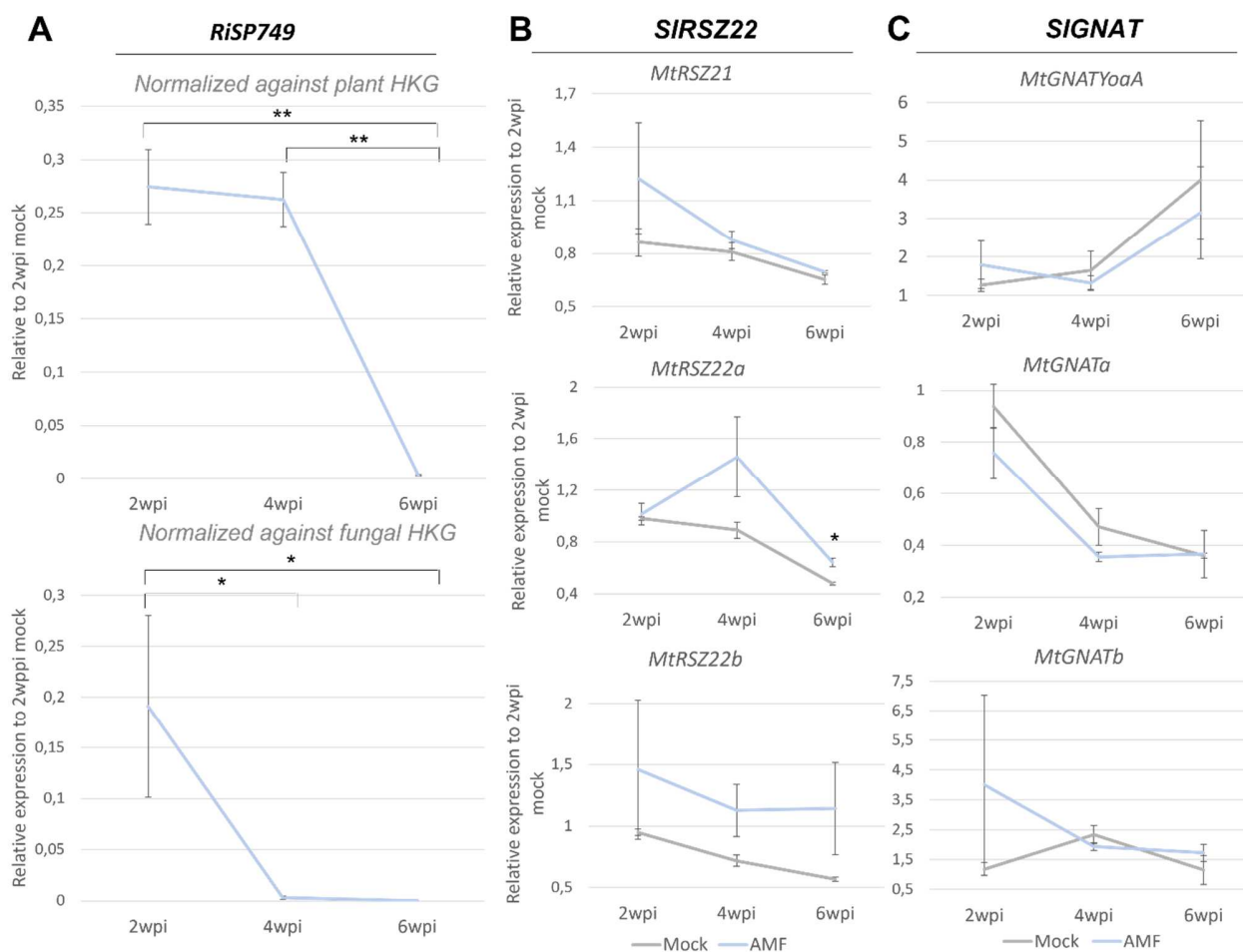


Figure 15: Expression of *RiSP749* and *M. truncatula* homologs of the tomato interactors *SRSZ22* and *SIGNAT* during AM symbiosis. *M. truncatula* WT plants were germinated, inoculated and their roots were harvested at 2, 4 and 6 weeks post inoculation (wpi). Non-inoculated plants were used as control. (A) Expression of the *R. irregularis* effector *RiSP749* in mycorrhized roots. Values are means of three independent repeats with their standard error. The top graph showed the relative expression to the control plants at 2wpi normalized against the plant HKG *MtTUB1* and *MtGADPH*. The bottom graph normalized the expression to the *R. irregularis* housekeeping gene *RiEF1 α* . Asterisks means that *RiSP749* expression is significantly different between the indicated samples (*, p -value<0.05; **, p -value<0.01; Student's t -test). (B) Expression of the *M. truncatula* homologs to *SIRSZ22* (*MtRSZ21*, *MtRSZ22a*, and *MtRSZ22b*) in mycorrhized and control roots. Values are means of three independent repeats with their standard error. Asterisks means that *MtRSZ22a* expression is significantly different in AMF compared to mock expression (*, p -value<0.05; Student's t -test). (C) Expression of the *M. truncatula* proteins homologs to *SIGNAT* (*MtGNATYoaA*, *MtGNATa*, *MtGNATb*) in mycorrhized and control roots. Values are means of three independent repeats with their standard error.

3.2. Effect of *RiSP749* overexpression on AM colonization of *M. truncatula* plants

In order to test the role of *RiSP749* in mycorrhization, *M. truncatula* plants with transgenic roots overexpressing *RiSP749-GFP Turbo* were generated (*RiSP749 OE*). For that purpose, we cloned *RiSP749* driven under the constitutive *CaMV35S* promoter. As control, plants were used which overexpressed *GFP Turbo* in their roots. The fusion to the *GFP Turbo* tag was done in order to use it in future experiments. After 5 weeks, the whole root system of 8 plants of each construct were

harvested, the root tips were used to assess the OE of *RiSP749* or *GFPTurbo* (Supplementary figure S4). Once, OE of *RiSP749* or *GFPTurbo*, respectively, was confirmed, colonization was evaluated through the Trouvelot method (Vierheilig et al., 1998b; Figure 16A). A small decrease in the colonization frequency (F%) and in the arbuscule abundance (a%, A%) was observed in *RiSP749* OE roots compared with the *GFPTurbo* OE control roots, although not significant (Figure 16A). This decrease in colonization was also not apparent visually in the ink coloured roots (Figure 16 B and C). Surprisingly, expression of the marker genes for functional symbiosis, *MtPT4*, and arbuscule development, *MtRAM1*, were strongly reduced in *RiSP749* OE lines compared with *GFPTurbo* OE roots (Figure 16E). Moreover, also the levels of *RiEF1 α* transcripts were lower in *RiSP749* OE roots (Figure 16F). This reduced expression of the arbuscule marker genes could be explained by the slight reduction in colonization as determined via the Trouvelot analysis or might indicate that arbuscules are not functional in *RiSP749* OE lines.

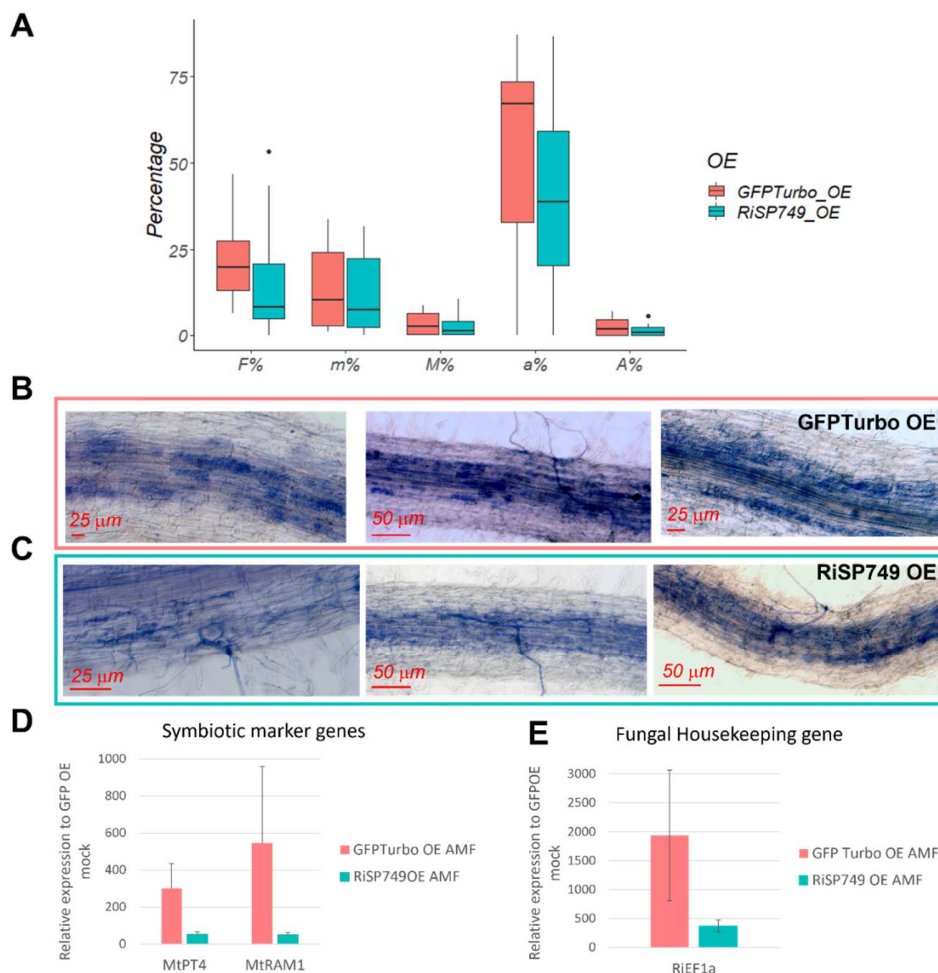


Figure 16: Colonization evaluation of *M. truncatula* hairy roots *RiSP749* overexpression (*RiSP749*OE) and *GFP Turbo* OE lines as control. (A) Colonization evaluation of *GFPTurbo* OE lines, as control, and *RiSP749* OE lines according to the Trouvelot method (Vierheilig et al, 1998b). F% represents the frequency of mycorrhiza in the root system, M% is the intensity of the mycorrhizal colonization in the root system, m% indicates the intensity of the mycorrhizal colonization in the root fragments, a% shows the arbuscule abundance in mycorrhizal parts of root fragments and A% is the arbuscule abundance in the root system. Colonization was measured in the full root system of 8 plants for

each line. (B) Illustrative images of the colonization in GFP Turbo OE lines. (C) Illustrative images of the colonization in RiSP749 OE lines. (D) Expression of the *M. truncatula* symbiotic responsive genes, *MtPT4* and *MtRAM1*, normalized to *M. truncatula* housekeeping genes *MtTUB1* and *MtGADPH* and relatively compared to expression in GFP Turbo OE. Values are the means of the expression in three independent repeats with their standard error. (E) Expression of *R. irregularis* housekeeping gene, *RiEF1 α* normalized to *M. truncatula* housekeeping genes and relatively compared to expression in GFPTurbo OE. Values are the means of the expression in three independent repeats with their standard error.

Although no clear and significant differences were observed in colonization (Figure 16 A, B and C), we observed a visual difference in the arbuscule formation pattern in *RiSP749 OE* roots compared with *GFP Turbo OE*. Normally, arbuscules are developed in the inner cortical cells, close to the vascular system. However, overexpression of *RiSP749* seemed to stimulate the development of arbuscules at outer layers of the cortex more distant from the vascular system. To confirm this, the layers of cortical cells containing arbuscules at one side of the vascular system was counted for 13 independent colonized root pieces, resulting in a significant difference between *RiSP749 OE* and *GFP Turbo OE* lines (p-value <0.01; Figure 17 A and B). However, this result needs additional experimental evaluation in plants where the control has at least 30% colonization frequency.

To get a better insight in the role of *RiSP749* in arbuscule functionality and because *RiSP749* accumulates mainly at the early stages of mycorrhization (Figure 15 A), we tested the expression of several genes involved in early mycorrhization stages and arbuscule development (*MtDELLA1*, *MtCYCLOPS*, *MtNSP2* and *MtNIN*) in the full root system of *GFP Turbo OE* and *RiSP749 OE* plants both from mock and AMF (Figure 17 C and D). First, the expression of these genes in all samples (*GFPTurbo AMF*, *RiSP749 OE* mock, and *RiSP749 OE AMF* lines) were compared with the *GFP Turbo OE* mock. This comparison revealed that all these genes were induced upon mycorrhization but not in *RiSP749 OE* mock and AMF lines. Even more, when *RiSP749* is overexpressed in mycorrhized roots, *MtNIN*, *MtCYCLOPS*, *MtNSP2* and *MtDELLA1* are significantly repressed compared with non-mycorrhized roots. Hence, the sustained expression of *RiSP749* during mycorrhization lead to the repression of these genes.

Next, the expression of *MtDELLA1* in mycorrhized plants (*GFPTurbo OE AMF* and *RiSP749 OE AMF*) was normalized to the *RiEF1 α* expression to correct for differences accounted by the plant colonization level (Figure 17D). Interestingly, in this analysis, the expression of *MtDELLA1* does not differ between control and *RiSP749 OE* plants. Thus, the repression of *MtDELLA1* observed when data is normalized against the *M. truncatula* housekeeping genes (Figure 17C) may be an artefact due to the reduced colonization level of *RiSP749 OE* lines compared to *GFP Turbo OE* plants. This comparison should be done also for *MtNIN*, *MtNSP2* and *MtCYCLOPS* to confirm if they are actually repressed by *RiSP749* in mycorrhized roots.

In summary, the overexpression of *RiSP749* slightly reduced the colonization frequency (F%) and seemed to have a phenotype in the arbuscule development pattern. *RiSP749* repressed the expression of *MtNIN*, *MtNSP2* and *MtCYCLOPS* three important players in the CSSP, in mycorrhized roots, although this result should be further confirmed.

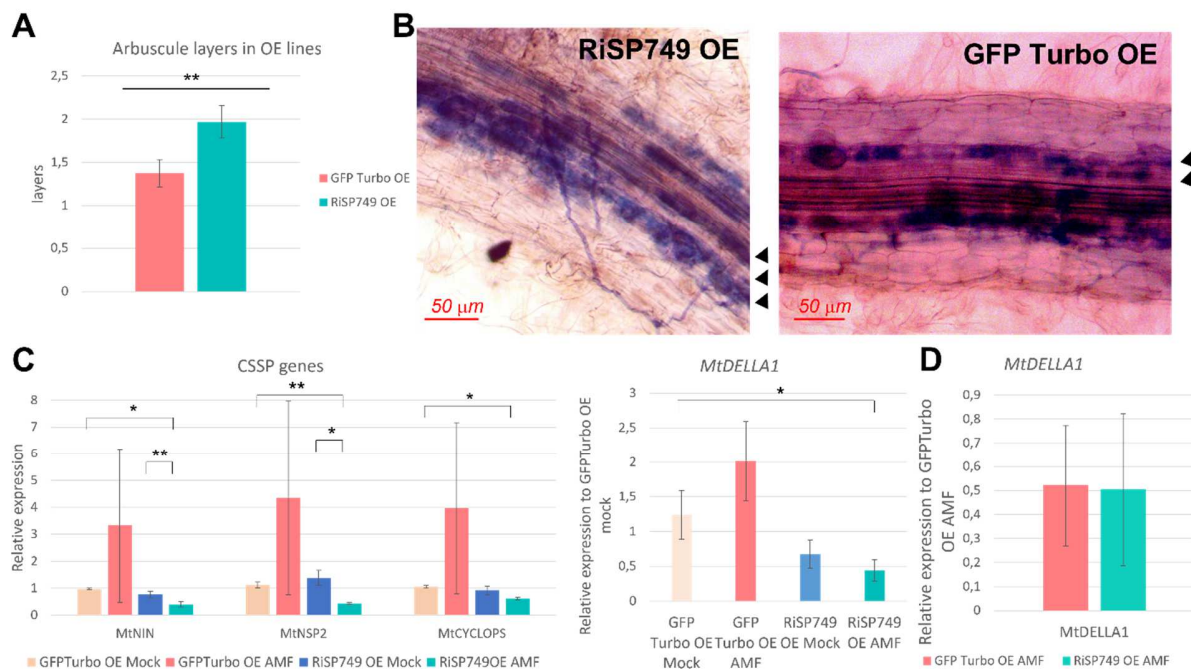


Figure 17: Phenotype of RiSP749 OE in development of arbuscule layers and effect of RiSP749 OE on the expression of AM related genes. (A) Quantification of the number of cortical cell layers with arbuscules in colonized root pieces both for mycorrhizal RiSP749 and GFP Turbo OE lines. Values represent the means 13 independent root pieces with the standard error. Asterisks means that it is significant (p -value < 0.01; Student's t -test). (B) Illustrative images of the referred phenotype. Each layer of arbusculated cortical cells is marked by an arrow. (C) Average expression of MtNIN, MtNSP2, MtCYCLOPS and MtDELLA1 in three biological repeats of GFP Turbo and RiSP749OE both in mock and AMF conditions with their standard error. Expression values were normalized to the *M. truncatula* genes MtTUB1 and MtGADPH and relatively compared to GFP Turbo OE mock expression. Asterisks means that it is significant (* p -value < 0.05; ** p -value < 0.01; Student's t -test) (D) AMF expression values were normalized to RiEF1 α expression to correct for fungal colonization differences.

3.3. Effect of RiSP749 OE on the expression of its protein interactors

In order to test whether *RiSP749 OE* has an effect on the expression of the *SIRSZ22* and *SIGNAT* *M. truncatula* homologs, their expression was checked in the roots of *RiSP749 OE* and *GFPTurbo OE* mock and AMF roots at 5wpi (Figure 18 A and B). Contrary to what was found in WT *M. truncatula* plants, the expression of the *SIRSZ22* *M. truncatula* homologs (*MtRSZ21*, *MtRSZ22a*, and *MtRSZ22b*) were repressed by mycorrhization in *GFPTurbo* AMF and by *RiSP749 OE* both in AMF and mock conditions, while *SIGNAT* *M. truncatula* homologs, *MtGNATyoaA* and *MtGNATb*, were induced by mycorrhization in *GFPTurbo* AMF and by *RiSP749 OE* both in AMF and mock conditions (Figure 18 A and B left side). However, when the expression is normalized to the *R. irregularis* housekeeping gene RiEF1 α , to correct for differences in mycorrhization levels, the expression of all *SIRSZ22* *M. truncatula* homologs were significantly induced *RiSP749 OE* AMF plants compared with the control (Figure 18A right side), while the expression of the *MtGNAT* *M. truncatula* homologs remained unchanged (Figure 18B right side).

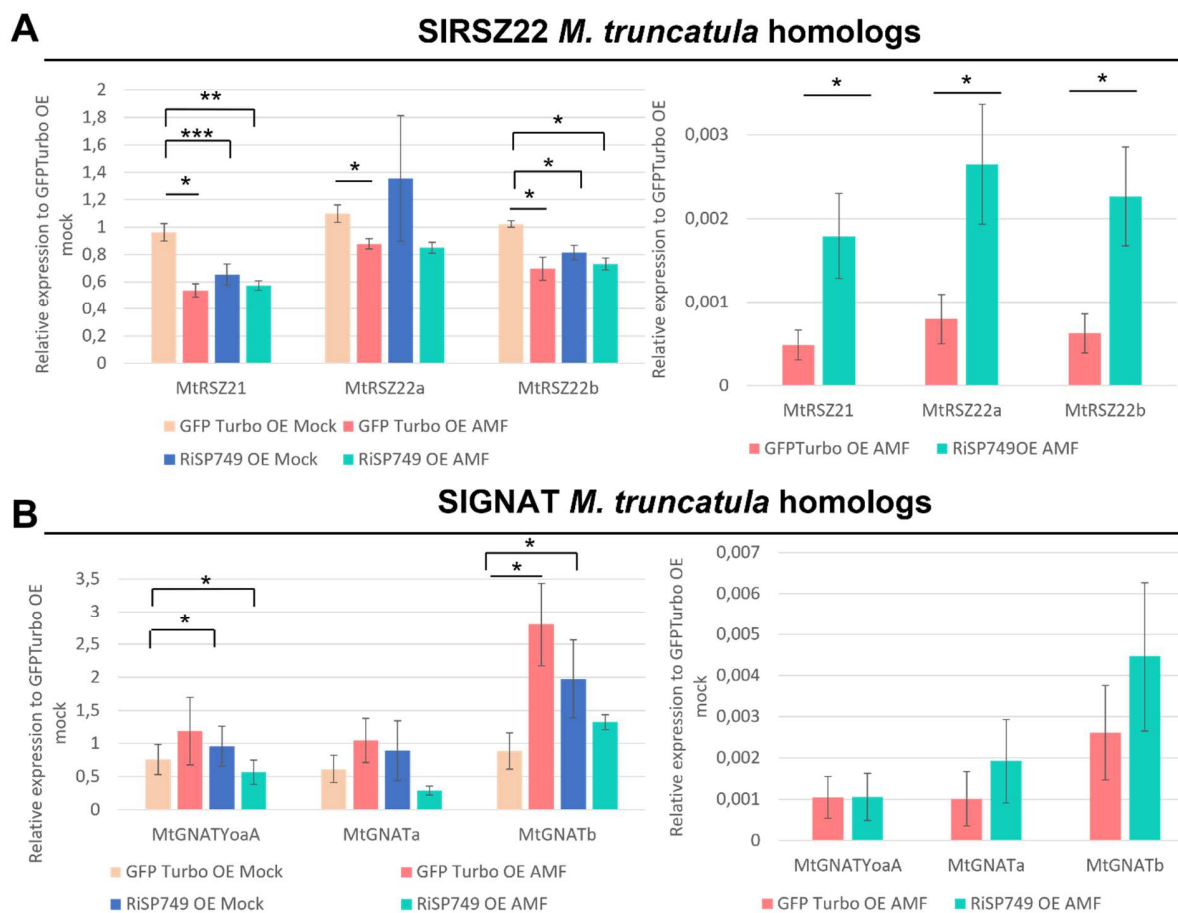


Figure 18: Expression of SIRSZ22 and SIGNAT *M. truncatula* homologs in GFP Turbo and RiSP749 OE lines in mock and AMF. (A) The average of the expression of the *M. truncatula* homologs of SIRSZ22 (*MtRSZ21*, *MtRSZ22a*, *MtRSZ22b*) measured in three independent biological replicates of GFP Turbo and RiSP749 OE both mock and AMF and their standard error is represented. In the left graph, samples are normalized to *M. truncatula* housekeeping genes (HKG) *MtTUB1* and *MtGADPH* while, in the right graph, AMF samples are normalized to *RiEF1α*, and the expression is in both cases relative to GFP Turbo OE mock. Asterisks means significant differences between indicated samples (*, p -value < 0.05; **, p -value < 0.01; ***, p -value < 0.001, Student's t -test). (B) The average of the expression of the *M. truncatula* homologs of SIGNAT (*MtGNATYoaA*, *MtGNATa*, *MtGNATb*) measured in three independent biological replicates of GFP Turbo and RiSP749 OE both mock and AMF and their standard error is represented. In the left graph, samples are normalized to *M. truncatula* HKG *MtTUB1* and *MtGADPH* while, in the right graph, AMF samples are normalized to *RiEF1α*, and the expression is in both cases relative to GFP Turbo OE mock. Asterisks means that significant difference between indicated samples (p -value < 0.05, for Student's t -test).

Overall, mycorrhization in GFP Turbo control roots repressed all SIRSZ22 homologs. RiSP749, in absence of mycorrhiza, also repressed the expression of *MtRSZ21* and *MtRSZ22b* in mock conditions while, in presence of mycorrhiza, all SIRSZ22 *M. truncatula* homologs showed a higher expression in RiSP749 OE lines than in GFP Turbo OE lines when normalized to the colonization level. This expression pattern could indicate that RiSP749 needs the presence of another fungal protein to induce the expression of these genes. The expression of the SIGNAT *M. truncatula* homologs was induced both by mycorrhization in GFP Turbo plants, and by RiSP749 OE in mock conditions, while in AMF conditions their expression remained unchanged.

4. Functional characterization of candidate interactors in tomato

Preliminary experiments were performed to investigate a possible role of *SIRSZ22* and *SIGNAT* in mycorrhization. Firstly, the promoter activity of *SIGNAT* was tested with pSIGNAT-GUS reporter lines. Secondly, RNA interference (RNAi) knock-down lines were generated for *SIRSZ22* to test the effect of *SIRSZ22* silencing on mycorrhization.

4.1. Pattern of promoter activity of *SIGNAT* in tomato mycorrhizal roots

To investigate the promoter activity of *SIGNAT* and its responsiveness to AMF colonization, we generated two pSIGNAT-GUS reporter lines, one containing 1 Kb of the *SIGNAT* promoter sequence (pSIGNAT_{1kb}:GUS) and another of 3 Kb length upstream of the starting codon (pSIGNAT_{3kb}:GUS). These two constructs of different promoter length were chosen because, according to both NCBI and Sol Genomics databases, 1 Kb upstream of the *SIGNAT* starting codon, another gene was annotated that might affect the expression by its regulatory elements. Plants with transgenic roots expressing one of each construct were generated and CaMV35S: GUS transgenic roots were used as control. The full root system was harvested after 5 weeks, part of the root system was ink stained to confirm the presence of colonization, and the other part of the root system was stained with 5-bromo-4-chloro-3-indolyl- β -glucuronide (X-Gluc) to visualize promoter activity.

The promoter activity of *SIGNAT* was visual along the whole root system, especially close to the root tips, as this is the most transcriptionally active region of the root (Figure 19). An overall increase in expression was observed in mycorrhized roots compared with mock controls, both for the pSIGNAT_{1kb}:GUS and pSIGNAT_{3kb}:GUS, visual by a more GUS intensity (Figure 19). In addition, the 1 Kb promoter seemed to be more active than the 3 Kb promoter, as the *GUS* expression is more intense and more evenly distributed in pSIGNAT_{1kb}:GUS compared with pSIGNAT_{3kb}:GUS. These results suggest that the presence of the upstream gene may influence the expression of *SIGNAT* or the presence of upstream located negative regulatory elements.

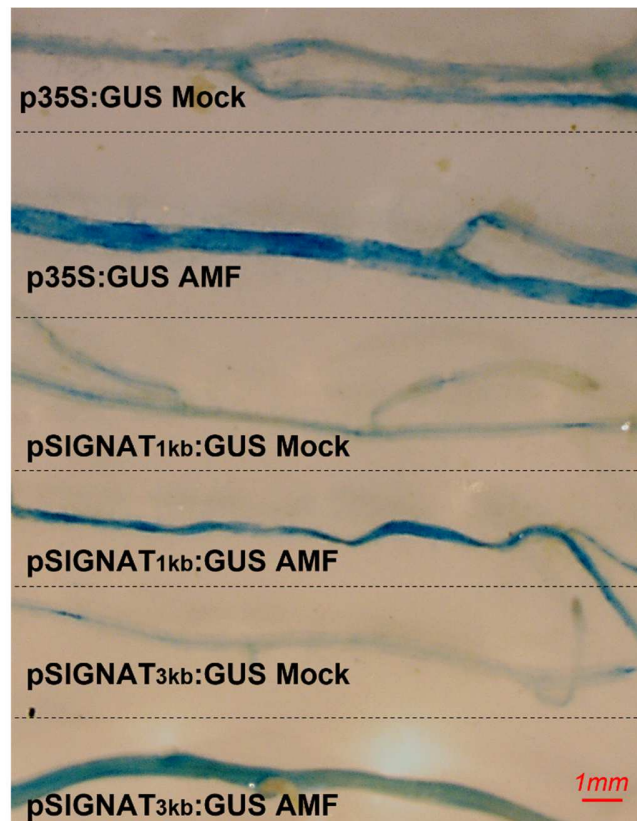


Figure 19: Promoter activity of *SIGNAT* in tomato roots using *pSIGNAT-GUS* reporter lines. The expression pattern of *SIGNAT* was analysed in 1kb (*pSIGNAT1Kb*) and 3kb (*pSIGNAT3Kb*) promoters of *SIGNAT* fused to *GUS*. *pCaMV35S:GUS* was used as control. Tomato roots were grown with or without *R. irregularis* spores. After 5 weeks post inoculated, roots were harvested and stained with X-Gluc.

4.2. Effects of tomato *SIRSZ22* silencing on mycorrhization

In order to analyze the role of *SIRSZ22* in mycorrhization and to further untangle the action mechanism of *RiSP749*, plants with transgenic roots expressing *SIRSZ22* RNAi constructs were generated. Plants transformed with the empty vector *pK7gwiwg2D Red root* (EV) were used as control. After five weeks, the full root system of transformed plants was harvested.

First, the downregulation of *SIRSZ22* expression compared to the expression in EV roots was confirmed by qRT-PCR analysis both in mock and AMF (Figure 20A). Additionally, the expression of the *R. irregularis* effector *RiSP749*, the fungal housekeeping gene *RiEF1 α* and the tomato functional symbiotic marker genes *SIPT4*, *SIPT5* and *SIRAM1* were checked. *RiSP749* and *RiEF1 α* expression was higher in *SIRSZ22* RNAi mycorrhized lines compared to EV plants (Figure 20B). *SIPT4* and *SIPT5* were more expressed in *SIRSZ22* RNAi lines compared with the EV when normalized against the tomato HKG *SIEF1 α* and *SIGADPH* (Figure 20C). However, a slight repression of *SIPT4* was seen when expressions were normalized to the *R. irregularis* housekeeping gene *RiEF1 α* and compared to EV expression (Figure 20D). Further supporting a possible role of *RiSP749* in arbuscule functionality by interacting with *SIRSZ22*. Experiments were performed in two to three independent root systems. Hence, additional experiments are necessary, and care should be taken in making strong conclusions.

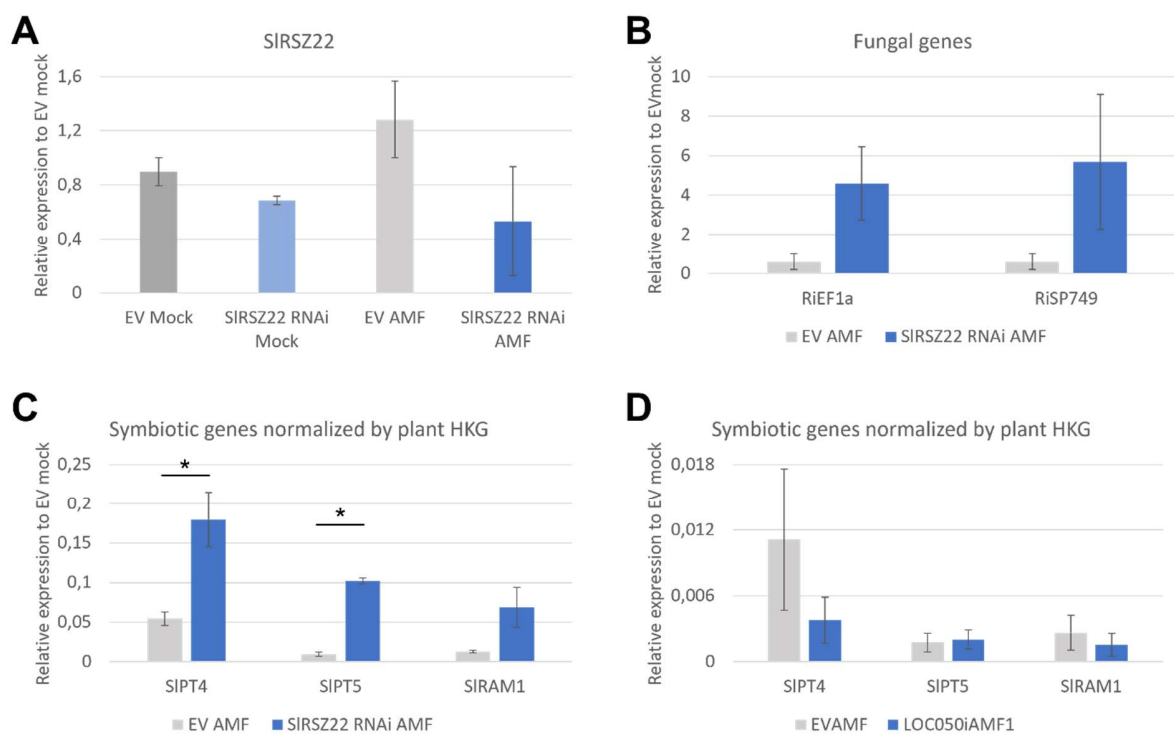


Figure 20: Expression analysis in root systems of SIRSZ22 RNAi lines and empty vector (EV) lines, as control. (A) Confirmation of SIRSZ22 expression downregulation in SIRSZ22 RNAi lines in mock and AMF conditions. (B) Expression of the *R. irregularis* genes *RiEF1 α* and *RiSP749* in the control and SIRSZ22 RNAi lines in AMF conditions. (C) Expression of the tomato AM symbiosis genes *SIPT4*, *SIPT5* and *SIRAM1* normalized to *SIEF1 α* and *SIGADPH* in mycorrhized control and SIRSZ22 RNAi lines. (D) Expression of the tomato AM symbiosis genes *SIPT4*, *SIPT5* and *SIRAM1* normalized to *RiEF1 α* in mycorrhized control and SIRSZ22 RNAi lines. Values are means of two or three biological repeats with their standard error. Asterisks mean that expression is significantly different between the signaled samples (p -value < 0.05, Student's *t*-test)

Part 4: Discussion

AMF establishes interactions with the majority of land plants, including important crops such as tomato, improving their performance in stress conditions such as during drought, high temperatures or waterlogged conditions (Chen *et al*, 2018). They can also prime and protect the host plant against multiple phytopathogens (Diagne *et al*, 2020), and improve the plant's nutrient content by transferring essential minerals to the plant roots (Cakmak, 2002; Peña Venegas *et al*, 2021). Overall, AMF are promising to be used as biofertilizers for a sustainable and eco-friendly agriculture (Nacoon *et al*, 2021).

In order to establish a successful interaction with the plant, a complex signal exchange happens between the host plant and the fungus, activating downstream signaling pathways to regulate symbiosis (Gutjahr & Parniske, 2013). During the first steps of the interaction, the plant recognizes AMF as possible pathogenic organisms by which it activates plant defenses. In phytopathogens, effectors are essential for overcoming these plant defenses (Lo Presti *et al*, 2015), which opened the question whether these effectors could also be involved in symbiotic interactions. Indeed, during nodulation, a symbiotic pathway that has much in common with AM symbiosis (Oldroyd, 2013), the secretion of effectors is necessary for the establishment of a successful symbiosis. Soybean plants mutated in Nod factor receptor genes could still form nodules as long as they are inoculated with their compatible rhizobia with an active type 3 secretion system (T3SS; Okazaki *et al*, 2013; Teulet *et al*, 2019). Interestingly, AMF also secrete a large number of effector proteins (Kamel *et al*, 2017; Sędziewska Toro & Brachmann, 2016; Zeng *et al*, 2018), but to date only for five of them a role during AM symbiosis establishment have been reported (Kloppholz *et al*, 2011; Tsuzuki *et al*, 2016; Zeng *et al*, 2020; Wang *et al*, 2021; Voß *et al*, 2018). The downregulation of these effectors negatively affects colonization, supporting the hypothesis that effectors are essential to regulate symbiosis. Therefore, the functional characterization of these AMF effectors will advance our understanding about AM symbiosis and, on the long term, this knowledge may be used to improve their performance as biofertilizers in crop agriculture.

In this master thesis, we studied the effector protein RiSP749 from the model AMF *R. irregularis* and its role in both *M. truncatula* and tomato mycorrhization. We found that *R. irregularis* interacts with the alternative splicing factor SIRSZ22 from tomato and probably also with the three protein homologs MtSRZ21, MtSRZ22a, and MtSRZ22b of *M. truncatula*. Moreover, during colonization of WT *M. truncatula* plants, we observed that RiSP749 is more highly expressed at early time points of colonization, whereas the expression of *MtSRZ22a* and *MtSRZ22b* is higher in mycorrhized *M. truncatula* roots than in the non-mycorrhized control at all time points during colonization and also decreases over time. Additionally, the overexpression of *RiSP749* in *M. truncatula* roots causes a slight reduction in colonization levels, together with a reduction in the expression of the symbiotic marker genes *MtPT4* and *MtRAM1* (Volpe *et al*, 2016; Park *et al*, 2015), indicating a possible dysfunction in arbuscule development. *MtDELLA1*, *MtNIN*, *MtNSP2* and *MtCYCLOPS*, genes involved in the CSSP during mycorrhization (Gobbato *et al*, 2012; Liu *et al*, 2011b; Pimprikar *et al*, 2016; Guillotin *et al*, 2016), are also repressed by *RiSP749* overexpression. Likewise, the expression of *SIRSZ22* *M. truncatula* homologs are also repressed

by *RiSP749* overexpression in mock conditions and during mycorrhization. However, when *RiSP749* is overexpressed in mycorrhized roots, their expression is induced, suggesting that other fungal proteins may be involved in the upregulation of these genes as seen by their induced expression in WT mycorrhized roots. Finally, some preliminary experiments in tomato showed that the *SIRSZ22* RNAi knock-down roots had more colonization as seen by a higher expression of the fungal marker gene *RiEF1 α* , although the symbiotic marker genes *SIPT4*, *SIPT5* and *SIRAM1* (Ho-Plágaro *et al*, 2019; Chen *et al*, 2014), were not increased and even slightly repressed, a similar trend as what was observed for the *RiSP749* OE lines.

1. *RiSP749* interacts with the tomato protein *SIRSZ22*

SIRSZ22 interacts with *RiSP749*, and the interaction was confirmed both through binary Y2H and rBiFC experiments. This interaction takes place in the nucleus at heterogeneous spots but not in the nucleolus. In addition, the three *M. truncatula* homologs of *SIRSZ22* (*MtRSZ21*, *MtRSZ22a* and *MtRSZ22b*) also interacted with *RiSP749* in binary Y2H experiments. On the other hand, *SIGNAT* showed interaction with *RiSP749* *in vitro*, but not *in planta*, indicating that *SIGNAT* may not be a real interactor of *RiSP749*.

A. thaliana splicing factor *AtRSZ22*, homologs to the human 9G8 splicing factor, has nucleocytoplasmic shuttling properties, alternating its location between the nucleus and the cytoplasm (Rausin *et al*, 2010). In the nucleus, *AtRSZ22* has a speckle-like distribution and a small fraction localizes the nucleolus which significantly increases upon phosphorylation inhibition or *AtRSZ22* overexpression (Rausin *et al*, 2010; Tillemans *et al*, 2006). Interestingly, the nucleolar accumulation decreases in RRM or Zn knuckle mutants, suggesting that the translocation to the nucleolus is dependent on *AtRSZ22* ability to bind RNA (Rausin *et al*, 2010). In contrast, *SIRSZ22* did not show a nucleolar localization, suggesting that the dynamics and functionality of *SIRSZ22* may differ from *AtRSZ22*. The heterogeneous distribution of *SIRSZ22* in the nucleus may correspond with assembling sites of splicing factors (Ohtani, 2018). Fluorescence Loss In Photobleaching (FLIP) could be done to investigate the nucleocytoplasmic shuttling of *SIRSZ22* by photobleaching the cytoplasm area around the nucleus and study the loss rate of fluorescence, while Fluorescence Recovery After Photobleaching (FRAP) can be used to study the nuclear dynamics and the accumulation in particular regions of the nucleus such as cajal bodies or speckles and test the accumulation in the nucleolus (Rino *et al*, 2007; Ohtani, 2018; Nissim-Rafinia & Meshorer, 2011).

The interaction between the three evaluated *M. truncatula* proteins *MtSRZ21*, *MtSRZ22a* and *MtSRZ22b*, and *RiSP749* should be further studied *in planta*, using additional experiments such as rBiFC or protein co-immunoprecipitation (CoIP) in mycorrhized roots. The fact that *RiSP749* interacts with all of them, indicates that the interaction motif might be conserved among these proteins. MSA of the four RSZ proteins showed that both the RRM and the Zn knuckle motifs are conserved among them, suggesting that the binding motif could be in these regions, as these domains are known to be involved in protein-protein and protein-RNA interactions in *AtRSZ22* (Tillemans *et al*, 2006). However, the RS domain of SF2/ASF, a human splicing factor closely related to *AtRSZ22* (Rausin *et al*, 2010), is essential for the interaction with U1 70K protein, homolog of *RiSP749* (Wu & Maniatis, 1993). Hence, further experiments with truncated forms of

SIRSZ22 are necessary to unravel the interacting motif of RiSP749. Moreover, even though the binary Y2H revealed that all studied SIRSZ22 *M. truncatula* homologous proteins interact with RiSP749, additional experiments are necessary to uncover the true orthologs of SIRSZ22 and the actual targets of RiSP749 during mycorrhization. Therefore, it would be interesting to evaluate the activity of each of them as well as the SIRSZ22 activity to identify which has similar functions as SIRSZ22. These proteins are splicing factors, involved in the mRNA processing (Lopato *et al*, 1999). In *A. thaliana*, AtRSZ22 recognized the RNA probe 5'-CUUCGAUCAACGCCACGCCA-3' and splice mRNAs containing this sequence (Lopato *et al*, 1999). This sequence can be tested as SIRSZ22 cis-element binding sequence for later *in silico* analysis of candidate target mRNAs. Moreover, target mRNAs of SIRSZ22 and its *M. truncatula* homologs could be studied through e.g. mRNA co-immunoprecipitation (RIP) (Gagliardi & Matarazzo, 2016), and compared between them to evaluate whether they are involved in processing the same mRNAs. Even more, RIP could also be performed using the effector RiSP749 to investigate which genes it regulates and if they overlap with SIRSZ22 targets.

The regulation of RiSP749 exerted on SIRSZ22 and its role during mycorrhization are unknown. RiSP749 is a homolog of the snRNA U11/U12 35K protein, involved in the U12 spliceosome, a minor spliceosome involved in the splicing of a small set of genes containing non-canonical U12 introns such as Dihydropyridine-sensitive L-type calcium channel alpha-1 subunit CACNL1A3 (CACNA1S) (Levine & Durbin, 2001; Lopato *et al*, 1999; Kamel *et al*, 2017; Golovkin & Reddy, 1998). Hence, RiSP749 is most likely participating in the alternative splicing of U12 intron containing mycorrhizal induced genes during symbiosis establishment. An *in vitro* analysis of the splicing activity of RiSP749 and its ability to efficiently complement the U11/U12 35K protein could be done to test this hypothesis (Albaqami, 2018).

Unlike SIRSZ22, the interaction between SIGNAT and RiSP749 could not be confirmed. Although the result from the binary Y2H supported this interaction, the rBiFC results could not confirm it. Additionally, yeast colonies co-transformed with SIGNAT and RiSP749 did not grow in 3-AT at concentrations higher than 2,5mM, suggesting a weak interaction, which can be even a false positive and MtGNATb co-transformed with RiSP749 did not grow in SD-LTH media. Besides a repetition of the rBiFC experiments, as only one repetition was done during this thesis, also other techniques such as coIP could be used, although it is very unlikely that SIGNAT and its *M. truncatula* homologs (MtGNATYoaA, MtGNATa, MtGNATb) are real interactors of RiSP749.

2. RiSP749 is expressed at early stages of mycorrhization in *M. truncatula*

The time series experiment performed in WT *M. truncatula* plants revealed that *RiSP749* expression decreases over time. *RiSP749* expression was two times higher at 2 wpi than at 6 wpi on average, indicating a role of RiSP749 in early stages of mycorrhization.

The role of RiSP749 in early stages of mycorrhization is supported by RNAseq results of Kamel *et al.*, 2017. In this study, the expression of *RiSP749* was two-fold times lower in the intraradical mycelium (IRM) of 5wpi *M. truncatula* plants compared with *in vitro* germinated spores of *R. irregularis* in presence of the synthetic SL GR24. However, the number of spores and colonization levels are not specified. Contrary, in tomato, *RiSP749* expression levels increased over time reaching maximum expression level at 6 wpi, although the expression remains low in all time

points (Toon Leroy master thesis). This difference in expression pattern could be due to the differences in colonization strategy between the two host plants, as it is known that the host plant strictly controls the mycorrhization process (Siciliano *et al*, 2007). Alternatively, the experimental set up could also influence this result. In T. Leroy master thesis only one plant was present in each biological repeat, while in this project three to four *M. truncatula* plants were pooled per biological repeat.

On the other hand, composite *M. truncatula* plants with roots overexpressing *RiSP749* harvested at 5 wpi showed a slightly but not significant decrease in the frequency of colonization (F%) and arbuscule abundance (A%, a%) compared with the control *GFPTurbo OE*. The absence of a clear difference in mycorrhization between *RiSP749 OE* and *GFPTurbo OE* could have several reasons. Firstly, the Trouvelot method (Vierheilig *et al*, 1998b) may not account for the phenotype of this transgenic line. Secondly, the colonization levels could be too low to distinguish a clear effect, as the F% was below 30% in the control *GFPTurbo OE* roots, which is low as generally at 5 weeks, *M. truncatula* plants have a colonization of approximately 40% (An *et al*, 2019). Thirdly, *RiSP749* might not have a role during mycorrhization, although this is highly unlikely considering the differences in gene expression of mycorrhiza inducible genes when *RiSP749* is overexpressed even in mock conditions. Finally, the harvesting time point selected might not be optimal for screening the role of *RiSP749* during mycorrhization. As endogenous *RiSP749* is more highly expressed at early time points during symbiosis, a role at early stages of symbiosis is anticipated. Hence, it would be interesting to evaluate phenotypes earlier during the AMF interaction that are not accounted for in the Trouvelot method, such as the number of entry points and colonization units as well as the effect of *RiSP749 OE* on the extraradical hyphal length. Effectors induced at early time points commonly show an early phenotype such as the Tin2 effector from the biotrophic fungus *Ustilago maydis* which prevents the lignification of the host plant vascular bundle at 6 days post inoculation (dpi; Tanaka *et al.*, 2014) or SIS1 effector from *R. irregularis* which promotes hyphal elongation at 7 dpi (Tsuzuki *et al*, 2016). Alternatively, Host-Induced Gene Silencing (HIGS) could be used to reduce the expression levels of *RiSP749* during mycorrhization to study the effect of *RiSP749* suppression on mycorrhization as was done for two other effectors of *R. irregularis* *RiSIS1* or *RiSLM* (Tsuzuki, 2016; Zeng, 2020). If *RiSP749 OE* actually decreases colonization then, at early points a reduced number of entry points and lower intraradical hyphal growth should be observed in the *RiSP749 OE* roots, while HIGS of *RiSP749* might result in higher level of colonization, as seem for *RXLR1* and *RXLR4* effectors from *Phytophthora capsici* (Cheng *et al*, 2022).

3. *RiSP749* overexpression reduces the expression of multiple AM symbiosis inducible genes

The *RiSP749 OE* lines did not show a significant difference in colonization compared with control plants according to the Trouvelot method (Vierheilig *et al*, 1998b). However, reduced levels of expression of early and late symbiotic marker genes *MtPT4*, *MtRAM1*, *MtNSP2*, *MtCYCLOPS* and *MtDELLA1* were observed in mycorrhized *RiSP749 OE* plants compared with the control *GFPTurbo OE*. In addition, the number of layers of cortical cells containing arbuscules in *RiSP749 OE* lines was higher.

The Trouvelot method for quantification of AMF colonization only suggested a small decrease in the colonization frequency (F%) and the number of arbuscules (A%, a%) at 5wpi in the *RiSP749* OE lines, but which is supported by the reduced levels of *RiEF1 α* expression in the same lines. However, the number of cortical cell layers containing arbuscules was increased in the *RiSP749* OE lines. The determination of this phenotype might be subjected to bias, due to the general low colonization levels in these experiments or the way how the mycorrhized parts are mounted on the slides, nevertheless the quantification revealed that the differences are significant. However, the expression of the arbuscule development-specific marker genes *MtPT4* and *MtRAM1* was reduced in *RiSP749* OE lines compared to GFPTurbo lines upon mycorrhization. Normalization against the *R. irregularis* HKG *RiEF1 α* will correct for differences in colonization levels between plants, providing a more robust result. For *MtRAM1*, the expression downregulation could be systemic but not local, which indicates that, although in the whole root system the expression of *MtRAM1* is lower in *RiSP749* OE roots, in the arbuscules the expression levels could still be the same or even higher than in the control, especially considering the low levels of colonization achieved. For *MtPT4*, this explanation is less probable as *MtPT4* is exclusively expressed in arbusculated cells (Volpe *et al*, 2016). The identification of systemic but not local changes in gene expression has been also reported for genes involved in other symbiotic interactions such as during nodulation. Here, the induced expression of *MtCLE12*, only expressed at the site of interaction, is masked when the complete root system is harvested (Mortier *et al*, 2010). To evaluate the expression levels of these genes specifically in arbusculated cells, RNA *in situ* hybridization or laser microdissection could be used to isolate the specific regions of the root that are colonized (Balestrini & Fiorilli, 2020; Kwon *et al*, 2017). Alternatively, *RiSP749* OE may indeed lead to a reduction in *MtPT4* and *MtRAM1* expression indicating an effect on arbuscule activity. The expression of nutrient transporters in arbuscules is essential to form fully functional arbuscules, hence, the overexpression of *RiSP749* may impair the formation of functional arbuscules. The absence of functional arbuscules might explain why the fungus keeps forming new arbuscules in the outer layers of the cortex in 749 OE lines. Promoter p*MtPT4*::GUS reporter lines in plants overexpressing *RiSP749* and WT plants could be used to study whether *MtPT4* is expressed in all arbusculated cells of all cortical cell layers or only in certain cells of the mycorrhized roots of *RiSP749* OE lines. Another way to test the functionality of arbuscules can be by determining the phosphate content and distribution by addressing the accumulation of polyphosphate (polyp) granules in arbuscules with toluidine blue staining (Chilvers, 1980) or neutral red dye, which allow measuring polyp in living tissues (Guttenberger, 2000). A differential distribution of polyp could indicate differences in P transport to the plant cells. The arbuscules observed in roots overexpressing *RiSP749* seem fully developed, improbable if the arbuscules are not functional. A more detailed phenotype of the arbuscule architecture in *RiSP749* OE lines could be checked by staining the arbuscules with fluorescein isothiocyanate-conjugated wheat germ agglutinin (FITC-WGA; Carotenuto & Genre, 2020). Finally, testing the expression of *MtSTR* and *MtRAM2* (Bravo *et al*, 2017) will indicate if the release of lipids is also affected in *RiSP749* OE roots.

Furthermore, *MtNIN*, *MtCYCLOPS*, *MtNSP2*, and *MtDELLA*, four genes from the CSSP pathway, which are normally induced upon mycorrhization (Gobbato *et al*, 2012; Liu *et al*, 2011b; Pimprikar

et al, 2016; Guillotin *et al*, 2016), are not or even repressed in the RiSP749 OE background. In mock conditions, RiSP749 OE does not affect the expression of *MtCYCLOPS*, and *MtNSP2*, but slightly represses *MtNIN* (22% reduction) and *MtDELLA1* (49% reduction). However, mycorrhized plants overexpressing RiSP749 shows a significant expression decrease of *MtNIN*, *MtNSP2*, *MtDELLA1* and *MtCYCLOPS*. Taken together, the CSSP pathway seemed to be repressed by RiSP749. These genes were selected due to their role in early stages of mycorrhization. *MtCYCLOPS* interacts with CCaMK and together induces the expression of *MtNSP2* and *MtNIN* (Horváth *et al*, 2011). *MtCyclops M. truncatula* mutant shows an overall lower level of colonization and a reduced number of arbuscules. Most likely due to the role of *MtCYCLOPS* as *MtRAM1* inducer in complex with *MtDELLA1* (Pimprikar *et al*, 2016). Besides, *MtDELLA1* has a role in cortical cell division by interaction with *MtMIG1* (Heck *et al*, 2016). *MtNSP2* is involved in SL biosynthesis, Myc factor detection and hyphal branching (Park *et al*, 2015; Maillet *et al*, 2011; Liu *et al*, 2011b). *MtNIN* expression is influenced by *MtNSP2* and *MtCYCLOPS*, as *mtnsp2* and *mtcyclops* mutants do not show an induction of *MtNIN* in mycorrhized roots (Guillotin *et al*, 2016). *MtNIN* is induced at early time points in response to Myc-LCOs factors and *mtnin* mutants showed a lower number of fungal entry points at 2wpi and reduced colonization levels at 9 wpi compared with WT *M. truncatula* plants (Guillotin *et al*, 2016). RiSP749 is higher expressed at earlier time points and represses all these early mycorrhiza-related genes of the CSSP, suggesting a role of RiSP749 at early stages of mycorrhization. We hypothesized that RiSP749 acts indirectly or upstream of *MtCYCLOPS* and *DELLA1*, the most upstream CSSP genes studied that appeared downregulated in RiSP749 OE lines, to control hyphal branching during symbiosis establishment by restricting the intraradical growth of the fungus. A reduced intraradical hyphal extension in RiSP749 OE lines would also explain the formation of arbuscules at outer layers of the cortex. However, the mycorrhization phenotype of *RiSP749 OE* does not resemble the previous reported mutant phenotypes of these CSSP genes (Maclean *et al.*, 2017; Table 5). However, RiSP749 OE downregulates but not eliminates the expression of these genes, suggesting that the downregulation exerted by RiSP749 may not be enough to result in the mutant phenotype.

Table 5: Mycorrhization phenotypes of the *mtcyclops*, *mtram1*, *mtpt4*, *mtnsp2*, *mtnin* and *mtdella1* mutants

Gene	Mutant phenotype	Reference
CYCLOPS	Reduced number of arbuscules	Horvath <i>et al.</i> , 2011
RAM1	Cortical cell penetration and trunk formation but almost no hyphal and arbuscule branching	Park <i>et al.</i> , 2015
PT4	Premature arbuscule degeneration	Javot <i>et al.</i> , 2007
NSP2	Reduced colonization	Maillet 2011
NIN	Reduced colonization	Guillotin <i>et al.</i> , 2016
DELLA1	Intraradical colonization but very limited formation of arbuscules	Foo <i>et al.</i> , 2013

Despite there are some indications to suggest that RiSP749 acts on the CSSP during mycorrhization, more repetitions of these experiments should first be done with a higher number of plants and by pooling plants grown in the same pot to reduce the biological variability derived from differences in colonization and plant root growth. Additionally, a higher colonization rate would help to visualize and quantify differences in the phenotype between the RiSP749 OE and GFPTurbo control lines. This effect is now probably masked by the overall reduced colonization levels, even in the control lines, for all experiments throughout the master thesis. Moreover, testing the expression of *MtENOD11* and *MtRAM2*, expressed at early stages of mycorrhization and involved in the hyphopodium formation, and *MtNF-Y* and *MtMIG1*, involved in cortical cell expansion and division, will indicate if RiSP749 is impaired at intraradical growth or even at earlier stages of mycorrhization (Kosuta *et al*, 2003; Heck *et al*, 2016). As mentioned above, testing the number of entry points at shorter times will also indicate a defect on early stages of colonization in RiSP749 OE lines. Finally, *in vitro* growth of the fungus in culture with *M. truncatula* roots would allow to monitor more easily the progression of the fungus and the rate of development *in vivo*.

4. RiSP749 induces SIRSZ22 *M. truncatula* homologs during mycorrhization

RiSP749 induced the expression of all three SIRSZ22 *M. truncatula* homologs *MtRSZ21*, *MtRSZ22a*, and *MtRSZ22b* in mycorrhized roots, although it repressed two of them, *MtRSZ21* and *MtRSZb*, in mock conditions. Moreover, the transcript levels of *MtRSZ22a* and *MtRSZ22b* are also increased in mycorrhized WT *M. truncatula* plants, but the opposite was observed for GFPTurbo OE lines upon mycorrhization, i.e a significant downregulation. The expression pattern of these proteins is clearly responsive to mycorrhization but whether it is induced or repressed by AMF needs further investigation as the opposite pattern is seen in WT and GFPTurbo plants. WT plants have been harvested at different time points as for the GFPTurbo lines, and although colonization frequencies are rather similar between both experiments (20% at 6wpi in WT and 22% at 5wpi in GFPTurbo lines), these differences in harvesting time could possibly explain the differences observed in the transcriptional responses of mycorrhized roots. Furthermore, both experiments strongly differ in their material as for the GFPTurbo material, composite plants generated by hairy root transformation are used. It is well known that hairy roots alter in their transcriptional responses compared with WT plants (Kastell *et al*, 2013). Results are also contrary than what would be predicted according to the information obtained from LEGOO database. According to LEGOO, *MtRSZ21* expression is induced by MtNIN, thus, we would expect *MtRSZ21* to be induced in WT *M. truncatula* and GFPTurbo mycorrhized plants and repressed in RiSP749OE lines, as MtNIN is repressed by RiSP749. However, the opposite expression pattern was seen. According to the results, at least two *MtRSZ22* homologs are responsive to RiSP749, as they are significantly reduced by RiSP749 in mock conditions and strongly increased in mycorrhized RiSP749OE samples when corrected for the level of colonization. Hence, *MtRSZ21* and *MtRSZ22b* expression is most likely influenced by RiSP749, although it is probably not the only fungal factor affecting their expression. Other fungal proteins may be necessary to control their transcriptional levels. Target redundancy is common in microbial effectors (Ghosh & O'Connor, 2017), explaining why the presence of the fungus alter the expression of *MtRSZ21*, *MtRSZ22a* and *MtRSZ22b*. For example, different TAL effectors from *Xanthomonas oryzae* regulates Os11N3 (Pérez-Quintero *et al*, 2013). Alternatively, the lower chromatin condensation level observed in mycorrhized cortical

cells may facilitate the induction of *MtRSZ21*, *MtRSZ22a* and *MtRSZ22b* expression by RiSP749 (Lingua *et al*, 2001).

MtGNAT homologs are slightly induced by mycorrhization in GFPTurbo lines and by RiSP749 in mock conditions, but not affected by RiSP749 in mycorrhization conditions. In general, the changes in expression of *MtGNATYoaA*, *MtGNATa* and *MtGNATb* are less pronounced compared with the *MtSRZ* homologs. In addition, we found that SIGNAT did not interact with RiSP749 in planta and in vitro. Hence, although an induction in GFPTurbo plants is seen upon mycorrhization, no further conclusions are made in relation to RiSP749. Perhaps, the changes in expression in mycorrhized GFPTurbo lines might be due to a role of these GNAT proteins in mycorrhization, although independent to RiSP749, but this is not evident in WT *M. truncatula* plants. However, the expression pattern of *MtGNATb* is in concordance with the information found in LEGOO. According to LEGOO database, *MtGNATb* is induced upon treatment with Myc factors but repressed later by AMF while our results showed a small induction of *MtGNATb* at early time points that disappeared later on, supporting this information.

First of all, to make these results more robust, a higher number of plants should be evaluated, to ensure that these results are not an artefact due to the intrinsic biological variability. Moreover, before further hypothesizing on these transcriptional responses, it is of utmost importance to first confirm whether and which of these *M. truncatula* homologous proteins are real targets of RiSP749 during mycorrhization and the nature of their interaction as it is possible that RiSP749 does not influence the expression level of these proteins but rather acts at protein level sequestering the proteins or altering its post translational modification state as seen for previous AMF effectors (SP7 and RiNLE1) (Kloppholz *et al*, 2011; Wang *et al*, 2021). If RiSP749 acts at the transcript level of *MtRSZ* homologous genes, we should expect a similar expression pattern for the fungal effector and the host plant genes, i.e. both decreased over time in mycorrhized WT plants, although the decrease of *MtRSZ* is not significant and parallel to a decrease in mock conditions. However, we do see a change in transcript levels upon RiSP749 OE both in mock and mycorrhiza condition, indicating an influence of RiSP749 on *MtRSZ* genes expression. Nevertheless, RiSP749 may act at the protein level changing the activity of SIRSZ22 by sequestering it (Real *et al*, 2017; De Jonge *et al*, 2010), modifying their targets by altering the cis-elements recognized by SIRSZ22 or the snRNP proteins that bind to the spliceosome complex (Ahmed *et al*, 2018) or marking it for degradation (Abramovitch *et al*, 2006). Therefore, further studies at the protein level are important to understand the consequences of the RiSP749 interaction with SIRSZ22. Changes in the spliceosome complex could be evaluated by coIP followed by mass spectrometry (MS) of SIRSZZ interacting proteins in presence or absence of RiSP749, while changes in the recognized cis-element could be by purifying the spliceosome complex and put it in presence of a synthesized pre-mRNA containing the cis-elements recognized by SIRSZ22 and analyzing changes in splicing activity in presence or absence of RiSP749.

5. *SIRSZ22* silencing increased AM colonization in tomato

Preliminary experiments demonstrated that silencing of *SIRSZ22* might cause an increase in tomato mycorrhization according to higher expression levels of the *R. irregularis* housekeeping gene *RiEF1 α* . *RiSP749* is also more highly expressed in *SIRSZ22* silenced tomato plants compared with EV control plants. Likewise, the symbiotic marker genes, *SIPT4*, *SIPT5* and *SIRAM1*, are upregulated in *SIRSZ22* silenced roots, although this upregulation disappears when expression is normalized to *RiEF1 α* .

The increased transcript levels of *RiEF1 α* in *SIRSZ22* silenced roots indicates that *SIRSZ22* has a negative role in mycorrhization. This result is in accordance with *RiSP749* OE in *M. truncatula*. In *M. truncatula* the overexpression of *RiSP749* induces *SIRSZ22* *M. truncatula* homologs, and colonization levels and *RiEF1 α* expression was reduced, while in tomato the downregulation of *SIRSZ22* increases *RiEF1 α* expression. Accordingly, *SIPT4*, *SIPT5* and *SIRAM1* expression levels were also higher in *SIRSZ22* silencing lines in accordance to what has been seen for *RiSP749* OE in *M. truncatula*. However, when we corrected by the level of colonization normalizing against the fungal HKG *RiEF1 α* the opposite tendency was seen. However, unlike with the normalization against the plant HKG *SIGADPH* and *SIEF1 α* , these differences are not significant. This suggests that the increase in *SIPT4*, *SIPT5* and *SIRAM1* is due to the increased colonization level but in arbuscules, equal amounts of transcripts of these marker genes are present both in *SIRSZ22* RNAi line and control. However, no phenotypic analysis of the colonization rate of these plants were done. Hence, it is possible that the higher level of *RiEF1 α* in *SIRSZ22* RNAi lines is due to higher rates of extraradical mycelium and not higher colonization percentages, thus fungal symbiosis genes such as the N transporter *AMT1* expressed in arbuscules may be better for normalization.

These results are only preliminary, additional experiments have to be performed in which more plants should be evaluated. Additionally, *SIRSZ22* could be overexpressed to check if there is a reduction in mycorrhization, confirming that *SIRSZ22* is a negative regulator of mycorrhization. In Toon Leroy master thesis, not significant differences of *SIRSZ22* were reported at different time points, 2, 4 and 6 wpi. This suggests that its role in mycorrhization is more likely exerted by a shift in its activity than by differences in its expression. Studying the interactome of this protein would provide a better understanding of its possible role in mycorrhization.

6. Conclusions

Based on the current results, we propose three models of the role of *RiSP749* OE during mycorrhization in *M. truncatula* AM symbiosis establishment (Figure 21). In the first model, we hypothesize that *RiSP749* is involved in the early stages of mycorrhization, probably controlling the intraradical hyphal elongation as it acts at the transcriptional level of early CSSP genes involved in Myc factor detection and hyphopodium formation (*MtNIN* and *MtNSP2*), root penetration (*MtCYCLOPS*), hyphal growth and branching (*MtNSP2*) and cortical cell expansion (*MtDELLA1*). When *RiSP749* is constitutively OE, the fungus experiences **difficulties in hyphal elongation**, arbuscules start to be formed in the outer layers of the cortex, compared with the GFPTurbo OE control, and colonization is more compact around each entry point of the fungus (Figure 21B). Hence, the expression of *MtPT4* and *MtRAM1* are reduced when the complete root system is harvested for RNA. To prove this hypothesis, a higher number of entry points and

colonization units should be observed in RiSP749 OE lines, and can be analyzed in e.g. earlier time points. In the second model, we hypothesized that the **functionality of the arbuscules** is impaired in the RiSP749 OE lines, by which more arbuscules are formed. The low expression levels of *MtPT4* and *MtRAM1* in RiSP749 OE lines suggests that constitutive expression of *RiSP749* prevents the formation of functional arbuscules and, thus, complete symbiosis. Therefore, the fungus keeps forming new arbuscules, filling also the outer layers of the root cortex to compensate for it (Figure 21C). In the last model, a combination of the previous models can happen, it is possible that RiSP749 OE results in **arbuscules in the outer layers due to the problems in hyphal elongation** and, at the same time, the formed arbuscules are **not functional** because of an impaired CSSP pathway. Alternatively, arbuscules located in outer layers may have a lower supply of nutrients as the passive diffusion of the nutrients from the vascular system is slow and hindered by the presence of the Casparian strip in the endodermis, reducing the arbuscule functionality (Kaiser *et al*, 2015). Hence, testing the functionality of arbuscules and the distribution of nutrients in the plant root by stable isotopes of carbon (^{13}C) and N (^{15}N) would be interesting to confirm or refuse this last **combined model** (Kilburn *et al.*, 2010; Figure 21D). Finally, RiSP749 interacts with SIRSZ22 in the nucleus of the host plant cell, as RSZ proteins are involved in mRNA processing, RiSP749 probably alters the mRNA processing or changes the target mRNAs of SIRSZ22 by which the interaction modifies gene expression during mycorrhization. However, a lower expression of *SIRSZ22* in *slrsz22* silenced lines does not seem to be responsible in modifying arbuscule specific genes (*SIPT4*, *SIPT5*, and *SIRAM1*), but might be affecting CSSP genes, which still need to be tested.

Taken together, although further experiments are necessary to prove the different hypothesis, and to untangle the mode-of-action of RiSP749 during *M. truncatula* and tomato mycorrhization, the results obtained in this thesis suggests that RiSP749 is an real effector of *R. irregularis* with a role during mycorrhization at least partly exerted by interacting with the splicing factors from the RSZ family in tomato and *M. truncatula*.

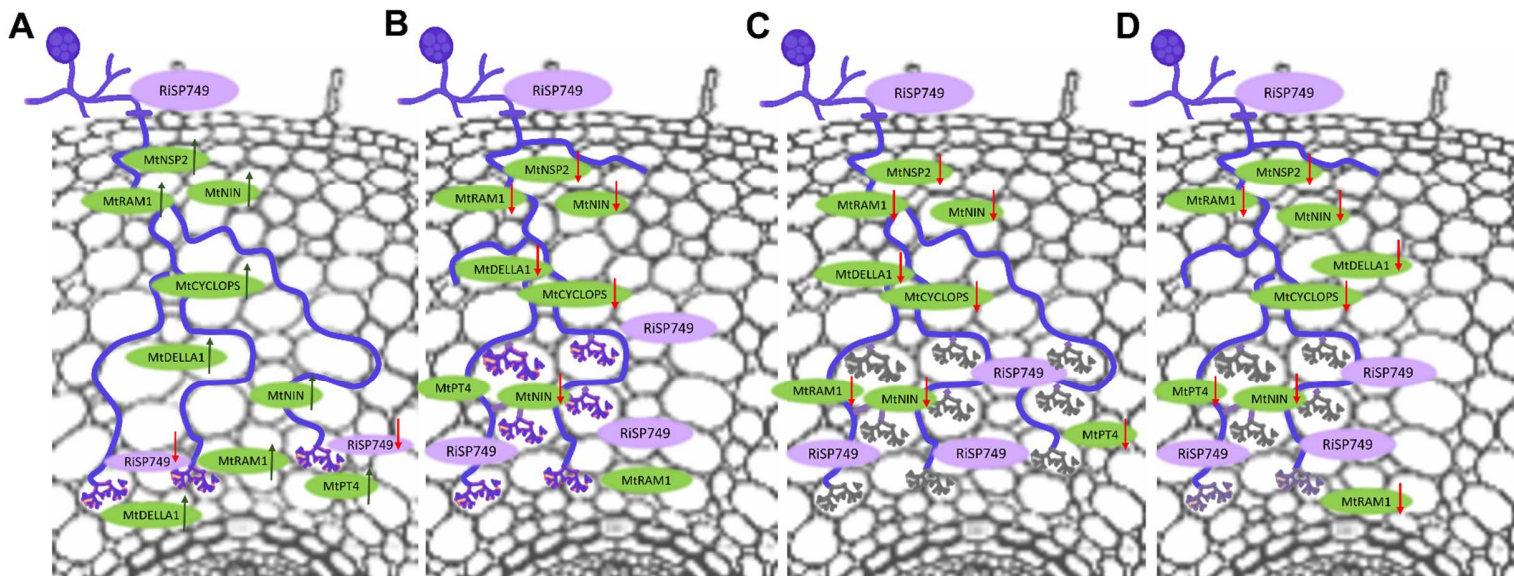


Figure 21: Hypothetical models of the role of RiSP749 in mycorrhization of *M. truncatula*. (A) *M. truncatula* colonization by *R. irregularis* and RiSP749 regulation of mycorrhization in wild-type conditions. (B) *M. truncatula* colonization by *R. irregularis* in roots overexpression RiSP749. Hyphal progression is restricted and more layers of arbuscules are formed. (C) *M. truncatula* colonization by *R. irregularis* in roots overexpression RiSP749. Arbuscules are not functional (grey) and more layers of arbuscules are formed (D) *M. truncatula* colonization by *R. irregularis* in roots overexpression RiSP749. Hyphal progression is restricted and more layers of arbuscules are formed, besides arbuscules are not functional, especially the ones more distant from the vascular bundle. Plant genes are indicated in green and the arrows indicate changes in their expression (green arrow = increased expression; red arrow = reduced expression normalized to plant housekeeping genes and compared to GFPTurbo mock).

Part 5: Materials and Methods

1. Plant and fungal material

M. truncatula plants Jemalong A17 were sterilized in concentrated sulphuric acid (96%) for 8 min, followed by six washes in sterile water, and incubation in 12% hypochlorite (commercial bleach) for 3 min and final washes in sterile water. Next, seeds were incubated in 1mg/l solution of 6-benzylaminopurine (BAP) at room temperature for three hours, washed three times with water and transferred to a Petri dish with filter papers for germination. After three days germinating in the dark at 21°C, seedlings were used for growth experiments or hairy root transformations. Tomato (*Solanum lycopersicum* cultivar MoneyMaker) seeds were sterilized in 4% hypochlorite (commercial bleach) for 15 min, washed three times in sterile water and transferred to Petri dishes with filter papers for germination for five days in the dark at 21°C.

M. truncatula plants were grown in pots of 14 cm in a mix of sand and vermiculite (1:1) at 21°C in long day conditions (16 h light, 8 h dark). Tomato plants were grown in pots of 16 cm in a mix of sand and vermiculite (1:2) at 24°C in long day conditions (16 h light, 8 h dark). *M. truncatula* and tomato plants were watered with 25 ml or 50 ml Hewitt solution (Hewitt, 1996) twice per week, respectively. *M. truncatula* and tomato plants were harvested at 5 wpi unless stated otherwise. The transgenic root system of each independent composite plant was taken as an independent repeat except for the time series experiments in which three to four WT *M. truncatula* plants were grown and pooled as one independent biological repeat sample.

Rhizophagus irregularis DAOM197198 spores were obtained from Agronutrition, France. To remove the conservation solution, spores were centrifuged for 15 min at 4°C, washed with sterile water, centrifuged again for 15 min, and resuspended in Hewitt solution (Hewitt, 1996). Plants were inoculated with three hundred spores per plant.

2. Cloning

Table S2 (Addendum) contains all the cloned genes, the vectors and the cloning methods. Gateway cloning (Reece-Hoyes & Walhout, 2018) and Golden Gate cloning (Green Gate system for plants; (Lampropoulos *et al*, 2013), were used according to the manufacturers description, and depending on the experiment. *Escherichia coli* DH5 α was used for the amplification of the plasmids, and ORF sequences of all newly cloned genes were confirmed by sequencing (Eurofins). The ORFs of *SIRSZ22* and *SIGNAT* from tomato and their *M. truncatula* homologs *MtRSZ21*, *MtRSZ22a*, *MtRSZ22b*, *MtGNATyaaA*, *MtGNATa* and *MtGNATb* were obtained from cDNA extracted from WT plants of tomato or *M. truncatula*, respectively, and cloned with Gateway specific primers to introduce them into the pDONR vector of interest. The ORF of RiSP749 was cloned from an in-house available vector with Gateway specific primers to introduce it into the donor vectors pDONR207 or the pDONR201 P1P4. For the construction of the rBiFC constructs, n-YFP-SIRSZ22 and c-YFP-RiSP749 in pBiFC-NN2in1, and n-YFP-SIGNAT and c-YFP-RiSP749 in pBiFCNN-2in1, Multisite Gateway cloning was used. The Y2H vectors with RiSP749, SIRSZ22 and SIGNAT, and vectors for co-localization assays (eCFP-tagged interactor proteins in the pK7WGC2 destination vector) were already available in-house and have been generated by Gateway cloning (Master thesis T. Leroy). The *M. truncatula* *MtRSZ21*, *MtRSZ22a*, *MtRSZ22b* and *MtGNATb*

interactors were cloned into the *pGADT7* vector for Y2H by Gateway cloning. For the overexpression of *RiSP749* and its control *GFPTurbo OE* in transgenic *M. truncatula* roots, the *35S::RiSP749-GFPTurbo:RoID_mRuby* and *35S::GFPTurbo:RoID_mRuby* constructs were available in-house and have been generated by Golden Gate cloning (Supervisor J. Van Dingenen). RNAi lines of *SIRSZ22* were generated by a hairpin construct to induce knock-down of *SIRSZ22*. For this, 140 bp long fragment in the middle of the ORF was selected and cloned from tomato cDNA with Gateway specific primers into pDONR207 and then introduced in pK7gwiwg2D Red root vector through LR Gateway reaction. Finally, the pGUS reporter lines were generated cloning the promoters (1Kb and 3Kb) upstream the ATG code of the *SIGNAT* ORF from tomato genomic DNA with specific primers to introduce it by Gibson cloning into pGGA and using a Golden gate reaction to introduce it into the final vectors pGGA-G to generate *pSIGNAT-1kb::GUS-GFP::RoID_mRuby* and *pSIGNAT-3kb::GUS-GFP::RoID_mRuby*.

3. *In silico* analysis

For the phylogenetic analysis of *SIRSZ22* and *SIGNAT* in *M. truncatula*, tomato and *A. thaliana* we used blastP algorithm from NCBI (Addendum Table S1). The selection of the candidate *M. truncatula* homologs of *SIRSZ22* and *SIGNAT* was done considering the identity %, e-value ($<10^{-10}$) and the presence of the conserved domains (RRM and Acetyltransferase, respectively) using PFAM. The effector *RiSP749* characteristics were studied using LOCALIZER for the NLS (Sperschneider *et al*, 2017), the fungal secretome database (Choi *et al*, 2010), the TargetP-2.0 and the SignalP-5.0 for the signal peptide (Armenteros *et al*, 2019; Almagro Armenteros *et al*, 2019), and ApoplastP for the non-apoplastic localization (Sperschneider *et al*, 2018).

4. Yeast-two-hybrid (Y2H) assay

In order to test the interaction between *RiSP749* and the tomato or *M. truncatula* interactors, both bait (Interactor *pGADT7*) and prey (*RiSP749 pGBKT7*) vectors (Addendum Table S2) were co-transformed in *Saccharomyces cerevisiae* strain PJ69-4a (MATa; *trp1-901*; *leu2-3,112*; *ura3-52*; *his3-200*; *gal4Δ*; *gal80Δ*; *Met2::GAL7-lacZ*; *LYS2::GAL1-HIS3*; *GAL2-ADE2*) by PEG/Lithium acetate method as described in (Fields & Song, 1989). Five transformed colonies were selected on Yeast minimal Synthetic Defined (SD) media without Leucine (L) and Threonine (T) (SD-LT) (Takara) and three of each bait-prey combination were dropped in five serial dilutions (1 , 10^{-1} , 10^{-2} , 10^{-3} and 10^{-4}) on control and selective media SD without L, T and histidine (H) (SD-LTH) supplemented with increasing concentrations of 3-amino-1,2,4-triazole (3-AT) (2.5, 5 and 10mM). Plates were incubated for three days at 30°C, and growth was evaluated.

5. Transient expression of proteins in leaves of *Nicotiana benthamiana*

5.1. Ratiometric bimolecular fluorescent complementation (BiFC)

Agrobacterium tumefaciens strain C58C1 was transformed with pBiFCt-2in1-NN (*SIRSZ22/RiSP749*) or pBiFCt-2in1-NN (*SIGNAT/RiSP749*) (Grefen & Blatt, 2012) to study the interaction of *RiSP749* and the tomato proteins *SIRSZ22* and *SIGNAT* *in planta*. pBiFCt-2in1-NN (*AtMAX2/AtSKP1*) was used as a positive control and pBiFCt-2in1-NN (*Solyc07g045450/RiSP190*) as a negative control for interaction. Leaves of four weeks old *Nicotiana benthamiana* (tobacco) plants were used for transient expression of the construct by *A. tumefaciens* mediated

transformation together with *35SP:p19:NosT* to prevent silencing of the constructs. Two days after infiltration, the interactions were examined by imaging using the confocal microscope Zeiss LSM 710 using the 40X magnification lens. The ratio between the yellow fluorescence signal and the background red fluorescence signal was determined in the nuclei of the cells expressing both constructs, to quantify the interaction.

5.2. Colocalization

Agrobacterium tumefaciens strain C58C1 was transformed with 35S:: RiSP749-GFP Turbo:RoID_mRuby, 35S:: SIRSZ22-eCFP: RoID_mRuby or 35S:: SIGNAT-eCFP:RoID_mRuby alone or in combination in order to check the subcellular localization of RiSP749 and its tomato interactors SIRSZ22 and SIGNAT. Leaves of four weeks old *Nicotiana benthamiana* (tobacco) plants were used for transient expression of the construct by *A. tumefaciens* mediated transformation together with *35SP:p19:NosT* to prevent silencing of the constructs. Two days after infiltration, imaging was done using the confocal microscope Zeiss LSM 710 using 20X magnification.

6. Generation of *M. truncatula* and tomato hairy root composite plants

RiSP749 was overexpressed to determine its role in mycorrhization of *M. truncatula*. For that purpose 35S:: *RiSP749-GFP Turbo:RoID_mRuby* and 35S:: *GFP Turbo:RoID_mRuby* constructs were used. To study the involvement of SIRSZ22 in tomato mycorrhization we used the RNAi hairpin construct introduced in the pK7gwiwg2D Red Root vector. Empty pK7gwiwg2D Red Root vector was used as control. All vectors were introduced into *Agrobacterium rhizogenes* strain ARQUA and used to transform *M. truncatula* or tomato seedlings by hairy root transformation (Boisson-Dernier *et al*, 2007). In short, the root tip was cut with a sterile scalpel from seedlings with a radicle length of approximately 10 mm, and scraped through the desired ARQUA colony. The seedlings were grown for one week in Murashige & Skoog (MS) media (Rezali *et al*, 2017) at 21°C, and transformed roots were weekly scored, non-transformed roots were excised and transgenic roots were selected under the fluorescence microscope based on the expression of the fluorescent tag. After four weeks, the hairy root transformed composite plants were transferred to pots and inoculated with *R. irregularis* for four to five weeks.

7. GUS staining and analysis

In order to localize the expression of *SIGNAT* and to determine the activity of its promoter, a short version of the promoter that contained only 1kb upstream of the starting codon of *SIGNAT* (pLOC101247959-1kb::GUS-GFP: RoID_mRuby) and a long version of 3kb (pLOC101247959-3kb::GUS-GFP: RoID_mRuby) were used to generate tomato composite plants. As control, we used the GUS driven by CaMV 35S promoter. Composite plants expressing these constructs were harvested at 5 wpi. Part of the root system of each plant was used for checking colonization and the other part was immersed in X-Gluc NT buffer and incubated at 37°C for four hours allowing GUS staining (Hong, 2000). Imaging of the mock and mycorrhized GUS stained roots was performed with the light microscope LEICA df.

8. Colonization analysis, ink staining and Trouvelot method

R. irregularis root colonization was evaluated according to the Trouvelot method (Vierheilig *et al*, 1998a) in ink coloured plant roots. Ink binds to the chitin present in the cell wall of the fungus staining the fungal structures and allowing its visualization under the light microscope. Roots are firstly permeabilized using 10% KOH and then stained in a solution of 2% ink in 5% acetic acid. To avoid decoloring and dehydration of the roots, the root system was immersed and maintained in 50% glycerol. Thirty slices of 1 cm each were examined per plant and the frequency of mycorrhiza in the root system (F%), the intensity of the mycorrhizal colonization in the root system (M%), the intensity of the mycorrhizal colonization in the root fragments (m%), the arbuscule abundance in mycorrhizal parts of the root fragments (a%) and the arbuscule abundance in the root system (A%) were determined according to Trouvelot (Vierheilig *et al*, 1998a).

9. RNA extraction, cDNA synthesis and qRT-PCR analysis

Total RNA from plant roots was extracted using the ReliaPrep RNA tissue Miniprep kit (Promega). The qScript cDNA supermix from Quanta biosciences was used to synthesize cDNA from 100 to 500 ng/ μ l RNA. The quantity and quality of RNA was measured with NanoDrop One (ThermoFisher). qRT-PCR was done on the LightCycler 480 with SYBR Green I master mix (Roche). Normalization was done against the geomean of the following housekeeping genes: *MtTUB1* and *MtGADPH* for *M. truncatula* experiments, and *SIGADPH* and *SIEF1 α* for tomato experiments. The primers used in these experiments are included in Addendum Table S3.

References

- Abramovitch RB, Janjusevic R, Stebbins CE & Martin GB (2006) Type III effector AvrPtoB requires intrinsic E3 ubiquitin ligase activity to suppress plant cell death and immunity. *Proc Natl Acad Sci U S A* 103: 2851–2856
- Ahmed MB, Santos KCG dos, Sanchez IB, Petre B, Lorrain C, Plourde MB, Duplessis S, Desgagné-Penix I & Germain H (2018) A rust fungal effector binds plant DNA and modulates transcription. *Sci Reports* 2018 8: 1–14
- Akiyama K, Matsuzaki KI & Hayashi H (2005) Plant sesquiterpenes induce hyphal branching in arbuscular mycorrhizal fungi. *Nature* 435: 824–827
- Almagro Armenteros JJ, Tsirigos KD, Sønderby CK, Petersen TN, Winther O, Brunak S, von Heijne G & Nielsen H (2019) SignalP 5.0 improves signal peptide predictions using deep neural networks. *Nat Biotechnol* 37: 420–423
- Amani Machiani M, Javanmard A, Morshedloo MR, Aghaee A & Maggi F (2021) Funneliformis mosseae inoculation under water deficit stress improves the yield and phytochemical characteristics of thyme in intercropping with soybean. *Sci Reports* 2021 11: 1–13
- An J, Zeng T, Ji C, de Graaf S, Zheng Z, Xiao TT, Deng X, Xiao S, Bisseling T, Limpens E, *et al* (2019) A Medicago truncatula SWEET transporter implicated in arbuscule maintenance during arbuscular mycorrhizal symbiosis. *New Phytol* 224: 396–408
- Angelard C, Colard A, Niculita-Hirzel H, Croll D & Sanders IR (2010) Segregation in a mycorrhizal fungus alters rice growth and symbiosis-specific gene transcription. *Curr Biol* 20: 1216–1221
- Antolín-Llovera M, Ried MK & Parniske M (2014) Cleavage of the SYMBIOSIS RECEPTOR-LIKE KINASE ectodomain promotes complex formation with Nod factor receptor 5. *Curr Biol* 24: 422–427
- Armbruster L, Linster E, Boyer JB, Brünje A, Eirich J, Stephan I, Bienvenut W V., Weidenhausen J, Meinel T, Hell R, *et al* (2020) NAA50 Is an Enzymatically Active N α -Acetyltransferase That Is Crucial for Development and Regulation of Stress Responses. *Plant Physiol* 183: 1502–1516
- Armenteros JJA, Salvatore M, Emanuelsson O, Winther O, Von Heijne G, Elofsson A & Nielsen H (2019) Detecting sequence signals in targeting peptides using deep learning. *Life Sci alliance* 2
- Avio L, Pellegrino E, Bonari E & Giovannetti M (2006) Functional diversity of arbuscular mycorrhizal fungal isolates in relation to extraradical mycelial networks. *New Phytol* 172: 347–357
- Badri A, Stefani FOP, Lachance G, Roy-Arcand L, Beaudet D, Vialle A & Hijri M (2016) Molecular diagnostic toolkit for Rhizophagus irregularis isolate DAOM-197198 using quantitative PCR assay targeting the mitochondrial genome. *Mycorrhiza* 26: 721–733
- Bago B, Pfeffer PE & Shachar-Hill Y (2000) Carbon metabolism and transport in arbuscular mycorrhizas. *Plant Physiol* 124: 949–957
- Balestrini R & Fiorilli V (2020) Laser Microdissection as a Useful Tool to Study Gene Expression in Plant and Fungal Partners in AM Symbiosis. *Methods Mol Biol* 2146: 171–184
- Balliu A, Sallaku G & Rewald B (2015) AMF Inoculation Enhances Growth and Improves the Nutrient Uptake Rates of Transplanted, Salt-Stressed Tomato Seedlings. *Sustain* 2015, Vol 7, Pages 15967-15981 7: 15967–15981
- Balergue C, Chabaud M, Barker DG, Bécard G & Rochange SF (2013) High phosphate reduces host ability to develop arbuscular mycorrhizal symbiosis without affecting root calcium spiking responses to the fungus. *Front Plant Sci* 4
- Balergue C, Puech-Pags V, Bécard G & Rochange SF (2011) The regulation of arbuscular mycorrhizal symbiosis by

- phosphate in pea involves early and systemic signalling events. *J Exp Bot* 62: 1049–1060
- Banasiak J, Borghi L, Stec N, Martinoia E & Jasiński M (2020) The Full-Size ABCG Transporter of *Medicago truncatula* Is Involved in Strigolactone Secretion, Affecting Arbuscular Mycorrhiza. *Front Plant Sci* 11: 1
- Banasiak J, Jamruszka T, Murray JD & Jasinski M (2021) A roadmap of plant membrane transporters in arbuscular mycorrhizal and legume–rhizobium symbioses. *Plant Physiol* 187: 2071–2091
- Banba M, Gutjahr C, Miyao A, Hirochika H, Paszkowski U, Kouchi H & Imaizumi-Anraku H (2008) Divergence of Evolutionary Ways Among Common sym Genes: CASTOR and CCaMK Show Functional Conservation Between Two Symbiosis Systems and Constitute the Root of a Common Signaling Pathway. *Plant Cell Physiol* 49: 1659–1671
- De Bang TC, Lundquist PK, Dai X, Boschiero C, Zhuang Z, Pant P, Torres-Jerez I, Roy S, Nogales J, Veerappan V, *et al* (2017) Genome-Wide Identification of *Medicago* Peptides Involved in Macronutrient Responses and Nodulation. *Plant Physiol* 175: 1669
- Bari R & Jones JDG (2009) Role of plant hormones in plant defence responses. *Plant Mol Biol* 69: 473–488
- Barta A, Kalyna M & Reddy ASN (2010) Implementing a Rational and Consistent Nomenclature for Serine/Arginine-Rich Protein Splicing Factors (SR Proteins) in Plants. *Plant Cell* 22: 2926
- Benedito VA, Torres-Jerez I, Murray JD, Andriankaja A, Allen S, Kakar K, Wandrey M, Verdier J, Zuber H, Ott T, *et al* (2008) A gene expression atlas of the model legume *Medicago truncatula*. *Plant J* 55: 504–513
- Besserer A, Puech-Pagès V, Kiefer P, Gomez-Roldan V, Jauneau A, Roy S, Portais JC, Roux C, Bécard G & Séjalon-Delmas N (2006) Strigolactones Stimulate Arbuscular Mycorrhizal Fungi by Activating Mitochondria. *PLoS Biol* 4: 1239–1247
- Bhattacharjee RB, Singh A & Mukhopadhyay SN (2008) Use of nitrogen-fixing bacteria as biofertiliser for non-legumes: prospects and challenges. *Appl Microbiol Biotechnol* 80: 199–209
- Bi K, Scalschi L, Jaiswal N, Mengiste T, Fried R, Sanz AB, Arroyo J, Zhu W, Masrati G & Sharon A (2021) The Botrytis cinerea Crh1 transglycosylase is a cytoplasmic effector triggering plant cell death and defense response. *Nat Commun* 2021 12: 1–15
- Bitterlich M, Krügel U, Boldt-Burisch K, Franken P & Kühn C (2014) The sucrose transporter SISUT2 from tomato interacts with brassinosteroid functioning and affects arbuscular mycorrhiza formation. *Plant J* 78: 877–889
- Bilou I, Bueno P, Ocampo JA & Garcia-Garrido JM (2000) Induction of catalase and ascorbate peroxidase activities in tobacco roots inoculated with the arbuscular mycorrhizal *Glomus mosseae*. *Mycol Res* 104: 722–725
- Bilou I, Ocampo JA & García-Garrido JM (1999) Resistance of pea roots to endomycorrhizal fungus or Rhizobium correlates with enhanced levels of endogenous salicylic acid. *J Exp Bot* 50: 1663–1668
- Boisson-Dernier A, Chabaud M, Garcia F, Bécard G, Rosenberg C & Barker DG (2007) *Agrobacterium rhizogenes*-Transformed Roots of *Medicago truncatula* for the Study of Nitrogen-Fixing and Endomycorrhizal Symbiotic Associations. <http://dx.doi.org/10.1094/MPMI2001146695> 14: 695–700
- Boller T & Felix G (2009) A Renaissance of Elicitors: Perception of Microbe-Associated Molecular Patterns and Danger Signals by Pattern-Recognition Receptors. <http://dx.doi.org/10.1146/annurev.arplant.57.032905.105346> 60: 379–407
- Bona E, Cantamessa S, Massa N, Manassero P, Marsano F, Copetta A, Lingua G, D'Agostino G, Gamalero E & Berta G (2017) Arbuscular mycorrhizal fungi and plant growth-promoting pseudomonads improve yield, quality and nutritional value of tomato: a field study. *Mycorrhiza* 27: 1–11
- Bozkurt TO, Schornack S, Win J, Shindo T, Ilyas M, Oliva R, Cano LM, Jones AME, Huitema E, Van Der Hoorn RAL, *et*

- al (2011) Phytophthora infestans effector AVRblb2 prevents secretion of a plant immune protease at the haustorial interface. *Proc Natl Acad Sci U S A* 108: 20832–20837
- Bravo A, Brands M, Wewer V, Dörmann P & Harrison MJ (2017) Arbuscular mycorrhiza-specific enzymes FatM and RAM2 fine-tune lipid biosynthesis to promote development of arbuscular mycorrhiza. *New Phytol* 214: 1631–1645
- Buendia L, Wang T, Girardin A & Lefebvre B (2016) The LysM receptor-like kinase SILYK10 regulates the arbuscular mycorrhizal symbiosis in tomato. *New Phytol* 210: 184–195
- Burleigh SH, Cavagnaro T & Jakobsen I (2002) Functional diversity of arbuscular mycorrhizas extends to the expression of plant genes involved in P nutrition. *J Exp Bot* 53: 1593–1601
- Caillaud MC, Asai S, Rallapalli G, Piquerez S, Fabro G & Jones JDG (2013) A Downy Mildew Effector Attenuates Salicylic Acid-Triggered Immunity in Arabidopsis by Interacting with the Host Mediator Complex. *PLoS Biol* 11: e1001732
- Cakmak I (2002) Plant nutrition research: Priorities to meet human needs for food in sustainable ways. *Plant Soil* 202 2471 247: 3–24
- Calabrese S, Pérez-Tienda J, Ellerbeck M, Arnould C, Chatagnier O, Boller T, Schüßler A, Brachmann A, Wipf D, Ferrol N, et al (2016) GintAMT3-a low-affinity ammonium transporter of the arbuscular mycorrhizal rhizophagus irregularis. *Front Plant Sci* 7: 679
- Calvo-Polanco M, Molina S, Zamarreño AM, García-Mina JM & Aroca R (2014) The Symbiosis with the Arbuscular Mycorrhizal Fungus Rhizophagus irregularis Drives Root Water Transport in Flooded Tomato Plants. *Plant Cell Physiol* 55: 1017–1029
- Camps C, Jardinaud MF, Rengel D, Carrère S, Hervé C, Debellé F, Gamas P, Bensmihen S & Gough C (2015) Combined genetic and transcriptomic analysis reveals three major signalling pathways activated by Myc-LCOs in Medicago truncatula. *New Phytol* 208: 224–240
- Capoen W, Sun J, Wysham D, Otegui MS, Venkateshwaran M, Hirsch S, Miwa H, Downie JA, Morris RJ, Ané JM, et al (2011) Nuclear membranes control symbiotic calcium signaling of legumes. *Proc Natl Acad Sci U S A* 108: 14348–14353
- Carotenuto G & Genre A (2020) Fluorescent Staining of Arbuscular Mycorrhizal Structures Using Wheat Germ Agglutinin (WGA) and Propidium Iodide. *Methods Mol Biol* 2146: 53–59
- Carrère S, Verdenaud M, Gough C, Gouzy J & Gamas P (2020) LeGOO: An Expertized Knowledge Database for the Model Legume Medicago truncatula. *Plant Cell Physiol* 61: 203–211
- Chen A, Chen X, Wang H, Liao D, Gu M, Qu H, Sun S & Xu G (2014) Genome-wide investigation and expression analysis suggest diverse roles and genetic redundancy of Pht1 family genes in response to Pi deficiency in tomato. *BMC Plant Biol* 14: 61
- Chen M, Arato M, Borghi L, Nouri E & Reinhardt D (2018) Beneficial services of arbuscular mycorrhizal fungi – from ecology to application. *Front Plant Sci* 9: 1270
- Cheng W, Lin M, Chu M, Xiang G, Guo J, Jiang Y, Guan D & He S (2022) RNAi-Based Gene Silencing of RXLR Effectors Protects Plants Against the Oomycete Pathogen Phytophthora capsici.
- Chialva M, Zouari I, Salvioli A, Novero M, Vrebalov J, Giovannoni JJ & Bonfante P (2016) Gr and hp-1 tomato mutants unveil unprecedented interactions between arbuscular mycorrhizal symbiosis and fruit ripening. *Planta* 244: 155–165
- Chitarra W, Pagliarani C, Maserti B, Lumini E, Siciliano I, Cascone P, Schubert A, Gambino G, Balestrini R & Guerrieri E (2016) Insights on the Impact of Arbuscular Mycorrhizal Symbiosis on Tomato Tolerance to Water Stress.

- Plant Physiol* 171: 1009–1023
- Choi J, Park J, Kim D, Jung K, Kang S & Lee YH (2010) Fungal Secretome Database: Integrated platform for annotation of fungal secretomes. *BMC Genomics* 11: 1–15
- Croll D, Wille L, Gamper HA, Mathimaran N, Lammers PJ, Corradi N & Sanders IR (2008) Genetic diversity and host plant preferences revealed by simple sequence repeat and mitochondrial markers in a population of the arbuscular mycorrhizal fungus *Glomus intraradices*. *New Phytol* 178: 672–687
- Delaux PM, Bécard G & Combier JP (2013) NSP1 is a component of the Myc signaling pathway. *New Phytol* 199: 59–65
- Diagne N, Ngom M, Djighaly PI, Fall D, Hocher V & Svistoonoff S (2020) Roles of Arbuscular Mycorrhizal Fungi on Plant Growth and Performance: Importance in Biotic and Abiotic Stressed Regulation. *Divers 2020, Vol 12, Page 370* 12: 370
- Dickson S (2004) The Arum–Paris continuum of mycorrhizal symbioses. *New Phytol* 163: 187–200
- Dickson S, Smith FA & Smith SE (2007) Structural differences in arbuscular mycorrhizal symbioses: more than 100 years after Gallaud, where next? *Mycorrhiza* 17: 375–393
- Duc NH, Csintalan Z & Posta K (2018) Arbuscular mycorrhizal fungi mitigate negative effects of combined drought and heat stress on tomato plants. *Plant Physiol Biochem* 132: 297–307
- Erfelinc ML, Ribeiro B, Perassolo M, Pauwels L, Pollier J, Storme V & Goossens A (2018) A user-friendly platform for yeast two-hybrid library screening using next generation sequencing. *PLoS One* 13
- Van Esse HP, Van't Klooster JW, Bolton MD, Yadeta KA, Van Baarlen P, Boeren S, Vervoort J, Dewit PJGM & Thomma BPHJ (2008) The *Cladosporium fulvum* Virulence Protein Avr2 Inhibits Host Proteases Required for Basal Defense. *Plant Cell* 20: 1948–1963
- Etesami H, Jeong BR & Glick BR (2021) Contribution of Arbuscular Mycorrhizal Fungi, Phosphate–Solubilizing Bacteria, and Silicon to P Uptake by Plant. *Front Plant Sci* 12: 1355
- Fabre G, Garroum I, Mazurek S, Daraspe J, Mucciolo A, Sankar M, Humbel BM & Nawrath C (2016) The ABCG transporter PEC1/ABCG32 is required for the formation of the developing leaf cuticle in *Arabidopsis*. *New Phytol* 209: 192–201
- Fan Z, Lin S, Zhang X, Jiang Z, Yang K, Jian D, Chen Y, Li J, Chen Q & Wang J (2014) Conventional flooding irrigation causes an overuse of nitrogen fertilizer and low nitrogen use efficiency in intensively used solar greenhouse vegetable production. *Agric Water Manag* 144: 11–19
- FAO F and AO (2020) The State of Food Security and Nutrition in the World 2020.
- Fields S & Song OK (1989) A novel genetic system to detect protein–protein interactions. *Nat* 1989 3406230 340: 245–246
- Figueroa M, Ortiz D & Henningsen EC (2021) Tactics of host manipulation by intracellular effectors from plant pathogenic fungi. *Curr Opin Plant Biol* 62: 102054
- Floss DS, Levy JG, Lévesque-Tremblay V, Pumplun N & Harrison MJ (2013) DELLA proteins regulate arbuscule formation in arbuscular mycorrhizal symbiosis. *Proc Natl Acad Sci U S A* 110
- Foo E, Ross JJ, Jones WT & Reid JB (2013) Plant hormones in arbuscular mycorrhizal symbioses: an emerging role for gibberellins. *Ann Bot* 111: 769–779
- Freeman BC & Beattie GA (2008) An Overview of Plant Defenses against Pathogens and Herbivores. *Plant Heal Instr*
- Fukuda M, Nagumo F, Nakamura S & Tobita S (2012) Alternative Fertilizer Utilizing Methods for Sustaining Low

Input Agriculture. *Soil Fertil*

- Gabriel-Neumann E, Neumann G, Leggewie G & George E (2011) Constitutive overexpression of the sucrose transporter SoSUT1 in potato plants increases arbuscular mycorrhiza fungal root colonization under high, but not under low, soil phosphorus availability. *J Plant Physiol* 168: 911–919
- Gagliardi M & Matarazzo MR (2016) RIP: RNA Immunoprecipitation. *Methods Mol Biol* 1480: 73–86
- García-Garrido JM & Ocampo JA (2002) Regulation of the plant defence response in arbuscular mycorrhizal symbiosis. *J Exp Bot* 53: 1377–1386
- Garcia K, Doidy J, Zimmermann SD, Wipf D & Courty PE (2016) Take a Trip Through the Plant and Fungal Transportome of Mycorrhiza. *Trends Plant Sci* 21: 937–950
- Gaude N, Schulze WX, Franken P & Krajinski F (2012) Cell type-specific protein and transcription profiles implicate periarbuscular membrane synthesis as an important carbon sink in the mycorrhizal symbiosis. <https://doi.org/104161/psb19650> 7: 461–464
- Gavrin A & Schornack S (2019) Medicago truncatula as a model organism to study conserved and contrasting aspects of symbiotic and pathogenic signaling pathways. *Model Legum Medicago truncatula*: 317–330
- Geng Y, Cao G, Wang L & Wang S (2019) Effects of equal chemical fertilizer substitutions with organic manure on yield, dry matter, and nitrogen uptake of spring maize and soil nitrogen distribution. *PLoS One* 14
- Genre A, Chabaud M, Balzergue C, Puech-Pagès V, Novero M, Rey T, Fournier J, Rochange S, Bécard G, Bonfante P, *et al* (2013) Short-chain chitin oligomers from arbuscular mycorrhizal fungi trigger nuclear Ca²⁺ spiking in Medicago truncatula roots and their production is enhanced by strigolactone. *New Phytol* 198: 190–202
- Genre A, Chabaud M, Timmers T, Bonfante P & Barker DG (2005) Arbuscular Mycorrhizal Fungi Elicit a Novel Intracellular Apparatus in Medicago truncatula Root Epidermal Cells before Infection. *Plant Cell* 17: 3489
- Genre A & Russo G (2016) Does a Common Pathway Transduce Symbiotic Signals in Plant–Microbe Interactions? *Front Plant Sci* 7
- Ghosh S & O'Connor TJ (2017) Beyond paralogs: The multiple layers of redundancy in bacterial pathogenesis. *Front Cell Infect Microbiol* 7: 467
- Gibelin-Viala C, Amblard E, Puech-Pages V, Bonhomme M, Garcia M, Bascaules-Bedin A, Fliegmann J, Wen J, Mysore KS, le Signor C, *et al* (2019) The Medicago truncatula LysM receptor-like kinase LYK9 plays a dual role in immunity and the arbuscular mycorrhizal symbiosis. *New Phytol* 223: 1516–1529
- Giovannetti M, Avio L, Barale R, Ceccarelli N, Cristofani R, Iezzi A, Mignolli F, Picciarelli P, Pinto B, Reali D, *et al* (2012) Nutraceutical value and safety of tomato fruits produced by mycorrhizal plants. *Br J Nutr* 107: 242–251
- Girardin A, Wang T, Ding Y, Keller J, Buendia L, Gaston M, Ribeyre C, Gascioli V, Auriac MC, Vernié T, *et al* (2019) LCO Receptors Involved in Arbuscular Mycorrhiza Are Functional for Rhizobia Perception in Legumes. *Curr Biol* 29: 4249–4259.e5
- Gobbato E (2015) Recent developments in arbuscular mycorrhizal signaling. *Curr Opin Plant Biol* 26: 1–7
- Gobbato E, Marsh JF, Vernié T, Wang E, Maillet F, Kim J, Miller JB, Sun J, Bano SA, Ratet P, *et al* (2012) A GRAS-type transcription factor with a specific function in mycorrhizal signaling. *Curr Biol* 22: 2236–2241
- Golovkin M & Reddy ASN (1998) The plant U1 small nuclear ribonucleoprotein particle 70K protein interacts with two novel serine/arginine-rich proteins. *Plant Cell* 10: 1637–1647
- Gomes CP & Selman B (2005) Cue for the branching connection. *Nat* 2005 4357043 435: 750–751

- Gómez-Gómez L & Boller T (2000) FLS2: An LRR Receptor-like Kinase Involved in the Perception of the Bacterial Elicitor Flagellin in Arabidopsis. *Mol Cell* 5: 1003–1011
- Gough C, Cottret L, Lefebvre B & Bono JJ (2018) Evolutionary history of plant LysM receptor proteins related to root endosymbiosis. *Front Plant Sci* 9
- Grefen C & Blatt MR (2012) A 2in1 cloning system enables ratiometric bimolecular fluorescence complementation (rBiFC). *Biotechniques* 53: 311–314
- Groth M, Takeda N, Perry J, Uchid H, Dräxl S, Brachmann A, Sato S, Tabata S, Kawaguchi M, Wang TL, *et al* (2010) NENA, a Lotus japonicus homolog of Sec13, is required for rhizodermal infection by arbuscular mycorrhiza fungi and rhizobia but dispensable for cortical endosymbiotic development. *Plant Cell* 22: 2509–2526
- Grunwald U, Guo W, Fischer K, Isayenkov S, Ludwig-Müller J, Hause B, Yan X, Küster H & Franken P (2009) Overlapping expression patterns and differential transcript levels of phosphate transporter genes in arbuscular mycorrhizal, Pi-fertilised and phytohormone-treated Medicago truncatula roots. *Planta* 229: 1023–1034
- Guenoune D, Galili S, Phillips DA, Volpin H, Chet I, Okon Y & Kapulnik Y (2001) The defense response elicited by the pathogen Rhizoctonia solani is suppressed by colonization of the AM-fungus Glomus intraradices. *Plant Sci* 160: 925–932
- Guether M, Neuhäuser B, Balestrini R, Dynowski M, Ludewig U & Bonfante P (2009) A Mycorrhizal-Specific Ammonium Transporter from Lotus japonicus Acquires Nitrogen Released by Arbuscular Mycorrhizal Fungi. *Plant Physiol* 150: 73–83
- Guillotin B, Couzigou JM & Combier JP (2016) NIN is involved in the regulation of arbuscular mycorrhizal symbiosis. *Front Plant Sci* 7
- Gutjahr C & Parniske M (2013) Cell and Developmental Biology of Arbuscular Mycorrhiza Symbiosis. <http://dx.doi.org/101146/annurev-cellbio-101512-122413> 29: 593–617
- Gutjahr C, Radovanovic D, Geoffroy J, Zhang Q, Siegler H, Chiapello M, Casieri L, An K, An G, Guiderdoni E, *et al* (2012) The half-size ABC transporters STR1 and STR2 are indispensable for mycorrhizal arbuscule formation in rice. *Plant J* 69: 906–920
- Guttenberger M (2000) A rapid staining procedure for arbuscules of living arbuscular mycorrhizas using neutral red as acidotropic dye. *Plant Soil* 2000 2262 226: 211–218
- Harrison MJ, Dewbre GR & Liu J (2002) A phosphate transporter from Medicago truncatula involved in the acquisition of phosphate released by arbuscular mycorrhizal fungi. *Plant Cell* 14: 2413–2429
- Hart M, Ehret DL, Krumbein A, Leung C, Murch S, Turi C & Franken P (2015) Inoculation with arbuscular mycorrhizal fungi improves the nutritional value of tomatoes. *Mycorrhiza* 25: 359–376
- Heck C, Kuhn H, Heidt S, Walter S, Rieger N & Requena N (2016) Symbiotic Fungi Control Plant Root Cortex Development through the Novel GRAS Transcription Factor MIG1. *Curr Biol* 26: 2770–2778
- Heil M & Bostock RM (2002) Induced Systemic Resistance (ISR) Against Pathogens in the Context of Induced Plant Defences. *Ann Bot* 89: 503–512
- Helber N & Requena N (2008) Expression of the fluorescence markers DsRed and GFP fused to a nuclear localization signal in the arbuscular mycorrhizal fungus Glomus intraradices. *New Phytol* 177: 537–548
- Herrera Medina MJ, Gagnon H, Piché Y, Ocampo JA, García Garrido JM & Vierheilig H (2003) Root colonization by arbuscular mycorrhizal fungi is affected by the salicylic acid content of the plant. *Plant Sci* 164: 993–998
- Ho-Plágaro T, Molinero-Rosales N, Fariña Flores D, Villena Díaz M & García-Garrido JM (2019) Identification and

- expression analysis of GRAS transcription factor genes involved in the control of arbuscular mycorrhizal development in tomato. *Front Plant Sci* 10: 268
- Hohnjec N, Vieweg MF, Pühler A, Becker A & Küster H (2005) Overlaps in the transcriptional profiles of *Medicago truncatula* roots inoculated with two different *Glomus* fungi provide insights into the genetic program activated during arbuscular mycorrhiza. *Plant Physiol* 137: 1283–1301
- Horváth B, Yeun LH, Domonkos Á, Halász G, Gobbato E, Ayaydin F, Miró K, Hirsch S, Sun J, Tadege M, *et al* (2011) *Medicago truncatula* IPD3 is a member of the common symbiotic signaling pathway required for rhizobial and mycorrhizal symbioses. *Mol Plant Microbe Interact* 24: 1345–1358
- Hou S, Liu Z, Shen H & Wu D (2019) Damage-associated molecular pattern-triggered immunity in plants. *Front Plant Sci* 10: 646
- Humphreys CP, Franks PJ, Rees M, Bidartondo MI, Leake JR & Beerling DJ (2010) Mutualistic mycorrhiza-like symbiosis in the most ancient group of land plants. *Nat Commun* 2010 11 1: 1–7
- Hung NB, Ramkumar G & Lee YH (2014) An effector gene hopA1 influences on virulence, host specificity, and lifestyles of *Pseudomonas cichorii* JBC1. *Res Microbiol* 165: 620–629
- Javot H, Penmetsa RV, Terzaghi N, Cook DR & Harrison MJ (2007) A *Medicago truncatula* phosphate transporter indispensable for the arbuscular mycorrhizal symbiosis. *Proc Natl Acad Sci U S A* 104: 1720–1725
- Jiang Y, Wang W, Xie Q, Liu N, Liu L, Wang D, Zhang X, Yang C, Chen X, Tang D, *et al* (2017) Plants transfer lipids to sustain colonization by mutualistic mycorrhizal and parasitic fungi. *Science* 356: 1172–1173
- De Jonge R, Van Esse HP, Kombrink A, Shinya T, Desaki Y, Bours R, Van Der Krol S, Shibuya N, Joosten MHAJ & Thomma BPHJ (2010) Conserved fungal LysM effector Ecp6 prevents chitin-triggered immunity in plants. *Science* (80-) 329: 953–955
- Jung SC, Martinez-Medina A, Lopez-Raez JA & Pozo MJ (2012) Mycorrhiza-induced resistance and priming of plant defenses. *J Chem Ecol* 38: 651–664
- Kaiser C, Kilburn MR, Clode PL, Fuchslueger L, Koranda M, Cliff JB, Solaiman ZM & Murphy D V. (2015) Exploring the transfer of recent plant photosynthates to soil microbes: mycorrhizal pathway vs direct root exudation. *New Phytol* 205: 1537
- Kamel L, Tang N, Malbreil M, San Clemente H, Le Marquer M, Roux C & dit Frey NF (2017) The comparison of expressed candidate secreted proteins from two arbuscular mycorrhizal fungi unravels common and specific molecular tools to invade different host plants. *Front Plant Sci* 8: 124
- Kanamori N, Madsen LH, Radutoiu S, Frantescu M, Quistgaard EMH, Miwa H, Downie JA, James EK, Felle HH, Haaning LL, *et al* (2006) A nucleoporin is required for induction of Ca²⁺ spiking in legume nodule development and essential for rhizobial and fungal symbiosis. *Proc Natl Acad Sci U S A* 103: 359–364
- Kaschuk G, Kuyper TW, Leffelaar PA, Hungria M & Giller KE (2009) Are the rates of photosynthesis stimulated by the carbon sink strength of rhizobial and arbuscular mycorrhizal symbioses? *Soil Biol Biochem* 41: 1233–1244
- Kastell A, Smetanska I, Schreiner M & Mewis I (2013) Hairy roots, callus, and mature plants of *Arabidopsis thaliana* exhibit distinct glucosinolate and gene expression profiles. *Plant Cell Tissue Organ Cult* 115: 45–54
- Kevei Z, Lougnon G, Mergaert P, Horváth G V., Kereszt A, Jayaraman D, Zaman N, Marcel F, Regulski K, Kiss GB, *et al* (2008) 3-Hydroxy-3-Methylglutaryl Coenzyme A Reductase1 Interacts with NORK and Is Crucial for Nodulation in *Medicago truncatula*. *Plant Cell* 19: 3974–3989
- Keymer A, Pimprikar P, Wewer V, Huber C, Brands M, Bucarius SL, Delaux PM, Klingl V, von Röpenack-Lahaye E, Wang TL, *et al* (2017) Lipid transfer from plants to arbuscular mycorrhiza fungi. *Elife* 6

- Kilburn MR, Jones DL, Clode PL, Cliff JB, Stockdale EA, Herrmann AM & Murphy D V. (2010) Application of nanoscale secondary ion mass spectrometry to plant cell research. *Plant Signal Behav* 5: 760–762
- Kloppholz S, Kuhn H & Requena N (2011) A Secreted Fungal Effector of *Glomus intraradices* Promotes Symbiotic Biotrophy. *Curr Biol* 21: 1204–1209
- Kobae Y (2019) Dynamic phosphate uptake in arbuscular mycorrhizal roots under field conditions. *Front Environ Sci* 6: 159
- Kobae Y & Fujiwara T (2014) Earliest Colonization Events of *Rhizophagus irregularis* in Rice Roots Occur Preferentially in Previously Uncolonized Cells. *Plant Cell Physiol* 55: 1497–1510
- Kobae Y & Hata S (2010) Dynamics of Periarbuscular Membranes Visualized with a Fluorescent Phosphate Transporter in Arbuscular Mycorrhizal Roots of Rice. *Plant Cell Physiol* 51: 341–353
- Kosuta S, Chabaud M, Loughon G, Gough C, Dénarié J, Barker DG & Bécard G (2003) A Diffusible Factor from Arbuscular Mycorrhizal Fungi Induces Symbiosis-Specific MtENOD11 Expression in Roots of *Medicago truncatula*. *Plant Physiol* 131: 952
- Krajinski F, Courty PE, Sieh D, Franken P, Zhang H, Bucher M, Gerlach N, Kryvoruchko I, Zoeller D, Udvardi M, *et al* (2014) The H⁺-ATPase HA1 of *Medicago truncatula* Is Essential for Phosphate Transport and Plant Growth during Arbuscular Mycorrhizal Symbiosis. *Plant Cell* 26: 1808–1817
- Kretschmar T, Kohlen W, Sasse J, Borghi L, Schlegel M, Bachelier JB, Reinhardt D, Bours R, Bouwmeester HJ & Martinoia E (2012) A petunia ABC protein controls strigolactone-dependent symbiotic signalling and branching. *Nat* 2012 4837389 483: 341–344
- Krüger M, Krüger C, Walker C, Stockinger H & Schüßler A (2012) Phylogenetic reference data for systematics and phylotaxonomy of arbuscular mycorrhizal fungi from phylum to species level. *New Phytol* 193: 970–984
- Kwon S, Chin K, Nederlof M & Gray JW (2017) Quantitative, in situ analysis of mRNAs and proteins with subcellular resolution. *Sci Reports* 2017 71 7: 1–11
- Lambais MR (2000) Regulation of plant defense-related genes in arbuscular mycorrhizae.
- Lambais MR & Mehdy MC (1998) Spatial distribution of chitinases and β -1,3-glucanase transcripts in bean arbuscular mycorrhizal roots under low and high soil phosphate conditions. *New Phytol* 140: 33–42
- Lampropoulos A, Sutikovic Z, Wenzl C, Maegele I, Lohmann JU & Forner J (2013) GreenGate - A Novel, Versatile, and Efficient Cloning System for Plant Transgenesis. *PLoS One* 8: e83043
- Lanfranco L, Fiorilli V & Gutjahr C (2018) Partner communication and role of nutrients in the arbuscular mycorrhizal symbiosis. *New Phytol* 220: 1031–1046
- Larose G, Chênevert R, Moutoglis P, Gagné S, Piché Y & Vierheilig H (2002) Flavonoid levels in roots of *Medicago sativa* are modulated by the developmental stage of the symbiosis and the root colonizing arbuscular mycorrhizal fungus. *J Plant Physiol* 159: 1329–1339
- Lee EH, Eo JK, Ka KH & Eom AH (2013) Diversity of Arbuscular Mycorrhizal Fungi and Their Roles in Ecosystems. *Mycobiology* 41: 121
- Lehnert H, Serfling A, Enders M, Friedt W & Ordon F (2017) Genetics of mycorrhizal symbiosis in winter wheat (*Triticum aestivum*). *New Phytol* 215: 779–791
- Levine A & Durbin R (2001) A computational scan for U12-dependent introns in the human genome sequence. *Nucleic Acids Res* 29: 4006–4013
- Li S, Liu Y, Wang J, Yang L, Zhang S, Xu C & Ding W (2017) Soil acidification aggravates the occurrence of bacterial wilt in south China. *Front Microbiol* 8: 703

- Liao D, Sun X, Wang N, Song F & Liang Y (2018) Tomato LysM receptor-like kinase SILYK12 is involved in arbuscular mycorrhizal symbiosis. *Front Plant Sci* 9
- Liao HL, Chen Y, Bruns TD, Peay KG, Taylor JW, Branco S, Talbot JM & Vilgalys R (2014) Metatranscriptomic analysis of ectomycorrhizal roots reveals genes associated with Piloderma-Pinus symbiosis: Improved methodologies for assessing gene expression in situ. *Environ Microbiol* 16: 3730–3742
- Lin K, Limpens E, Zhang Z, Ivanov S, Saunders DGO, Mu D, Pang E, Cao H, Cha H, Lin T, *et al* (2014) Single Nucleus Genome Sequencing Reveals High Similarity among Nuclei of an Endomycorrhizal Fungus. *PLOS Genet* 10: e1004078
- Lingua G, Fusconi A & Berta G (2001) The nucleus of differentiated root plant cells: modifications induced by arbuscular mycorrhizal fungi. *Eur J Histochem* 45: 9–20
- Liu J, Liu J, Liu J, Cui M, Huang Y, Tian Y, Chen A & Xu G (2019a) The Potassium Transporter SIHAK10 Is Involved in Mycorrhizal Potassium Uptake. *Plant Physiol* 180: 465–479
- Liu J, Nannas NJ, Fu FF, Shi J, Aspinwall B, Parrott WA & Dawe RK (2019b) Genome-scale sequence disruption following biolistic transformation in rice and maize. *Plant Cell* 31: 368–383
- Liu T, Ye W, Ru Y, Yang X, Gu B, Tao K, Lu S, Dong S, Zheng X, Shan W, *et al* (2011a) Two host cytoplasmic effectors are required for pathogenesis of *Phytophthora sojae* by suppression of host defenses. *Plant Physiol* 155: 490–501
- Liu W, Kohlen W, Lillo A, den Camp RO, Ivanov S, Hartog M, Limpens E, Jamil M, Smaczniak C, Kaufmann K, *et al* (2011b) Strigolactone biosynthesis in *Medicago truncatula* and rice requires the symbiotic GRAS-type transcription factors NSP1 and NSP2. *Plant Cell* 23: 3853–3865
- Lopato S, Gattoni R, Fabini G, Stevenin J & Barta A (1999) A novel family of plant splicing factors with a Zn knuckle motif: examination of RNA binding and splicing activities. *Plant Mol Biol* 39: 761–773
- López-Ráez JA, Charnikhova T, Gómez-Roldán V, Matusova R, Kohlen W, De Vos R, Verstappen F, Puech-Pages V, Bécard G, Mulder P, *et al* (2008) Tomato strigolactones are derived from carotenoids and their biosynthesis is promoted by phosphate starvation. *New Phytol* 178: 863–874
- Luginbuehl LH & Oldroyd GED (2017) Current Biology Review Understanding the Arbuscule at the Heart of Endomycorrhizal Symbioses in Plants. *Curr Biol* 27: R952–R963
- Macleán AM, Bravo A & Harrison MJ (2017) Plant Signaling and Metabolic Pathways Enabling Arbuscular Mycorrhizal Symbiosis. *Plant Cell* 29: 2319–2335
- Maharshi A, Kumar G, Mukherjee A, Raghuwanshi R, Singh HB & Sarma BK (2019) Arbuscular mycorrhizal colonization and activation of plant defense responses against phytopathogens. *Microb Interv Agric Environ Vol 1 Res Trends, Priorities Prospect*: 219–240
- Maillet F, Poinot V, André O, Puech-Pagés V, Haouy A, Gueunier M, Cromer L, Giraudet D, Formey D, Niebel A, *et al* (2011) Fungal lipochitooligosaccharide symbiotic signals in arbuscular mycorrhiza. *Nat* 2011 4697328 469: 58–63
- Manck-Götzenberger J & Requena N (2016) Arbuscular mycorrhiza symbiosis induces a major transcriptional reprogramming of the potato SWEET sugar transporter family. *Front Plant Sci* 7: 487
- Martin F, Aerts A, Ahrén D, Brun A, Danchin EGJ, Duchaussoy F, Gibon J, Kohler A, Lindquist E, Pereda V, *et al* (2008) The genome of *Laccaria bicolor* provides insights into mycorrhizal symbiosis. *Nat* 2008 4527183 452: 88–92
- Mentlak TA, Kombrink A, Shinya T, Ryder LS, Otomo I, Saitoh H, Terauchi R, Nishizawa Y, Shibuya N, Thomma BPHJ, *et al* (2012) Effector-Mediated Suppression of Chitin-Triggered Immunity by *Magnaporthe oryzae* Is

- Necessary for Rice Blast Disease. *Plant Cell* 24: 322–335
- Mortier V, den Herder G, Whitford R, van de Velde W, Rombauts S, D'haeseleer K, Holsters M & Goormachtig S (2010) CLE Peptides Control Medicago truncatula Nodulation Locally and Systemically. *Plant Physiol* 153: 222–237
- Munkvold L, Kjølner R, Vestberg M, Rosendahl S & Jakobsen I (2004) High functional diversity within species of arbuscular mycorrhizal fungi. *New Phytol* 164: 357–364
- Murray JD, Cousins DR, Jackson KJ & Liu C (2013) Signaling at the Root Surface: The Role of Cutin Monomers in Mycorrhization. *Mol Plant* 6: 1381
- Nacoon S, Jogloy S, Riddech N, Mongkolthanaruk W, Ekprasert J, Cooper J & Boonlue S (2021) Combination of arbuscular mycorrhizal fungi and phosphate solubilizing bacteria on growth and production of Helianthus tuberosus under field condition. *Sci Reports* 2021 111 11: 1–10
- Nadal M, Sawers R, Naseem S, Bassin B, Kulicke C, Sharman A, An G, An K, Ahern KR, Romag A, *et al* (2017) An N-acetylglucosamine transporter required for arbuscular mycorrhizal symbioses in rice and maize. *Nat plants* 3
- Nagy R, Karandashov V, Chague V, Kalinkevich K, Tamasloukht M, Xu G, Jakobsen I, Levy AA, Amrhein N & Bucher M (2005) The characterization of novel mycorrhiza-specific phosphate transporters from Lycopersicon esculentum and Solanum tuberosum uncovers functional redundancy in symbiotic phosphate transport in solanaceous species. *Plant J* 42: 236–250
- Naveed ZA, Wei X, Chen J, Mubeen H & Ali GS (2020) The PTI to ETI Continuum in Phytophthora-Plant Interactions. *Front Plant Sci* 11: 2030
- Nissim-Rafinia M & Meshorer E (2011) Photobleaching Assays (FRAP & FLIP) to Measure Chromatin Protein Dynamics in Living Embryonic Stem Cells. *J Vis Exp* 52
- De Novais CB, Pepe A, Siqueira JO, Giovannetti M & Sbrana C (2017) Compatibility and incompatibility in hyphal anastomosis of arbuscular mycorrhizal. *Sci Agric* 74: 411–416
- Nzanza B, Marais D & Soundy P (2012) Yield and nutrient content of tomato (Solanum lycopersicum L.) as influenced by Trichoderma harzianum and Glomus mosseae inoculation. *Sci Hortic (Amsterdam)* 144: 55–59
- Ohtani M (2018) Plant snRNP biogenesis: A perspective from the nucleolus and cajal bodies. *Front Plant Sci* 8: 2184
- Okazaki S, Kaneko T, Sato S & Saeki K (2013) Hijacking of leguminous nodulation signaling by the rhizobial type III secretion system. *Proc Natl Acad Sci U S A* 110: 17131–17136
- Oldroyd GED (2013) Speak, friend, and enter: signalling systems that promote beneficial symbiotic associations in plants. *Nat Rev Microbiol* 11: 252–263
- Pahalvi HN, Rafiya L, Rashid S, Nisar B & Kamili AN (2021) Chemical Fertilizers and Their Impact on Soil Health. *Microbiota Biofertilizers, Vol 2* 2: 1–20
- Park HJ, Floss DS, Levesque-Tremblay V, Bravo A & Harrison MJ (2015) Hyphal Branching during Arbuscule Development Requires Reduced Arbuscular Mycorrhiza1. *Plant Physiol* 169: 2774–2788
- Parniske M (2008) Arbuscular mycorrhiza: the mother of plant root endosymbioses. *Nat Rev Microbiol* 2008 610 6: 763–775
- Paszkowski U, Kroken S, Roux C & Briggs SP (2002) Rice phosphate transporters include an evolutionarily divergent gene specifically activated in arbuscular mycorrhizal symbiosis. *Proc Natl Acad Sci U S A* 99: 13324–13329
- Pedone-Bonfim MV, Lins MA, Coelho IR, Santana AS, Silva FS & Maia LC (2013) Mycorrhizal technology and phosphorus in the production of primary and secondary metabolites in cebil (Anadenanthera colubrina (Vell.) Brenan) seedlings. *J Sci Food Agric* 93: 1479–1484

- Peña Venegas RA, Lee SJ, Thuita M, Mlay DP, Masso C, Vanlauwe B, Rodriguez A & Sanders IR (2021) The Phosphate Inhibition Paradigm: Host and Fungal Genotypes Determine Arbuscular Mycorrhizal Fungal Colonization and Responsiveness to Inoculation in Cassava With Increasing Phosphorus Supply. *Front Plant Sci* 12: 693037
- Péret B, Clément M, Nussaume L & Desnos T (2011) Root developmental adaptation to phosphate starvation: better safe than sorry. *Trends Plant Sci* 16: 442–450
- Pérez-Quintero AL, Rodríguez-R LM, Dereeper A, López C, Koebnik R, Szurek B & Cunnac S (2013) An Improved Method for TAL Effectors DNA-Binding Sites Prediction Reveals Functional Convergence in TAL Repertoires of *Xanthomonas oryzae* Strains. *PLoS One* 8: e68464
- Pimprikar P, Carbonnel S, Paries M, Katzer K, Klingl V, Bohmer MJ, Karl L, Floss DS, Harrison MJ, Parniske M, *et al* (2016) A CcAMK-CYCLOPS-DELLA Complex Activates Transcription of RAM1 to Regulate Arbuscule Branching. *Curr Biol* 26: 1126
- Pimprikar P & Gutjahr C (2018) Transcriptional Regulation of Arbuscular Mycorrhiza Development. *Plant Cell Physiol* 59: 678–695
- Pingali PL (2012) Green revolution: Impacts, limits, and the path ahead. *Proc Natl Acad Sci U S A* 109: 12302–12308
- Plett JM & Martin F (2015) Reconsidering mutualistic plant-fungal interactions through the lens of effector biology. *Curr Opin Plant Biol* 26: 45–50
- Prasad Singh P, Srivastava D, Jaiswar A & Adholeya A (2019) Effector proteins of *Rhizophagus proliferus*: conserved protein domains may play a role in host-specific interaction with different plant species. *Brazilian J Microbiol* 50: 593
- Lo Presti L, Lanver D, Schweizer G, Tanaka S, Liang L, Tollot M, Zuccaro A, Reissmann S & Kahmann R (2015) Fungal Effectors and Plant Susceptibility. <http://dx.doi.org/10.1146/annurev-arplant-043014-114623> 66: 513–545
- Pumpkin N, Zhang X, Noar RD & Harrison MJ (2012) Polar localization of a symbiosis-specific phosphate transporter is mediated by a transient reorientation of secretion. *Proc Natl Acad Sci U S A* 109
- Raffaele S, Win J, Cano LM & Kamoun S (2010) Analyses of genome architecture and gene expression reveal novel candidate virulence factors in the secretome of *Phytophthora infestans*. *BMC Genomics* 11
- Rausin G, Tillemans V, Stankovic N, Hanikenne M & Motte P (2010) Dynamic nucleocytoplasmic shuttling of an Arabidopsis SR splicing factor: role of the RNA-binding domains. *Plant Physiol* 153: 273–284
- Real E, Rodrigues L, Cabal GG, Enguita FJ, Mancio-Silva L, Mello-Vieira J, Beatty W, Vera IM, Zuzarte-Luís V, Figueira TN, *et al* (2017) Plasmodium UIS3 sequesters host LC3 to avoid elimination by autophagy in hepatocytes. *Nat Microbiol* 2017 31 3: 17–25
- Reece-Hoyes JS & Walhout AJM (2018) Gateway recombinational cloning. *Cold Spring Harb Protoc* 2018: 1–6 doi:10.1101/pdb.top094912 [PREPRINT]
- Rey T, Laporte P, Bonhomme M, Jardinaud MF, Huguet S, Balzergue S, Dumas B, Niebel A & Jacquet C (2016) MtNF-YA1, A Central Transcriptional Regulator of Symbiotic Nodule Development, Is Also a Determinant of *Medicago truncatula* Susceptibility toward a Root Pathogen. *Front Plant Sci* 7
- Rezali NI, Jaafar Sidik N, Saleh A, Osman NI & Mohd Adam NA (2017) The effects of different strength of MS media in solid and liquid media on in vitro growth of *Typhonium flagelliforme*. *Asian Pac J Trop Biomed* 7: 151–156
- Riely BK, Loughon G, Ané JM & Cook DR (2007) The symbiotic ion channel homolog DMI1 is localized in the nuclear membrane of *Medicago truncatula* roots. *Plant J* 49: 208–216
- Rino J, Carvalho T, Braga J, Desterro JMP, Lührmann R & Carmo-Fonseca M (2007) A Stochastic View of

- Spliceosome Assembly and Recycling in the Nucleus. *PLOS Comput Biol* 3: e201
- Rodriguez A & Sanders IR (2015) The role of community and population ecology in applying mycorrhizal fungi for improved food security. *ISME J* 9: 1053–1061
- Rosikiewicz P, Bonvin J & Sanders IR (2017) Cost-efficient production of in vitro Rhizophagus irregularis. *Mycorrhiza* 27: 477–486
- Rovenich H, Boshoven JC & Thomma BPHJ (2014) Filamentous pathogen effector functions: of pathogens, hosts and microbiomes. *Curr Opin Plant Biol* 20: 96–103
- Ryan MH, Small DR & Ash JE (2000) Phosphorus controls the level of colonisation by arbuscular mycorrhizal fungi in conventional and biodynamic irrigated dairy pastures. *Aust J Exp Agric* 40: 663–670
- Saito K, Yoshikawa M, Yano K, Miwa H, Uchida H, Asamizu E, Sato S, Tabata S, Imaizumi-Anraku H, Umehara Y, et al (2007) NUCLEOPORIN85 is required for calcium spiking, fungal and bacterial symbioses, and seed production in *Lotus japonicus*. *Plant Cell* 19: 610–624
- Salvioli A, Ghignone S, Novero M, Navazio L, Venice F, Bagnaresi P & Bonfante P (2016) Symbiosis with an endobacterium increases the fitness of a mycorrhizal fungus, raising its bioenergetic potential. *ISME J* 10: 130–144
- Salvioli A, Zouari I, Chalot M & Bonfante P (2012) The arbuscular mycorrhizal status has an impact on the transcriptome profile and amino acid composition of tomato fruit. *BMC Plant Biol* 12
- Salzer P, Corbière H & Boller T (1999) Hydrogen peroxide accumulation in *Medicago truncatula* roots colonized by the arbuscular mycorrhiza-forming fungus *Glomus intraradices*. *Planta* 199: 2083–2088: 319–325
- Sasse J, Simon S, Gübeli C, Liu GW, Cheng X, Friml J, Bouwmeester H, Martinoia E & Borghi L (2015) Asymmetric localizations of the ABC transporter PaPDR1 trace paths of directional strigolactone transport. *Curr Biol* 25: 647–655
- Schachtman DP, Reid RJ & Ayling SM (1998) Phosphorus Uptake by Plants: From Soil to Cell. *Plant Physiol* 116: 447–453
- Schubert R, Werner S, Cirka H, Rödel P, Moya YT, Mock HP, Hutter I, Kunze G & Hause B (2020) Effects of Arbuscular Mycorrhization on Fruit Quality in Industrialized Tomato Production. *Int J Mol Sci* 21: 1–15
- Sędzielewska Toro K & Brachmann A (2016) The effector candidate repertoire of the arbuscular mycorrhizal fungus *Rhizophagus clarus*. *BMC Genomics* 17: 1–13
- Serghi EU, Kokkoris V, Cornell C, Dettman J, Stefani F & Corradi N (2021) Homo- and Dikaryons of the Arbuscular Mycorrhizal Fungus *Rhizophagus irregularis* Differ in Life History Strategy. *Front Plant Sci* 12: 1544
- Sharda JN & Koide RT (2008) Can hypodermal passage cell distribution limit root penetration by mycorrhizal fungi? *New Phytol* 180: 696–701
- Siciliano V, Genre A, Balestrini R, DeWit PJGM & Bonfante P (2007) Pre-Penetration Apparatus Formation During AM Infection is Associated With a Specific Transcriptome Response in Epidermal Cells. *Plant Signal Behav* 2: 533
- Sievers F & Higgins DG (2018) Clustal Omega for making accurate alignments of many protein sequences. *Protein Sci* 27: 135
- Silverstone AL, Ciampaglio CN & Sun T (1998) The Arabidopsis RGA Gene Encodes a Transcriptional Regulator Repressing the Gibberellin Signal Transduction Pathway. *Plant Cell* 10: 155
- Singh S, Katzer K, Lambert J, Cerri M & Parniske M (2014) CYCLOPS, a DNA-binding transcriptional activator, orchestrates symbiotic root nodule development. *Cell Host Microbe* 15: 139–152

- Smith SE, Jakobsen I, Grønlund M & Smith FA (2011) Roles of Arbuscular Mycorrhizas in Plant Phosphorus Nutrition: Interactions between Pathways of Phosphorus Uptake in Arbuscular Mycorrhizal Roots Have Important Implications for Understanding and Manipulating Plant Phosphorus Acquisition. *Plant Physiol* 156: 1050–1057
- Smith SE, Smith FA & Jakobsen I (2004) Functional diversity in arbuscular mycorrhizal (AM) symbioses: the contribution of the mycorrhizal P uptake pathway is not correlated with mycorrhizal responses in growth or total P uptake. *New Phytol* 162: 511–524
- Song F, Song G, Dong A & Kong X (2011) Regulatory mechanisms of host plant defense responses to arbuscular mycorrhiza. *Acta Ecol Sin* 31: 322–327
- Song OK, Wang X, Waterborg JH & Sternglanz R (2003) An N-alpha-acetyltransferase responsible for acetylation of the N-terminal residues of histones H4 and H2A. *J Biol Chem* 278: 38109–38112
- Soyano T, Kouchi H, Hirota A & Hayashi M (2013) Nodule inception directly targets NF-Y subunit genes to regulate essential processes of root nodule development in *Lotus japonicus*. *PLoS Genet* 9
- Sperschneider J, Catanzariti AM, Deboer K, Petre B, Gardiner DM, Singh KB, Dodds PN & Taylor JM (2017) LOCALIZER: subcellular localization prediction of both plant and effector proteins in the plant cell. *Sci Reports* 2017 71 7: 1–14
- Sperschneider J, Dodds PN, Singh KB & Taylor JM (2018) ApoplastP: prediction of effectors and plant proteins in the apoplast using machine learning. *New Phytol* 217: 1764–1778
- St-Arnaud M, Hamel C, Vimard B, Caron M & Fortin JA (1996) Enhanced hyphal growth and spore production of the arbuscular mycorrhizal fungus *Glomus intraradices* in an in vitro system in the absence of host roots. *Mycol Res* 100: 328–332
- Stirnberg P, Furner IJ & Ottoline Leyser HM (2007) MAX2 participates in an SCF complex which acts locally at the node to suppress shoot branching. *Plant J* 50: 80–94
- Stoian V, Vidican R, Crișan I, Puia C, Șandor M, Stoian VA, Păcurar F & Vaida I (2019) Sensitive approach and future perspectives in microscopic patterns of mycorrhizal roots. *Sci Reports* 2019 91 9: 1–8
- Stracke S, Kistner C, Yoshida S, Mulder L, Sato S, Kaneko T, Tabata S, Sandal N, Stougaard J, Szczyglowski K, et al (2002) A plant receptor-like kinase required for both bacterial and fungal symbiosis. *Nature* 417: 959–962
- Tadege M, Wen J, He J, Tu H, Kwak Y, Eschstruth A, Cayrel A, Endre G, Zhao PX, Chabaud M, et al (2008) Large-scale insertional mutagenesis using the Tnt1 retrotransposon in the model legume *Medicago truncatula*. *Plant J* 54: 335–347
- Tanaka S, Brefort T, Neidig N, Djamei A, Kahnt J, Vermerris W, Koenig S, Feussner K, Feussner I & Kahmann R (2014) A secreted *Ustilago maydis* effector promotes virulence by targeting anthocyanin biosynthesis in maize. *Elife* 2014
- Tang N, San Clemente H, Roy S, Bécard G, Zhao B & Roux C (2016) A Survey of the Gene Repertoire of *Gigaspora rosea* Unravels Conserved Features among Glomeromycota for Obligate Biotrophy. *Front Microbiol* 7
- Teixeira PJP, Colaianni NR, Fitzpatrick CR & Dangl JL (2019) Beyond pathogens: microbiota interactions with the plant immune system. *Curr Opin Microbiol* 49: 7–17
- Teulet A, Busset N, Fardoux J, Gully D, Chaintreuil C, Cartieaux F, Jauneau A, Comorge V, Okazaki S, Kaneko T, et al (2019) The rhizobial type III effector ErnA confers the ability to form nodules in legumes. *Proc Natl Acad Sci U S A* 116: 21758–21768
- Tillemans V, Leponce I, Rausin G, Dispa L & Motte P (2006) Insights into Nuclear Organization in Plants as Revealed by the Dynamic Distribution of Arabidopsis SR Splicing Factors. *Plant Cell* 18: 3218–3234

- Tisserant E, Kohler A, Dozolme-Seddas P, Balestrini R, Benabdellah K, Colard A, Croll D, da Silva C, Gomez SK, Koul R, *et al* (2012) The transcriptome of the arbuscular mycorrhizal fungus *Glomus intraradices* (DAOM 197198) reveals functional tradeoffs in an obligate symbiont. *New Phytol* 193: 755–769
- Tisserant E, Malbreil M, Kuo A, Kohler A, Symeonidi A, Balestrini R, Charron P, Duensing N, Frei Dit Frey N, Gianinazzi-Pearson V, *et al* (2013) Genome of an arbuscular mycorrhizal fungus provides insight into the oldest plant symbiosis. *Proc Natl Acad Sci U S A* 110: 20117–20122
- Toth R & Miller RM (1984) Dynamics of Arbuscule Development and Degeneration in a Zea Mays Mycorrhiza. *Am J Bot* 71: 449
- Truong HN, Thalineau E, Bonneau L, Fournier C, Potin S, Balzergue S, Van Tuinen D, Jeandroz S & Morandi D (2015) The *Medicago truncatula* hypermycorrhizal B9 mutant displays an altered response to phosphate and is more susceptible to *Aphanomyces euteiches*. *Plant Cell Environ* 38: 73–88
- Tsuzuki S, Handa Y, Takeda N & Kawaguchi M (2016) Strigolactone-induced putative secreted protein 1 is required for the establishment of symbiosis by the arbuscular mycorrhizal fungus *Rhizophagus irregularis*. *Mol Plant-Microbe Interact* 29: 277–286
- Ud-Din AIMS, Tikhomirova A & Roujeinikova A (2016) Structure and Functional Diversity of GCN5-Related N-Acetyltransferases (GNAT). *Int J Mol Sci* 17
- Vierheilig H, Coughlan AP, Wyss U & Piché Y (1998a) Ink and Vinegar, a Simple Staining Technique for Arbuscular-Mycorrhizal Fungi. *Appl Environ Microbiol* 64: 5004
- Vierheilig H, Coughlan AP, Wyss U & Piché Y (1998b) Ink and Vinegar, a Simple Staining Technique for Arbuscular-Mycorrhizal Fungi. *Appl Environ Microbiol* 64: 5004
- Volpe V, Giovannetti M, Sun XG, Fiorilli V & Bonfante P (2016) The phosphate transporters LjPT4 and MtPT4 mediate early root responses to phosphate status in non mycorrhizal roots. *Plant Cell Environ* 39: 660–671
- Voß S, Betz R, Heidt S, Corradi N & Requena N (2018) RiCRN1, a crinkler effector from the arbuscular mycorrhizal fungus *Rhizophagus irregularis*, functions in arbuscule development. *Front Microbiol* 9: 2068
- Wang E, Schornack S, Marsh JF, Gobbato E, Schwessinger B, Eastmond P, Schultze M, Kamoun S & Oldroyd GED (2012) A common signaling process that promotes mycorrhizal and oomycete colonization of plants. *Curr Biol* 22: 2242–2246
- Wang J, Grishin N, Kinch L, Cohen JC, Hobbs HH & Xie XS (2011) Sequences in the nonconsensus nucleotide-binding domain of ABCG5/ABCG8 required for sterol transport. *J Biol Chem* 286: 7308–7314
- Wang P, Jiang H, Boeren S, Dings H, Kulikova O, Bisseling T & Limpens E (2021) A nuclear-targeted effector of *Rhizophagus irregularis* interferes with histone 2B mono-ubiquitination to promote arbuscular mycorrhization. *New Phytol* 230: 1142
- Wang S, Chen A, Xie K, Yang X, Luo Z, Chen J, Zeng D, Ren Y, Yang C, Wang L, *et al* (2020) Functional analysis of the OsNPF4.5 nitrate transporter reveals a conserved mycorrhizal pathway of nitrogen acquisition in plants. *Proc Natl Acad Sci U S A* 117: 16649–16659
- Wang W, Shi J, Xie Q, Jiang Y, Yu N & Wang E (2017) Nutrient Exchange and Regulation in Arbuscular Mycorrhizal Symbiosis. *Mol Plant* 10: 1147–1158
- Wewer V, Brands M & Dörmann P (2014) Fatty acid synthesis and lipid metabolism in the obligate biotrophic fungus *Rhizophagus irregularis* during mycorrhization of *Lotus japonicus*. *Plant J* 79: 398–412
- Wu JY & Maniatis T (1993) Specific interactions between proteins implicated in splice site selection and regulated alternative splicing. *Cell* 75: 1061–1070

- Wu Y & Zhou JM (2013) Receptor-Like Kinases in Plant Innate Immunity. *J Integr Plant Biol* 55: 1271–1286
- Xu F, Huang Y, Li L, Gannon P, Linster E, Huber M, Kapos P, Bienvenut W, Plevoda B, Meinel T, *et al* (2015) Two N-terminal acetyltransferases antagonistically regulate the stability of a nod-like receptor in Arabidopsis. *Plant Cell* 27: 1547–1562
- Yang C, Dolatabadian A & Fernando WGD (2021) The wonderful world of intrinsic and intricate immunity responses in plants against pathogens. <https://doi.org/10.1080/0706066120211960610> 44: 1–20
- Yang SY, Grønlund M, Jakobsen I, Grottemeyer MS, Rentsch D, Miyao A, Hirochika H, Kumar CS, Sundaresan V, Salamin N, *et al* (2012) Nonredundant Regulation of Rice Arbuscular Mycorrhizal Symbiosis by Two Members of the PHOSPHATE TRANSPORTER1 Gene Family. *Plant Cell* 24: 4236–4251
- Yano K, Yoshida S, Müller J, Singh S, Banba M, Vickers K, Markmann K, White C, Schuller B, Sato S, *et al* (2008) CYCLOPS, a mediator of symbiotic intracellular accommodation. *Proc Natl Acad Sci U S A* 105: 20540–20545
- Ye L, Zhao X, Bao E, Li J, Zou Z & Cao K (2020) Bio-organic fertilizer with reduced rates of chemical fertilization improves soil fertility and enhances tomato yield and quality. *Sci Reports* 2020 101 10: 1–11
- Yoneyama K, Yoneyama K, Takeuchi Y & Sekimoto H (2007) Phosphorus deficiency in red clover promotes exudation of orobanchol, the signal for mycorrhizal symbionts and germination stimulant for root parasites. *Planta* 225: 1031–1038
- Young ND, Debellé F, Oldroyd GED, Geurts R, Cannon SB, Udvardi MK, Benedito VA, Mayer KFX, Gouzy J, Schoof H, *et al* (2011) The Medicago genome provides insight into the evolution of rhizobial symbioses. *Nature* 480: 520–524
- Yousaf M, Li J, Lu J, Ren T, Cong R, Fahad S & Li X (2017) Effects of fertilization on crop production and nutrient-supplying capacity under rice-oilseed rape rotation system. *Sci Reports* 2017 71 7: 1–9
- Van Zandt PA (2007) PLANT DEFENSE, GROWTH, AND HABITAT: A COMPARATIVE ASSESSMENT OF CONSTITUTIVE AND INDUCED RESISTANCE. *Ecology* 88: 1984–1993
- Zeng T, Holmer R, Hontelez J, te Lintel-Hekkert B, Marufu L, de Zeeuw T, Wu F, Schijlen E, Bisseling T & Limpens E (2018) Host- and stage-dependent secretome of the arbuscular mycorrhizal fungus *Rhizophagus irregularis*. *Plant J* 94: 411–425
- Zeng T, Rodriguez-Moreno L, Mansurkhodzaev A, Wang P, van den Berg W, Gascioli V, Cottaz S, Fort S, Thomma BPHJ, Bono JJ, *et al* (2020) A lysin motif effector subverts chitin-triggered immunity to facilitate arbuscular mycorrhizal symbiosis. *New Phytol* 225: 448–460
- Zhang Q, Blaylock LA & Harrison MJ (2010) Two Medicago truncatula half-ABC transporters are essential for arbuscule development in arbuscular mycorrhizal symbiosis. *Plant Cell* 22: 1483–1497
- Zhong Z, Norvienyeku J, Chen M, Bao J, Lin L, Chen L, Lin Y, Wu X, Cai Z, Zhang Q, *et al* (2016) Directional Selection from Host Plants Is a Major Force Driving Host Specificity in Magnaporthe Species. *Sci Rep* 6
- Ziane H, Hamza N & Meddad-Hamza A (2021) Arbuscular mycorrhizal fungi and fertilization rates optimize tomato (*Solanum lycopersicum* L.) growth and yield in a Mediterranean agroecosystem. *J Saudi Soc Agric Sci* 20: 454–458
- Zurbriggen MD, Carrillo N & Hajirezaei MR (2010) ROS signaling in the hypersensitive response: When, where and what for? *Plant Signal Behav* 5: 393

Addendum

1. Figures

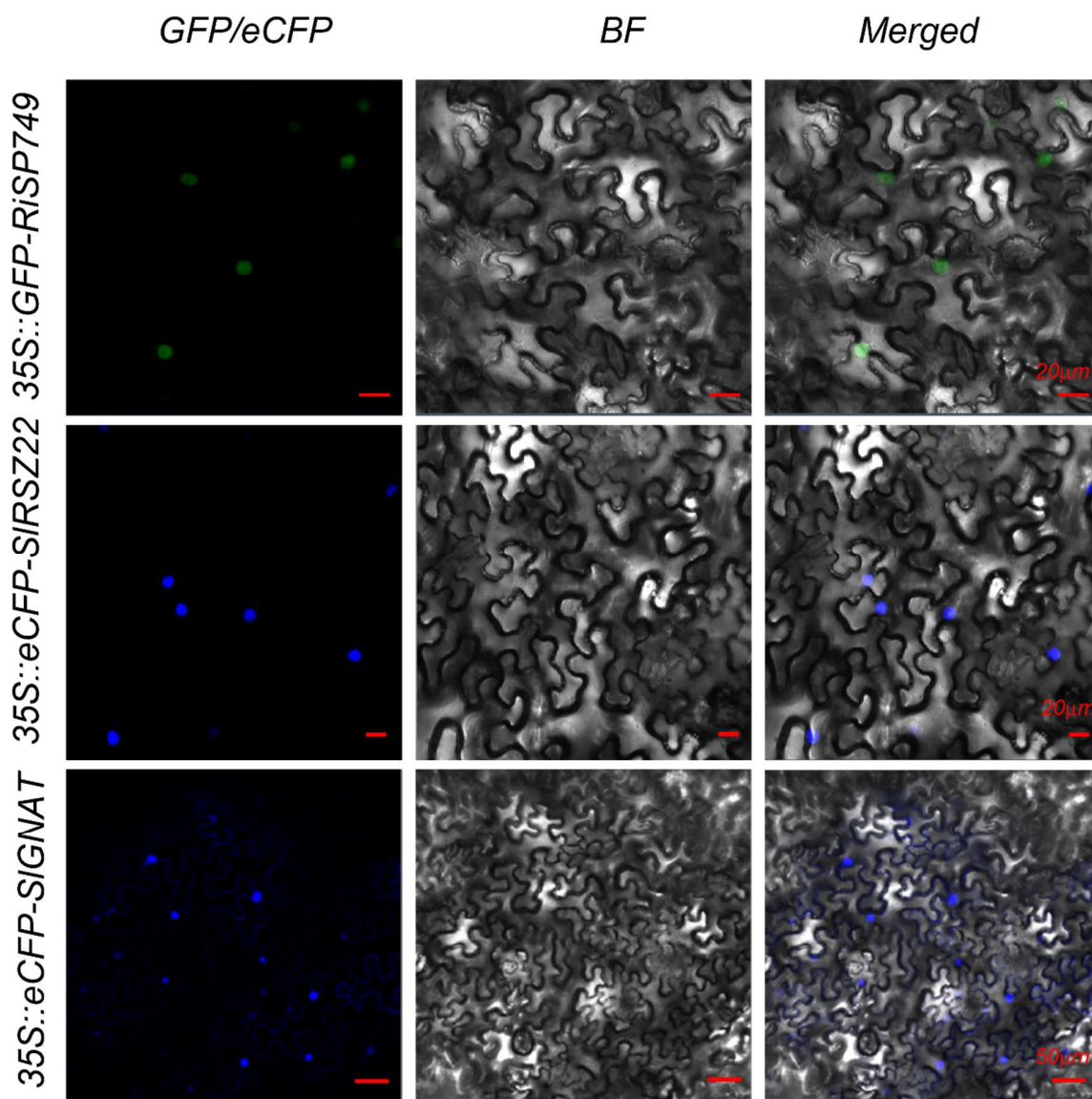


Figure S1: Localization of RiSP749 and tomato interactors SIRSZ22 and SIGNAT. RiSP749 was fused to GFP at the N-terminus, while the tomato interactors SIRSZ22 and SIGNAT were N-terminally fused to eCFP. SIRSZ22 and RiSP749 were exclusively located in the nucleus, while SIGNAT was located both in the nucleus and in cytoplasm.

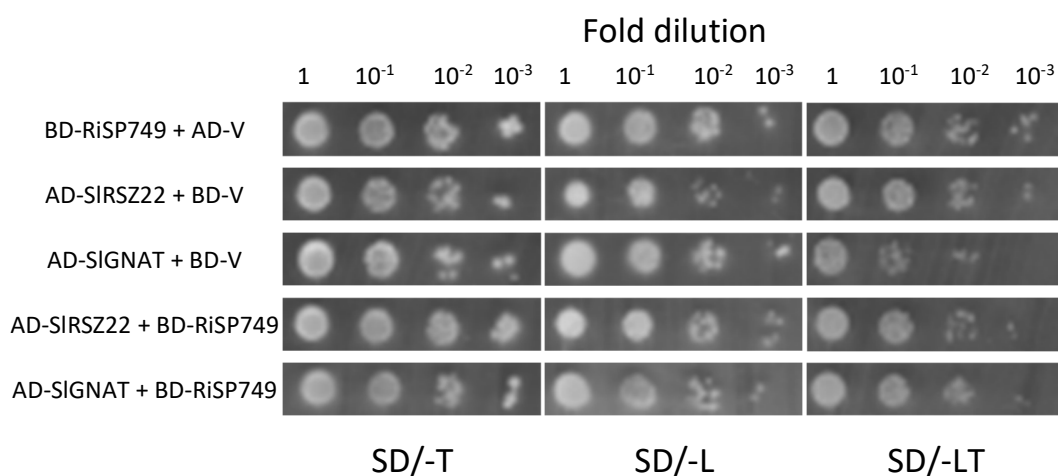


Figure S2: Controls of the binary Y2H-assay of RiSP749 and the candidate tomato interactors SIRSZ22 and SIGNAT. Transformation of *S. cerevisiae* strain PJ69-4 with the *R. irregularis* effector RiSP749 fused to the binding domain (BD) of the TF GAL4, and the empty pGADT7 vector (AD-V) or with the tomato proteins SIRSZ22 and SIGNAT fused to the activation domain (AD) of the TF GAL4 and the empty pGBKT7 vector (BD-V) resulted in growth in the control media SD-L, SD-T and SD_LT. Four serial dilutions of the culture were done.

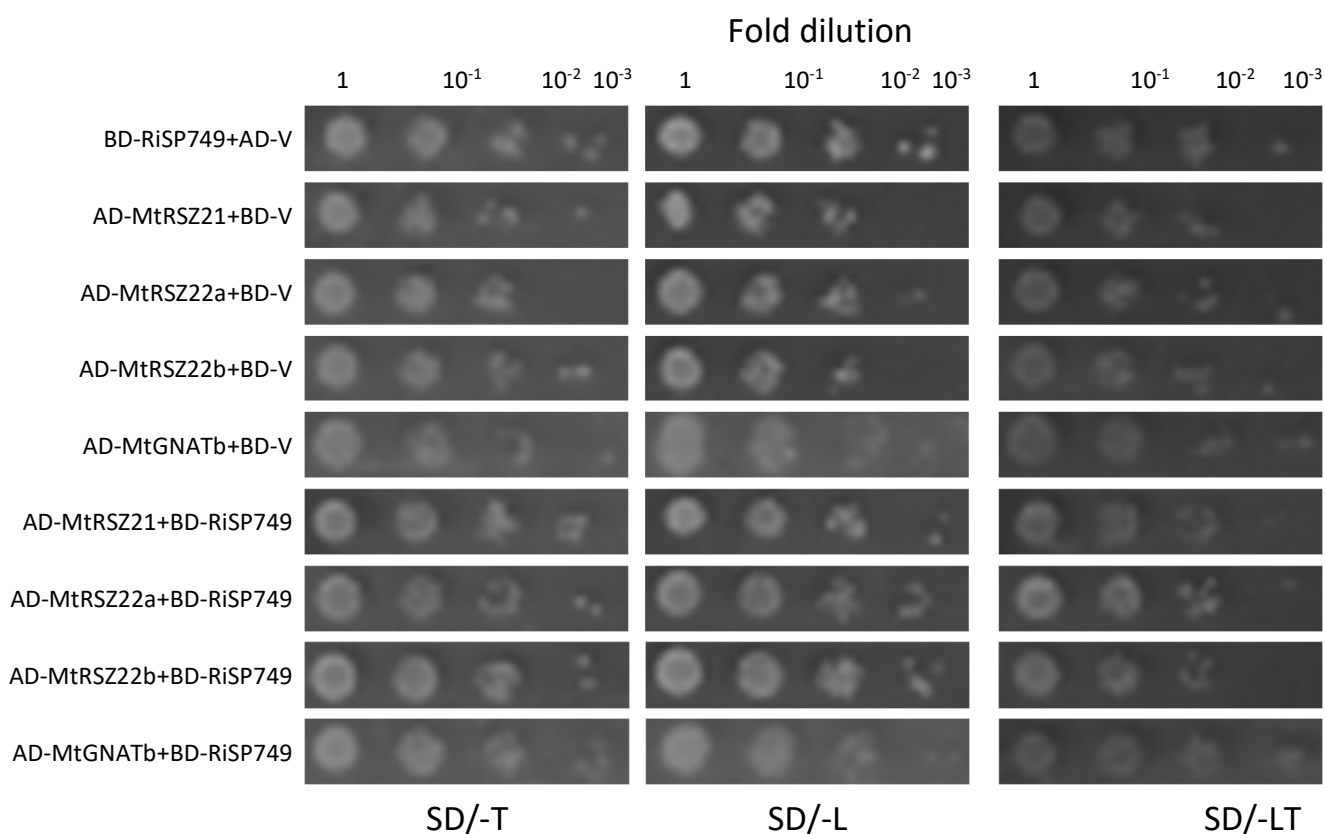


Figure S3: Figure 12: Controls of the binary Y2H assay of RiSP749 and the *M. truncatula* candidate orthologs of SIRSZ22 and SIGNAT. Transformation of *S. cerevisiae* strain PJ69-4 with the *R. irregularis* effector RiSP749 fused to the binding domain (BD) of the TF GAL4 and the empty pGADT7 vector (AD-V) or with the interactors MtRSZ21,

MtRSZ22a, *MtRSZ22b* and *MtGNATb* and the empty *pGBKT7* vector (*BD-V*). Four serial dilutions of the culture were done for each construct. All grew in *SD-L*, *SD-T* and *SD-LT* media.

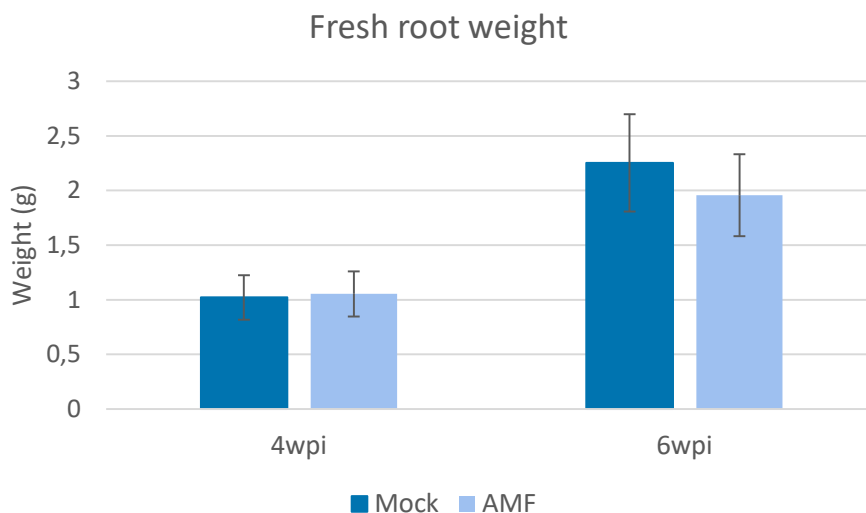


Figure S4: Fresh root weight of mycorrhized and mock wild-type (WT) *M. truncatula* plants harvested at 4 and 6 weeks post inoculation. No difference between mock and mycorrhized WT *M. truncatula* plants were seen at 4 and 6 wpi. The average of eleven WT *M. truncatula* were represented with their standard error (SE).

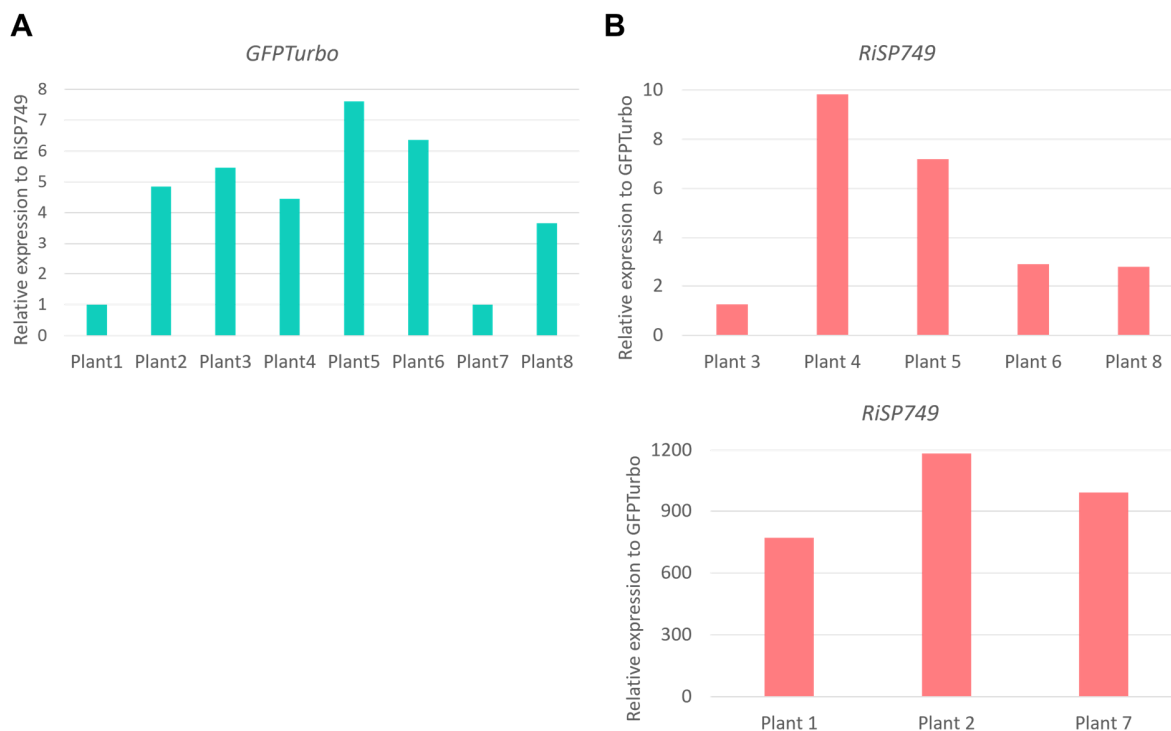


Figure S5: *GFPTurbo* and *RiSP749* expression in the root tips of each of the plants used for colonization analysis. (A) Relative expression of *GFPTurbo* to *RiSP749* expression in plant 1 in the 8 plants used for colonization analysis compared normalized against the plant housekeeping genes *MtTUB1* and *MtGADPH*. (B) Relative expression of

RiSP749 to GFPTurbo in the 8 plants used for colonization analysis. Plants 1, 2 and 7 were separated for proper visualization.

2. Tables

Table S1: Tomato and *M. truncatula* interactor references. Gene codes for the Tomato and *M. truncatula* *RiSP749* candidate interactors in different databases. NCBI code, Sol Genomics code, *A. thaliana* homolog TAIR code, PFAM code of their domains and LEGOO code.

Organism	NCBI gene code	Sol Genomics code	TAIR accession	Abbreviation	PFAM codes	LEGOO code
Tomato	LOC101266050	Solyc08g069120	AT4G31580	SIRSZ22	PFAM00076	-
<i>M. truncatula</i>	LOC112417497	-	AT2G24590	MtRSZ21	PFAM00076	MtrunA17Chr8g0365051
<i>M. truncatula</i>	LOC112418704	-	AT2G24590	MtRSZ22a	PFAM00076	MtrunA17_Chr1g0147821
<i>M. truncatula</i>	LOC112419871	-	AT2G24590	MtRSZ22b	PFAM00076	MtrunA17Chr3g0139061
Tomato	LOC101247959	Solyc09g082240	AT2G32030	SIGNAT	PFAM13302	-
<i>M. truncatula</i>	LOC25490856	-	AT2G32030	SIGNATa	PFAM13302	Medtr3g463610
<i>M. truncatula</i>	LOC11420857	-	AT2G32030	SIGNATYoaA	PFAM13302	Medtr7g114410
<i>M. truncatula</i>	LOC11443152	-	AT2G32030	SIGNATb	PFAM13302	Medtr5g006450

Table S2: Constructs generated and used* during this master thesis. The experiment in which they were used, the construct or gene introduced, the vector and the cloning system are described. Construct with an asterisk means that they were already available in the host laboratory.

Experiment	Construct	Vector	Cloning system
Yeast two hybrid*	LOC101266050 (SIRSZ22)	pDONR207	Gateway cloning BP reaction
Yeast two hybrid*	LOC101247959 (SIGNAT)	pDONR207	Gateway cloning BP reaction
Yeast two hybrid*	RiSP749	pDONR207	Gateway cloning BP reaction
Yeast two hybrid	LOC112417497 (MtRSZ21)	pDONR207	Gateway cloning BP reaction

Yeast two hybrid	LOC112418704 (MtRSZ22a)	pDONR207	Gateway cloning BP reaction
Yeast two hybrid	LOC112419871 (MtRSZ22b)	pDONR207	Gateway cloning BP reaction
Yeast two hybrid	LOC11443152 (MtGNATb)	pDONR207	Gateway cloning BP reaction
Colocalization*	SIRSZ22	pK7wgc2	Gateway cloning LR reaction
Colocalization*	SIGNAT	pK7wgc2	Gateway cloning LR reaction
Colocalization*	35S::RiSP749-GFPTurbo:RoID_mRuby	pGGPAG	Golden Gate
RiSP749 OE*	35S::GFPTurbo-RiSP749:RoID_mRuby	pGGPAG	Golden Gate
Yeast two hybrid*	LOC101266050 (SIRSZ22)	pGADT7	Gateway cloning LR reaction
Yeast two hybrid*	LOC101247959 (SIGNAT)	pGADT7	Gateway cloning LR reaction
Yeast two hybrid	LOC112417497	pGADT7	Gateway cloning LR reaction
Yeast two hybrid	LOC112418704	pGADT7	Gateway cloning LR reaction
Yeast two hybrid	LOC112419871	pGADT7	Gateway cloning LR reaction
Yeast two hybrid	LOC11443152	pGADT7	Gateway cloning LR reaction
Yeast two hybrid*	RiSP749	pGBKT7	Gateway cloning LR reaction
rBiFC	LOC101266050 (SIRSZ22)	pDONR201 P2P3	Gateway cloning BP reaction
rBiFC	LOC101247959 (SIGNAT)	pDONR201 P2P3	Gateway cloning BP reaction
rBiFC	RiSP749	pDONR201 P1P4	Gateway cloning BP reaction

rBiFC	nYFP-SIRSZ22 cYFP-RiSP749	BiFC NN 2 in 1	Gateway cloning LR reaction
rBiFC	nYFP-SIGNAT cYFP-RiSP749	BiFC NN 2 in 1	Gateway cloning LR reaction
RiSP749 OE	35S::GFPTurbo: RoID_mRuby	pGGPAG	Golden Gate
SIRSZ22 silencing	LOC101266050 RNAi	pDONR207	Gateway cloning BP reaction
SIRSZ22 silencing	LOC101266050 RNAi	pK7gwiwg2D Red root	Gateway cloning LR reaction
pSIGNAT activity	pLOC101247959-1kb::GUS-GFP: RoID_mRuby	pGGPAG	Golden Gate
pSIGNAT activity	pLOC101247959-3kb::GUS-GFP: RoID_mRuby	pGGPAG	Golden Gate

Table S3: List of qPCR primers used in this thesis. They are divided by organism, the top ones are from *R. irregularis*, then are the tomato ones and finally, *M. truncatula* gene primers

Primer name Fw	Primer sequence	Primer name Rv	Primer sequence
RiEF1 α _Fw	TGTTGCTTCGTCCTCAATATC	RiEF1 α _Rv	GGTTTATCGGTAGGTCGAG
RiSP749_Fw	CAAACGAATTTACCAAGCA	RiSP749_Rv	GCGCCTCTCGTGACTTTTAT
SIGAPDH_Fw	GCTGCTGGTGATGATCCTGT	SIGAPDH_Rv	GCGTTTGTGGTCCGAGAGAA
SIEF1 α _Fw	ACAGGCGTTCAGGTAAGGAA	SIEF1 α _Rv	CTTGACAACACCGACAGCAA
SILOC101266050_Fw	CAATCAGGGATCTGGATGGT	SILOC101266050_Rv	TTCACGAGCAAATGACCAG
SIRAM1_Fw	GTGCAAATGCAGTCACACAA	SIRAM1_Rv	TATCTTGCCATCCCAAAAGC
SIPT4_Fw	GTTTTTGGCATTACAAAATATGAT	SIPT4_Rv	CTTCTCATCTCCCCTGAAA
SIPT5_Fw	CCGAGACAAAAGGGAGATCA	SIPT5_Rv	TCTTGATGGCCAGAGACAGG
MtRAM1_Fw	ACTTTTTGGCCGATTTCTC	MtRAM1_Rv	CTTCACATGCCACGATGTTC
MtNSP2_Fw	CAAATCATTGTCAAGCAAAGC	MtNSP2_Rv	GAATCTGAAGAAGAACAAGTCCAA
MtPT4_Fw	CGGGCTAACATTCTTCTTCG	MtPT4_Rv	TTGCGCGTCTAATCTTCCTT
MtTUB1_Fw	TTTGCTCCTTACATCCCGTG	MtTUB_Rv	GCAGCACACATCATGTTTTTGG
MtGAPDH_Fw	TGCCTACCGTCGATGTTTCAGT	MtGADPH_Rv	TTGCCCTCTGATCCTCCTTG
MtLOC112418704_Fw	AGGTCGTGGCCGCGGAGGTG	MtLOC112418704_Rv	ACGCCACGAGGTGACACAC
MtLOC112417497_Fw	GTTACGCGGTGGTTCACG	MtLOC112417497_Rv	CATAAGGTGAATCACGGCGAG
MtLOC112419871_Fw	CGGTCTGGTGGGGTGGTTC	MtLOC112419871_Rv	ATAGCTGCGCCGGCGAGGTG
MtLOC11420857_Fw	GCAAAGCTGACATGGGTTATG	MtLOC11420857_Rv	GGCTAATTGAGCTCTCTCCAAG
MtLOC25490856_Fw	TCCAGCTGGATCTGGTGATG	MtLOC25490856_Rv	GTAGAGAATGAGTGTCTCTGAC
MtLOC11443152_Fw	CTCTATCCTCGAGTTCACCTG	MtLOC11443152_Rv	GGGGATCAGTAAAGAGAACAAC
MtDELLA1_Fw	TTCAAATGCGTTTAAACAAGCTA	MtDELLA1_Rv	CACTTGGACTCATTTTGTGGAA
MtNIN_Fw	GTGCTTTCAGAGTGAAGGCAAC	MtNIN_Rv	CATTCTCAAGATCAGCATCACATG

MtCYCLOPS_Fw

CGATCACTAAAGCTTAATTTGTCCT

MtCYCLOPS_Rv

CTCTTTTTCATCCGCCAAGTCT

3. Detailed Protocols

3.1. Tomato and *M. truncatula*-AMF bioassay

3.1.1. M. truncatula seed sterilization and germination

1. In 50ml falcon add seeds and 96% Sulfuric acid
2. 8 min on rotator
3. Rinse 3 x with water
4. Add 12% Bleach
5. 3 min on rotator
6. Rinse 3 x with water
7. Add 1mM solution of BAP
8. 3h on rotator
9. Add 3 sterile wet WM papers in a Petri dish lid
10. Place \pm 30 seeds on the papers
11. Add water in the dish and place the lid on the dish
12. Wrap the Petri dishes in aluminum foil and germinate the seed at 21°C GC for 4 days
13. Transfer plantlets to square plates with MS medium
14. 10-13 plants per plate
15. Keep in 21°C GC for 7 days

3.1.2. Tomato seed sterilization and germination

1. In 50ml falcon add seeds and 4% Bleach
2. 15 min on rotator
3. Rinse 3 x with water
4. Add 3 sterile wet WM papers in a Petri dish lid
5. Place \pm 30 seeds on the papers
6. Add water in the dish and place the lid on the dish
7. Wrap the Petri dishes in aluminum foil and germinate the seed at 21°C GC for 4 days
8. Transfer plantlets to square plates with MS medium
9. 10-13 plants per plate
10. Keep in 21°C GC for 7 days

3.1.3. Plant inoculation

1. Sterilize sand (S) and vermiculite (V)
2. Add S & V in a 1:1 ratio in a basket
3. Add water and mix thoroughly
4. Fill pots 2/3 of the way
5. Centrifuge 15 min at 4°C and 3000rpm the spore suspension (300 spores/plant)
6. Wash the spores with water

7. Centrifuge the spores 15 min at 4°C and 3000rpm
8. Resuspend in Hewitt to a final concentration of 750 spores/ml and add 400 µl in each hole done of the sand.
9. Gently place the plantlets in the holes
10. Add some tap water to the trays and put the cover on.

3.1.4. Harvesting

1. At 2, 4 and 6 weeks post inoculation (wpi) we harvest 12 plants for the time course experiment. For the rest of the experiments plants were harvested at 5wpi.
 - Time course experiment: the three or four plants of each pot were washed in tap water, the root system was dry out with tissue and the fresh root weight was measured. Then they were pulled together and randomly divided in two. Half was ink stained and the other half was frozen for RNA extraction.
 - Overexpression and RNAi experiments: Plants were washed, the root system was dry out with tissue and the fresh root weight was measured. Plants were divided for ink staining or for gene expression. The root tip of the stained roots and the full root system of the plants harvested for gene expression were frozen for later RNA extraction.

3.1.5. Root staining

1. Harvested roots are immersed in 10% KOH
2. Incubate the root samples at 95°C for 10 minutes
3. Remove KOH (caution when working with hot KOH) and roots are rinsed three times with water and once with 5% acetic acid
4. Add 5% black ink in 5% acetic acid and incubate at 95°C for 4 minutes
5. Remove the ink solution and rinse with tap water
6. Transfer the roots to 50% glycerol to conserve the staining

3.1.6. Colonization quantification, Trouvelot method

1. Cut the stained roots into equal 1 cm fragments
2. Randomly select 30 fragments and mount onto glass slide in 50% glycerol
3. For each fragment score the presence or absence for colonization and specific structures

3.2. Cloning

3.2.1. PCR reactions

Q5 High fidelity polymerase-cloning

1. ddH₂O: 10,75 µl
2. 5x NEB GC buffer: 5 µl
3. dNTPs: 0,5 µl
4. Forward and reverse primers: 1,25 µl each
5. Q5 polymerase: 0.25 µl
6. DNA template: 1 µl (±200ng)

Q5 PCR cycle

1. Initial denaturation a. 98°C : 30 seconds
2. Amplification: 25 – 35 cycles a. 98°C : 30 seconds b. Annealing T°C (depending on primer pair) : 30 seconds c. 72°C : 15-30° seconds per kb
3. Final extension a. 72°C : 5 minutes

GoTaq flexi – Colony PCR

1. GoTaq all-in one: 5 µl
2. ddH₂O: 4 µl
3. Forward and reverse primers: 0,5 µl each
4. Pick and add a colony

GoTaq PCR cycle

1. Initial denaturation a. 98°C : 2 minutes
2. Amplification: 25 – 35 cycles a. 95°C : 1 minute b. Annealing T°C (depending on primer pair) : 1 minute c. 72°C : 1 minute per kb
3. Final extension a. 72°C : 5 minutes

3.2.2. Golden gate assembly

1. Add 100 ng (1µl) destination vector
2. Add 100 ng (1µl) of each entry vector
3. Add 1,5 µl 10X cutsmart buffer
4. Add 1 mM ATP (1,5 µl)
5. Add 200U T4 DNA ligase
6. Add 0,5µl Bsa-HF v2 restriction enzyme

Golden Gate assembly cycle

37°C	2 min	20 x
16°C	2 min	
50°C	5 min	
80°C	5 min	
16°C	hold	

3.2.3. Gateway cloning

1. Add 100 ng destination vector
2. Add 50 ng of the insert
3. Add 2 µl of BP or LP clonase
4. Incubate from 1h to over night at 25°C

3.2.4. Gibson cloning

1. Add 100 ng destination vector
2. Add 50 ng of the insert
3. Add 2 µl of NEB builder
4. Incubate at 50°C for 15 min

3.2.5. E. coli heat shock transformation

1. Mix 50 µl DH5a competent cells with 5 µl of plasmid
2. Incubate 20 min on ice
3. Heat shock at 42°C for 45s
4. Add 900 µl LB

5. Incubate at 37°C for 1 hour with shaking
6. Centrifuge 2 min at 6000rpm and remove the supernatant
7. Resuspend in the residual media and add 40 µl on selective plate
8. Grow overnight at 37°C

3.2.6. Agrobacterium electroporation transformation

1. Mix 30 µl competent cells (C58C1) with 2 µl construct in 2ml cuvette and kept on ice
2. Electroporate at 2500 V, 25F, 400 Ω
3. Add 1 ml YEB medium and transfer all liquid to Eppendorf
4. Incubate at 28°C with shaking at 200 rpm for 1-2 hours
5. Centrifuge at 6000 rpm 3 min
6. Remove the supernatant leaving around 50 µl
7. Resuspend the bacteria and plate it on YEB medium with selective antibiotics
8. Incubate at 28°C for two days

3.3. Yeast transformation

1. Inoculate single yeast colony into 20 ml YPAD and incubate overnight at 30°C
2. The next day, measure the OD600 and start a new culture in a flask (in 20 ml YPAD) with OD600 = 0.17 – 0.2
3. Incubate at 30°C with shaking
4. Grow until OD = 0.6 – 0.8 (± 3-4 hours)
5. While you wait for the yeast to grow, prepare for each transformation in one tube:
 - A. 250 ng bait and 250 ng prey plasmid or 500 ng of a single plasmid
 - B. 306 µl mastermix:
 - a. 240 µl 50% PEG
 - b. 36 µl 1M LiAc
 - c. 30 µl ss-DNA

Vortex
6. Transfer cultures to 50 ml falcon tubes and spin at 3000 rpm for 5 minutes
7. Resuspend the yeast cells in 1 ml sterile H₂O and add 200 µl of the resuspended cells to the transformation tube prepared in step 5
8. Vortex 1 minute
9. Incubate at 42°C for 45 minutes
10. Spin down the cells at 3000 rpm for 5 minutes and discard as much supernatant as possible
11. Resuspend in 100 µl 0.9% NaCl
12. Plate all on SD-LT plates, seal with parafilm and incubate at 30°C for 2-3 days

3.3.1. Yeast assays

1. Grow five transformed colonies overnight at 30°C and 200 rpm in 200 µL appropriate SD medium in 96-well plates
2. Make 10x, 100x and 1000x dilutions in sterile MilliQ water
3. Plate on control plates and selective media using a replicator
4. Grow for two days at 30°C

3.4. Tobacco transformation

1. *Agrobacterium tumefaciens* (C58C1) were transformed with the constructs of interest as previously described
2. An *Agrobacterium* colony was picked and incubated in liquid YEB (with appropriate antibiotics) for 2 days at 28°C with shaking (200 rpm)
3. The cultures are resuspended in infiltration buffer to obtain an OD600 of 1,5
4. Incubate at room temperature for 2 hours with shaking
5. Per transformation 0,33 ml of *Agrobacterium* containing the desired construct, 0,33ml of the *35SP:p19:NosT* *Agrobacterium* culture and 0,33 ml of the infiltration solution were mixed to obtain a final OD600 of 0,5 for each strain
6. 0,5 ml of the bacterial solutions were co-infiltrated per leaf of 3-4 weeks old *N. benthamiana* plants using a 1 ml syringe
7. Plants were grown for 2-3 days in the greenhouse
8. Samples of infiltrated leaves were analyzed using confocal microscopy

3.5. RT-qPCR

3.5.1. RNA extraction according to the ReliaPrep RNA tissue Miniprep kit from Promega

1. Frozen full root system was ground with cooled pestle and mortar (don't allow samples to thaw). Root tips were crushed using Retsch machine and a metal balls
2. 500 µl of LBA buffer with 1-Thioglycerol for cell lysis and mix by pipetting
3. Clear homogenates by centrifugation for 3 minutes at 14,000 × g, then transfer them to a clean tube.
4. Add Isopropanol as recommended in the table above. Mix by vortexing 5 seconds.
5. Transfer lysate to a Minicolumn in a Collection Tube. Centrifuge at 12,000–14,000 × g for 1 minute at 20–25°C.
6. Remove the ReliaPrep™ Minicolumn, and discard liquid in the Collection Tube. Replace the Minicolumn in the Collection Tube.
7. Add 500µl of RNA Wash Solution to the Minicolumn. Centrifuge at 12,000–14,000 × g for 30 seconds. Empty the Collection Tube, and place it in the microcentrifuge rack.
8. Prepare DNase I incubation mix by combining the following amounts of reagent, per sample, in the order listed:
 - a) 24µl Yellow Core Buffer
 - b) 3µl MnCl₂, 0.09M
 - c) 3µl DNase I
 Mix by gently pipetting
9. Apply 30µl of DNase I incubation mix to the Minicolumn membrane. Incubate for 15 minutes at 20°–25°C.
10. Add 200µl of Column Wash Solution (with ethanol added) to the Minicolumn. Centrifuge at 12,000–14,000 × g for 15 seconds.
11. Add 500µl of RNA Wash Solution (with ethanol added). Centrifuge at 12,000–14,000 × g for 30 seconds. Discard the wash solutions and the Collection Tube.
12. Place the ReliaPrep™ Minicolumn into a new Collection Tube. Add 300µl of RNA Wash Solution and centrifuge at high speed for 2 minutes

13. Transfer the ReliaPrep™ Minicolumn from the Collection Tube to an Elution Tube. Add 30 µl of Nuclease-Free Water to the Minicolumn membrane as recommended in the table below. Place the Minicolumn and Elution Tube into a centrifuge with the Elution Tube lid facing to the outside. Centrifuge at 12,000–14,000 × g for 1 minute.

3.5.2. cDNA preparation

1. cDNA was created using the qScript cDNA superMix (Quantabio)
 - a) 1 µg of RNA
 - b) 4 µl of qScript superMix
 - c) Adjust to 20 µl using RNase-free water
 - d) Incubate for 5 minutes at 25°C
 - e) Incubate for 30 minutes at 42°C
 - f) Incubate for 5 minutes at 85°C
2. Dilute 1:5 in Nuclease Free Water
3. Prepare a 5:1 (SyberSafe:cDNA) mix for every condition

3.5.3. Primer preparation

1. Dilute the stock primers (Fw & Rv) 10x
2. Add 10 µl Fw primer and 10 µl Rv primer to 180 µl miliQ

3.5.4. qPCR plate

1. In a 384 well-plate, on ice, add 3 µl cDNA mix per reaction
2. Gently tap the plate to allow the cDNA droplets to drop to the bottom
3. Add 2 µl primer mix per reaction
4. Add the transparent layer over the plate
5. Spin down for 2 minutes and place in the machine
6. Run PSB protocol (5µl)

3.6. GUS staining

1. The roots with the β-glucuronidase (GUS) construct are harvested
2. Roots are washed with water
3. X-Gal solution in NT buffer is added to the roots
4. They are incubated at 37°C until blue colour appears
5. Reaction is stopped adding 70% ethanol